

MICROCOPY RESOLUTION TEST CHART
NATIONAL BUREAU OF STANDARDS-1963-A

REPORT DOCUMENTATION PAGE

1a REPORT SECURITY CLASSIFICATION UNCLASSIFIED		1b RESTRICTIVE MARKINGS	
2a SECURITY CLASSIFICATION AUTHORITY		3 DISTRIBUTION/AVAILABILITY OF REPORT Approved for public release; distribution is unlimited	
2b DECLASSIFICATION/DOWNGRADING SCHEDULE			
4 PERFORMING ORGANIZATION REPORT NUMBER(S)		5 MONITORING ORGANIZATION REPORT NUMBER(S)	
6a NAME OF PERFORMING ORGANIZATION Naval Postgraduate School	6b OFFICE SYMBOL (if applicable) Code 69	7a NAME OF MONITORING ORGANIZATION Naval Postgraduate School	
6c ADDRESS (City, State, and ZIP Code) Monterey, California 93943-5000		7b ADDRESS (City, State, and ZIP Code) Monterey, California 93943-5000	
8a NAME OF FUNDING/SPONSORING ORGANIZATION	8b OFFICE SYMBOL (if applicable)	9 PROCUREMENT INSTRUMENT IDENTIFICATION NUMBER	
8c ADDRESS (City, State, and ZIP Code)		10 SOURCE OF FUNDING NUMBERS	
		PROGRAM ELEMENT NO	PROJECT NO
		TASK NO	WORK UNIT ACCESSION NO
11 TITLE (include Security Classification) A MULTIBODY DYNAMIC ANALYSIS OF THE N-ROSS SATELLITE ROTATING FLEXIBLE REFLECTOR USING KANE'S METHOD			
12 PERSONAL AUTHOR(S) Heffernan, Natalie F.			
13a TYPE OF REPORT Masters and Engineers Thesis	13b TIME COVERED FROM TO	14 DATE OF REPORT (Year Month Day) June 1987	15 PAGE COUNT 128
16 SUPPLEMENTARY NOTATION			
17 COSATI CODES		18 SUBJECT TERMS (Continue on reverse if necessary and identify by block number)	
FIELD	GROUP	SUB GROUP	
		Spacecraft, Dynamics, Flexible body, Substructuring	
19 ABSTRACT (Continue on reverse if necessary and identify by block number)			
<p>The Navy Remote Ocean Sensing System (N-ROSS) satellite is being developed to supply accurate data on ocean parameters for fleet operations. A Low Frequency Microwave Radiometer (LFMR), a large flexible reflector attached to an angled flexible boom, is a sea surface temperature sensor on this satellite which rotates at 15 RPM. The dynamic interaction between the reflector and the boom, and the effects of the reflector orientation and flexibility on the pointing error of the LFMR during a spin-up procedure are investigated by performing dynamic simulations. Dynamical equations of this flexible multibody system are formulated using Kane's method. Efficient computer simulations were achieved by developing a FORTRAN program and using Dynamic Simulation Language (DSL).</p>			
20 DISTRIBUTION/AVAILABILITY OF ABSTRACT <input checked="" type="checkbox"/> UNCLASSIFIED/UNLIMITED <input type="checkbox"/> SAME AS RPT <input type="checkbox"/> OTIC USERS		21 ABSTRACT SECURITY CLASSIFICATION UNCLASSIFIED	
22a NAME OF RESPONSIBLE INDIVIDUAL Young S. Shin		22b TELEPHONE (Include Area Code) (408-646-2568)	22c OFFICE SYMBOL 69Sg

Approved for public release; distribution is unlimited.

A Multibody Dynamic Analysis of the
N-ROSS Satellite Rotating Flexible
Reflector Using Kane's Method

by

Natalie F. Heffernan
Lieutenant, United States Navy
B.S.E., Duke University, 1981

Submitted in partial fulfillment of the
requirements for the degrees of

MASTER OF SCIENCE IN MECHANICAL ENGINEERING
and
MECHANICAL ENGINEER

from the

NAVAL POSTGRADUATE SCHOOL
June 1987

Author:

Natalie F. Heffernan
Natalie F. Heffernan

Approved by:

Young S. Shin
Y.S. Shin, Thesis Advisor

Kim S. Kim
K.S. Kim, Co-Advisor

Anthony J. Healy
A.J. Healy, Chairman,
Department of Mechanical Engineering

G.E. Schacher
G.E. Schacher,
Dean of Science and Engineering

ABSTRACT

The Navy Remote Ocean Sensing System (N-ROSS) satellite is being developed to supply accurate data on ocean parameters for fleet operations. A Low Frequency Microwave Radiometer (LFMR), a large flexible reflector attached to an angled flexible boom, is a sea surface temperature sensor on this satellite which rotates at 15 RPM. The dynamic interaction between the reflector and the boom, and the effects of the reflector orientation and flexibility on the pointing error of the LFMR during a spin-up procedure are investigated by performing dynamic simulations. Dynamical equations of this flexible multibody system are formulated using Kane's method. Efficient computer simulations were achieved by developing a FORTRAN program and using Dynamic Simulation Language (DSL).

Accession For	
NTIS	CRA&I <input checked="" type="checkbox"/>
DTIC	TAB <input type="checkbox"/>
Unannounced <input type="checkbox"/>	
Justification	
By	
Distribution/	
Availability Codes	
Dist	Avail and/or Special
A-1	

QUALITY INSPECTED
2

TABLE OF CONTENTS

I. INTRODUCTION	10
A. BACKGROUND	10
B. PROBLEM STATEMENT	10
C. THESIS OUTLINE	11
II. FORMULATION OF 3-D EQUATIONS OF MOTION	13
A. MODEL DESCRIPTION	13
B. EQUATION FORMULATION	13
III. COMPUTER IMPLEMENTATION	36
A. INTRODUCTION	36
B. MODAL ANALYSIS	36
C. EVALUATION OF TIME CONSTANTS	37
D. DSL IMPLEMENTATION	38
IV. RESULTS	40
A. MATERIAL PROPERTIES AND PARAMETERS	39
B. EFFECTS OF THE REFLECTOR FLEXIBILITY	39
C. EFFECTS OF IN-PLANE ORIENTATION CHANGES	41
D. EFFECT OF OUT-OF-PLANE ORIENTATIO OF REFLECTOR	44

V. CONCLUSIONS AND RECOMMENDATIONS	45
A. CONCLUSIONS	45
B. RECOMMENDATIONS	45

APPENDICES

A MODAL ANALYSIS OF REFLECTOR AND BOOM	46
B REPRESENTATIVE EFFECT OF REFLECTOR FLEXIBILITY	47
C REPRESENTATIVE EFFECT OF IN-PLANE REFLECTOR ROTATION	48
D REPRESENTATIVE EFFECT OF OUT-OF-PLANE REFLECTOR ROTATION	49
E PROGRAMS	50
F FIGURES	81
LIST OF REFERENCES	126
INITIAL DISTRIBUTION LIST	127

LIST OF FIGURES

2.1	NROSS Baseline Configuration	82
2.2	LFMR Model	83
A.1	Undeformed Reflector	84
A.2	First Mode of Reflector	85
A.3	Second Mode of Reflector	86
A.4	Third Mode of Reflector	87
A.5	Fourth Mode of Reflector	88
A.6	Undeformed Boom	89
A.7	First Mode of Boom	90
A.8	Second Mode of Boom	91
A.9	Third Mode of Boom	92
A.10	Fourth Mode of Boom	93
4.1	Finite Element Model of LFMR System	94
4.2	Applied Torque History During the Spin-up Procedure	95
B.1	Angular Velocity of Stiffer Reflector at -155°	96
B.2	Angular Velocity of More Flexible Reflector at -155°	97
B.3	Fourth Boom Generalized Coordinate of Stiffer Reflector at -155°	98
B.4	Fourth Boom Generalized Coordinate of More Flexible Reflector at -155°	99
B.5	Third Reflector Generalized Coordinate of Stiffer Reflector at -155°	100
B.6	Third Reflector Generalized Coordinate of More Flexible Reflector at -155°	101
B.7	Vertical Deflection at Boom Tip of Stiffer Reflector at -155°	102
B.8	Vertical Deflection at Boom Tip of More Flexible Reflector at -155°	103

B.9	Rotation of Boom Tip About Vertical Axis of Stiffer Reflector at -155°	104
B.10	Rotation of Boom Tip About Vertical Axis of More Flexible Reflector at -155°	105
C.1	Angular Displacement of Stiffer Reflector at -135°	106
C.2	Angular Displacement of Stiffer Reflector at -145°	107
C.3	Angular Displacement of Stiffer Reflector at -155°	108
C.4	Horizontal Deflection of Boom Tip of Stiffer Reflector at -135°	109
C.5	Horizontal Deflection of Boom Tip of Stiffer Reflector at -145°	110
C.6	Horizontal Deflection of Boom Tip of Stiffer Reflector at -155°	111
C.7	Rotation of Boom Tip About Horizontal Axis of Stiffer Reflector at -135°	112
C.8	Rotation of Boom Tip About Horizontal Axis of Stiffer Reflector at -145°	113
C.9	Rotation of Boom Tip About Horizontal Axis of Stiffer Reflector at -155°	114
C.10	Horizontal Deflection of Dish Point 1 of Stiffer Reflector at -135°	115
C.11	Horizontal Deflection of Dish Point 1 of Stiffer Reflector at -145°	116
C.12	Horizontal Deflection of Dish Point 1 of Stiffer Reflector at -155°	117
D.1	First Boom Generalized Coordinate of Stiffer Reflector at -155°	118
D.2	First Boom Generalized Coordinate of Stiffer Reflector Tilted 5° Out of Plane	119
D.3	Fourth Reflector Generalized Coordinate of Stiffer Reflector at -155°	120
D.4	Fourth Reflector Generalized Coordinate of Stiffer Reflector Tilted 5° Out of Plane	121
D.5	Out-of-Plane Deflection at Boom Tip of Stiffer Reflector at -155°	122
D.6	Out-of-Plane Deflection at Boom Tip of Stiffer Reflector Tilted 5° Out of Plane	123
D.7	Out-of-Plane Deflection at Dish Point 4 of Stiffer Reflector at -155°	124
D.8	Out-of-Plane Deflection at Dish Point 4 of Stiffer Reflector Tilted 5° Out of Plane	125

LIST OF TABLES

2.1	PARTIAL VELOCITIES OF BODY A AND BODY B.....	24
2.2	PARTIAL VELOCITIES OF BODY C	25
3.1	REAL EIGENVALUES	37
4.1	BOOM AND REFLECTOR PROPERTIES	41
4.2	GEOMETRIC PARAMETERS	42

ACKNOWLEDGEMENT

I wish to express my gratitude to Dr. Kil Soo Kim and Professor Young Sik Shin for their immense guidance and encouragement in completing this thesis. Without their intellectual as well as emotional support, this work could not have been accomplished.

I. INTRODUCTION

A. BACKGROUND

The Navy has great interest in obtaining accurate, real-time data on various ocean parameters. Presently, research is being conducted on the merits of using a satellite system to collect this data. The Navy Remote Ocean Sensing System (N-ROSS) satellite has been developed to achieve this goal [Ref. 1]. This satellite scans the earth's surface and will provide the Navy with such parameters as wind speed, wind direction, ocean temperature, ice edge detection, wave height, and ocean photography [Ref. 2].

One of the sensor systems to accomplish this goal is the Low Frequency Microwave Radiometer (LFMR). The LFMR consists of a large reflector dish connected to an angled boom. The LFMR scans the ocean surfaces and records the temperature. Increased scanning area is accomplished by spinning the reflector at 15 RPM. A rigid electronics box is attached at the base of the LFMR boom. Therefore, the rotating LFMR system consists of the flexible boom and reflector and the rigid electronics box. Considering the nature of the system, accurate analysis and suppression of the vibration and deflection of the LFMR is essential for the satisfaction of the pointing error requirement of the system and for the accomplishment of the mission of the N-ROSS satellite[Ref. 2].

B. PROBLEM STATEMENT

A three-dimensional dynamic analysis has been performed using a model that consists of a flexible angled boom with a point mass at the tip [Ref. 3]. Lagrangian equations of motion were employed to achieve a good dynamic simulation.

In this study, the LFMR is analyzed as a multibody system. A multibody approach will provide a means to analyze the dynamic interaction between substructures of a complicated structure with greater ease. In dynamic analysis of a multibody system, maintaining computational efficiency is a key factor and "The emphasis of researchers working with multibody systems has been the expanded generality of mathematical models and the formulation of equations of motion that are amenable to computer solution." [Ref. 4]

Therefore, it is the intent of this thesis to apply an efficient multibody dynamic analysis to the LFMR system. The LFMR is broken down into two bodies; the first body is the flexible boom and the second body is the flexible reflector. Kane's method is used to formulate these equations of motion, "since it combines the computational advantages of both Newton's laws and the Lagrangian formulation." [Ref. 4]

C. THESIS OUTLINE

In Chapter II, the analytic model of the LFMR used for this thesis is described. The dynamical equations are formulated using Kane's method. This method is briefly explained prior to the formulation.

Chapter III contains an explanation of the three computer programs used to solve the equations of motion. NASA Structural Analysis (NASTRAN) calculates the mode shapes and natural frequencies for both bodies. A FORTRAN program reads the data output from NASTRAN and calculates the time constants. The time constants are applied in a Dynamic Simulation Language (DSL) program to solve the simultaneous differential equations.

In Chapter IV, the simulation results are presented to investigate deflections and rotations at various points on the LFMR. Three parameters are varied: (1) the flexibility of the reflector; (2) the in-plane orientation of the reflector; and (3) the out-of-plane orientation of the reflector. The effects of these changes are compared.

Chapter V presents conclusions and recommendations for application and extension of this work.

II. FORMULATION OF EQUATIONS OF MOTION

A. MODEL DESCRIPTION

The configuration of the LFMR is shown in Figure 2.1. The LFMR consists of a boom mounted on a rigid electronics box. A complex reflector is attached at the tip of the boom. The boom hinge is to be rigid after the deployment of the LFMR, allowing no relative motion between the upper and lower booms. The LFMR system rotates at 15 RPM about a spin axis fixed in a local reference frame of the N-ROSS satellite. The spin axis always points at the earth's center while the satellite is in its orbit. Therefore, the gravitational force and the centrifugal force are assumed in equilibrium. This observation allows the spacecraft's local reference frame to be considered the inertial (Newtonian) reference frame and the LFMR to be in a zero-gravity environment.

The model of the LFMR used in this thesis is shown in Figure 2.2. The angled boom was analyzed as one body and the reflector as the second body. Body A represents the electronics box, body B is the angled boom, and body C is the reflector dish.

The a_1, a_2, a_3 coordinate system rotates in the inertial reference frame, with a_3 coinciding with the spin axis. The c_1, c_2, c_3 coordinate system is the local reference frame of the reflector and its origin is at the connection point between the deflected boom and reflector (point h).

B. EQUATION FORMULATION

1. Kane's Dynamical Equations

The equations of motion for the LFMR were formulated using Kane's method [Ref. 5]. This method is a Lagrange form of D'Alambert's principle, which is equivalent to Newton's law cast into a different form. Newton's law for a differential element is

$$(Eqn. 2.1) \quad df - a^K dm = 0$$

where

df - differential force

a^K - acceleration of differential element on body K

dm - differential mass

Kane's method introduces the generalized active and inertia forces. The dynamical equations are

$$(Eqn. 2.2) \quad F_r + F_r^* = 0 \quad r = 1, \dots, \text{total degree of freedom}$$

F_r represents the generalized active forces and F_r^* is the generalized inertia forces. F_r is the sum of the dot product between the partial velocity and the differential force as shown in equation 2.3.

$$(Eqn. 2.3) \quad F_r = \int \underline{v}_r \cdot df$$

F_r^* is the sum of the dot product between the partial velocity and the differential inertia force as shown in equation 2.4.

$$(Eqn. 2.4) \quad \int \underline{v}_r \cdot (-a^K) dm$$

The partial velocity \underline{v}_r comes from the definition of velocity where

$$(Eqn. 2.5) \quad \underline{v} = \sum_{r=1}^V \underline{v}_r \dot{q}_r \quad r=1, \dots, \text{total degrees of freedom}$$

\dot{q}_r is the time derivative of the generalized coordinates.

For this model, there are three types of dynamical equations. Equation 2.6 is derived from the large rotational motion of the system. Equation 2.7 is derived from the small boom motion. The number of equations of this type depends on the number of modes (V_1) used to characterize the boom motion. Equation 2.8 is derived from the small

reflector motion. The number of equations of this type depends on the number of modes (v_2) used to characterize the reflector motion.

$$(Eqn. 2.6) \quad F_1 + F_1^* = 0$$

$$(Eqn. 2.7) \quad F_{1+j} + F_{1+j}^* = 0 \quad j=1, \dots, v_1$$

$$(Eqn. 2.8) \quad F_{1+v_1+k} + F_{1+v_1+k}^* = 0 \quad k=1, \dots, v_2$$

2. Generalized Coordinates and Generalized Speed

The first generalized speed U_1 is defined as follows:

$$(Eqn. 2.9) \quad U_1 = \underline{\omega}^N \cdot a_3$$

where $\underline{\omega}^N$ is the angular velocity of body A in the inertial reference frame. Subsequent generalized speeds are defined from the generalized coordinates q_i, \bar{q}_j which are model coordinates of bodies B and C, respectively, as follows:

$$(Eqn. 2.10) \quad \begin{aligned} U_{1+i} &= \dot{q}_i & (i = 1, \dots, v_1) \\ U_{1+v_1+j} &= \dot{\bar{q}}_j & (j = 1, \dots, v_2) \end{aligned}$$

where v_1 and v_2 represent the number of modes used to describe the displacement of body B and C, respectively. Thus, there are $1 + v_1 + v_2$ generalized speeds.

3. Angular Velocities

The angular velocity of body C with respect to body A is the time derivative of the small rotation of the hinge point H. Point H is the connection between body B and body C. This angular velocity can be represented using matrices as follows:

$$(Eqn. 2.11) \quad \underline{\omega}^{A,C} = [C]^T [\dot{C}] = \begin{bmatrix} 1 & \psi_3 & -\psi_2 \\ -\psi_3 & 1 & \psi_1 \\ \psi_2 & -\psi_1 & 1 \end{bmatrix} \begin{bmatrix} 0 & -\dot{\psi}_3 \dot{\psi}_2 \\ \dot{\psi}_3 & 0 & -\dot{\psi}_1 \\ -\dot{\psi}_2 & \dot{\psi}_1 & 0 \end{bmatrix} = \begin{bmatrix} 0 & -\dot{\psi}_3 \dot{\psi}_2 \\ \dot{\psi}_3 & 0 & -\dot{\psi}_1 \\ -\dot{\psi}_2 & \dot{\psi}_1 & 0 \end{bmatrix}$$

where $\dot{\psi}_i = \sum_{k=1}^{v_1} \dot{\psi}_k^i$ (H) U_{1+k} and ψ_k^i is the small angle displacement for the i^{th}

degree of freedom and the k^{th} mode at point H. Therefore, the angular velocity is

$$(Eqn. 2.12) \quad \overset{A}{\omega}^C = \psi_1 \underline{e}_1 + \psi_2 \underline{e}_2 + \psi_3 \underline{e}_3$$

4. Velocity and Accelerations

a. Velocity and Acceleration of Body A

From the generalized speed definition, the angular velocity of Body A is

$$(Eqn. 2.13) \quad \overset{NA}{\omega} = u_1 \underline{a}_3$$

The angular acceleration is merely the time derivative of the angular velocity, because the \underline{a}_3 axis is fixed in the inertial reference frame.

$$(Eqn. 2.14) \quad \overset{NA}{\alpha} = \dot{u}_1 \underline{a}_3$$

The velocity of A is defined relative to point Q, the origin of the $\underline{a}_1, \underline{a}_2, \underline{a}_3$ coordinate system. Point Q is fixed in the inertial reference frame. Since body A is a rigid body, the velocity is merely the rotational velocity of the mass center A*.

$$(Eqn. 2.15) \quad \overset{NA^*}{v} = (\overset{NA}{\omega} \times -b\underline{a}_1) = -bu_1 \underline{a}_2$$

where b is the distance from point Q to the mass center A*.

Similarly, the acceleration of body A is the rotational acceleration comprised of tangential and normal components.

$$(Eqn. 2.16) \quad \begin{aligned} \overset{NA^*}{a} &= \overset{NA}{\omega} \times (\overset{NA}{\omega} \times -b\underline{a}_1) + \overset{NA}{\alpha} \times (-b\underline{a}_1) \\ &= bu_1^2 \underline{a}_1 - b\dot{u}_1 \underline{a}_2 \end{aligned}$$

The $\underline{a}_1, \underline{a}_2, \underline{a}_3$ coordinate system was chosen so that the mass center of body A moves in plane motion, simplifying the equations.

b. Velocity and Acceleration of Body B

The position of an arbitrary point P on body B is described in the $\underline{a}_1, \underline{a}_2, \underline{a}_3$ coordinate system.

$$\begin{aligned}
 \text{(Eqn. 2.17)} \quad \mathbf{B}^P &= P_1 \mathbf{a}_1 + P_2 \mathbf{a}_2 + P_3 \mathbf{a}_3 + \sum_{i=1}^{V_1} \phi_i^x q_i \mathbf{a}_1 \\
 &+ \sum_{i=1}^{V_1} \phi_i^y q_i \mathbf{a}_2 + \sum_{i=1}^{V_1} \phi_i^z q_i \mathbf{a}_3
 \end{aligned}$$

The position vector \mathbf{B}^P is the sum of the undeformed position vector and the summations of the translational mode shape deformations. P_1, P_2 , and P_3 describe the undeformed position.

The position of point P changes with time, therefore the velocity of point P is the time derivative of the position added to the rotational velocity.

$$\begin{aligned}
 \text{(Eqn. 2.18)} \quad \mathbf{V}^{NP} &= \frac{B^P}{B} + \underline{\omega}^{NA} \times \frac{B^P}{B} \\
 &= \sum_{i=1}^{V_1} \phi_i^x u_{i+1} \mathbf{a}_1 + \sum_{i=1}^{V_1} \phi_i^y u_{i+1} \mathbf{a}_2 + \sum_{i=1}^{V_1} \phi_i^z u_{i+1} \mathbf{a}_3 \\
 &+ u_1 \left[P_1 + \sum_{i=1}^{V_1} \phi_i^x q_i \right] \mathbf{a}_2 - u_1 \left[P_1 + \sum_{i=1}^{V_1} \phi_i^y q_i \right] \mathbf{a}_1
 \end{aligned}$$

The acceleration of point P is derived from differentiating the velocity with respect to time.

$$\begin{aligned}
 \text{(Eqn. 2.19)} \quad \underline{\alpha}^{NP} &= \underline{\alpha}^{NA} \times \frac{B^P}{B} + \underline{\omega}^{NA} \times (\underline{\omega}^{NA} \times \frac{B^P}{B}) + 2 \underline{\omega}^{NA} \times \frac{B^P}{B} + \frac{B^P}{B} \\
 &= \left\{ -\dot{u}_1 \left[P_2 + \sum_{i=1}^{V_1} \phi_i^y q_i \right] - u_1^2 \left[P_1 + \sum_{i=1}^{V_1} \phi_i^x q_i \right] \right.
 \end{aligned}$$

$$\begin{aligned}
& 2u_1 \left\{ \sum_{i=1}^{v_1} \phi_i^y u_{1+i} \right\} + \sum_{i=1}^{v_1} \phi_i^x \dot{u}_{1+i} \left. \right\} \mathbf{a}_1 + \\
& \left\{ \dot{u}_1 \left[P_1 + \sum_{i=1}^{v_1} \phi_i^x q_i \right] - u_1^2 \left[P_2 + \sum_{i=1}^{v_1} \phi_i^y q_i \right] \right. \\
& \left. + 2u_1 \left\{ \sum_{i=1}^{v_1} \phi_i^x u_{1+i} \right\} + \sum_{i=1}^{v_1} \phi_i^y \dot{u}_{1+i} \right\} \mathbf{a}_2 \\
& + \sum_{i=1}^{v_1} \phi_i^z \dot{u}_{1+i} \mathbf{a}_3
\end{aligned}$$

c. Velocity and Acceleration of Body C

The position vector of an arbitrary point X on body C is described in the local coordinate system C, analogous to the representation of a point on body B.

$$\begin{aligned}
\text{(Eqn. 2.20)} \quad \mathbf{r}_{B^X}^C &= \left(x_1 + \sum_{j=1}^{v_2} \bar{\phi}_j^x \bar{q}_j \right) \mathbf{e}_1 + \left(x_2 + \sum_{j=1}^{v_2} \bar{\phi}_j^y \bar{q}_j \right) \mathbf{e}_2 \\
&+ \left(x_3 + \sum_{j=1}^{v_2} \bar{\phi}_j^z \bar{q}_j \right) \mathbf{e}_3
\end{aligned}$$

The velocity of point X in the inertial reference frame is the sum of the velocity at the hinge point H in the inertial reference frame and the rotational velocity with the time derivative of the position calculated in the local coordinate system C.

(Eqn. 2.21)
$$\underline{V}^{NX} = \underline{V}^{NH} + (\underline{\omega}^{NC} \times \underline{R}^{CX}) + \underline{C}^{CX}$$

where

$$\begin{aligned} \underline{\omega}^{NC} &= u_1 \underline{a}_3 + \psi_1 \underline{e}_1 + \psi_2 \underline{e}_2 + \psi_3 \underline{e}_3 \\ \underline{V}^{NH} &= \left\{ \sum_{i=1}^{v_1} \phi_i^x(H) u_{i+1} - u_1 \left[H_2 + \sum_{i=1}^{v_1} \phi_i^y(H) q_i \right] \right\} \underline{a}_1 + \\ &\quad \left\{ \sum_{i=1}^{v_1} \phi_i^y(H) u_{i+1} + u_1 \left[H_1 + \sum_{i=1}^{v_1} \phi_i^x(H) q_i \right] \right\} \underline{a}_2 + \\ &\quad \sum_{i=1}^{v_1} \phi_i^z(H) u_{i+1} \underline{a}_3 \end{aligned}$$

Thus the velocity of point X is

(Eqn. 2.22)
$$\begin{aligned} \underline{V}^{NX} &= \left\{ \sum_{i=1}^{v_1} \phi_i^x(H) u_{i+1} - u_1 \left[H_2 + \sum_{i=1}^{v_1} \phi_i^y(H) q_i \right] \right\} \underline{a}_1 + \\ &\quad \left\{ \sum_{i=1}^{v_1} \phi_i^y(H) u_{i+1} + u_1 \left[H_1 + \sum_{i=1}^{v_1} \phi_i^x(H) q_i \right] \right\} \underline{a}_2 + \\ &\quad \sum_{i=1}^{v_1} \phi_i^z(H) u_{i+1} \underline{a}_3 + \left\{ \sum_{j=1}^{v_2} \phi_j^x u_{1+v_1+j} + \psi_2 \left(x_3 + \sum_{j=1}^{v_2} \bar{\phi}_j^z q_j \right) \right\} \underline{a}_3 \end{aligned}$$

$$\begin{aligned}
& \left. \psi_3 \left(x_2 + \sum_{j=1}^{v_2} \bar{\phi}_j^y \bar{q}_j \right) \right\} \underline{c}_1 + \left\{ \sum_{j=1}^{v_2} \bar{\phi}_j^y u_{1+v_1+j} \right\} \\
& \left. \psi_3 \left(x_1 + \sum_{j=1}^{v_2} \bar{\phi}_j^x \bar{q}_j \right) - \psi_1 \left(x_3 + \sum_{j=1}^{v_2} \bar{\phi}_j^z \bar{q}_j \right) \right\} \underline{c}_2 + \\
& \left\{ \sum_{j=1}^{v_2} \bar{\phi}_j^z u_{1+v_1+j} + \psi_1 \left(x_2 + \sum_{j=1}^{v_2} \bar{\phi}_j^y \bar{q}_j \right) - \psi_2 \left(x_1 + \sum_{j=1}^{v_2} \bar{\phi}_j^x \bar{q}_j \right) \right\} \underline{c}_3 + \\
& \left\{ u_1 \left(x_1 + \sum_{j=1}^{v_2} \bar{\phi}_j^x \bar{q}_j \right) \right\} \underline{d}_1 + \left\{ u_1 \left(x_2 + \sum_{j=1}^{v_2} \bar{\phi}_j^y \bar{q}_j \right) \right\} \underline{d}_2 + \\
& \left\{ u_1 \left(x_3 + \sum_{j=1}^{v_2} \bar{\phi}_j^z \bar{q}_j \right) \right\} \underline{d}_3.
\end{aligned}$$

A third nonorthogonal coordinate system (d) is defined for computing the velocity and acceleration of body C more easily.

$$a_3 \times \underline{c}_i = \underline{d}_i$$

The following tables depict the relationship between the three coordinate systems.

	a_1	a_2	a_3
d_1	$-\psi_3$	1	0
d_2	-1	$-\psi_3$	0
d_3	ψ_1	ψ_2	0

	Ω_1	Ω_2	Ω_3
d_1	0	1	$-\psi_1$
d_2	-1	0	$-\psi_2$
d_3	ψ_1	ψ_2	0

	d_1	d_2	d_3
d_1	1	0	ψ_2
d_2	0	1	$-\psi_1$
d_3	ψ_2	$-\psi_1$	0

(not orthogonal)

	a_1	a_2	a_3
Ω_1	1	ψ_3	$-\psi_2$
Ω_2	$-\psi_3$	1	ψ_1
Ω_3	ψ_2	$-\psi_1$	1

The acceleration of point X with respect to the inertial reference frame is expressed as the hinge point H acceleration and the acceleration relative to the hinge point

$$\text{(Eqn. 2.23) } \dot{\mathbf{a}}^{NX} = \dot{\mathbf{a}}^{NH} + \dot{\boldsymbol{\alpha}}^{NC} \times \mathbf{B}^{CX} + \dot{\boldsymbol{\omega}}^{NC} \times (\dot{\boldsymbol{\omega}}^{NC} \times \mathbf{B}^{CX}) + 2 \dot{\boldsymbol{\omega}}^{NC} \times \mathbf{B}^{CX} + \dot{\mathbf{a}}^{CX}$$

where

$$\begin{aligned} \dot{\boldsymbol{\alpha}}^{NC} &= \dot{\boldsymbol{\alpha}}^{NA} + \frac{\text{Ad}(\dot{\boldsymbol{\omega}}^{AC})}{dt} + \dot{\boldsymbol{\omega}}^{NA} \times \dot{\boldsymbol{\omega}}^{AC} \\ &= \dot{u}_1 \mathbf{a}_3 + \dot{\psi}_1 \boldsymbol{\alpha}_1 + \dot{\psi}_2 \boldsymbol{\alpha}_2 + \dot{\psi}_3 \boldsymbol{\alpha}_3 + u_1 \dot{\psi}_1 \mathbf{a}_1 \\ &= u_1 \dot{\psi}_2 \mathbf{a}_2 + u_1 \dot{\psi}_3 \mathbf{a}_3 \end{aligned}$$

and

$$\begin{aligned} \dot{\mathbf{a}}^{NH} &= \left\{ -\dot{u}_1 \left[H_2 + \sum_{i=1}^{v_1} \phi_i^y(H) q_i \right] - u_1^2 \left[H_1 + \sum_{i=1}^{v_1} \phi_i^x(H) q_i \right] \right. \\ &\quad \left. - 2u_1 \sum_{i=1}^{v_1} \phi_i^y(H) u_{1+i} + \sum_{i=1}^{v_1} \phi_i^x(H) \dot{u}_{1+i} \right\} \mathbf{a}_1 + \end{aligned}$$

$$\begin{aligned} &\left\{ \dot{u}_1 \left[H_1 + \sum_{i=1}^{v_1} \phi_i^x(H) q_i \right] - u_1^2 \left[H_2 + \sum_{i=1}^{v_1} \phi_i^y(H) q_i \right] \right. \\ &\quad \left. - 2u_1 \sum_{i=1}^{v_1} \phi_i^x(H) u_{1+i} + \sum_{i=1}^{v_1} \phi_i^y(H) \dot{u}_{1+i} \right\} \mathbf{a}_2 + \end{aligned}$$

$$\sum_{i=1}^{v_1} \phi_i^z(H) \dot{u}_{1+i} \mathbf{a}_3$$

The acceleration equation for body C was too unwieldy for higher terms to be considered. Therefore, only first-order terms were used to produce

$$\begin{aligned}
 \text{(Eqn. 2.24)} \quad \underline{\ddot{a}}^{NX} = \underline{\ddot{a}}^{NH} + & \left[-\psi_2 u_1^2 x_1 + \psi_1 u_1^2 x_2 + u_1^2 \left(x_3 + \sum_{j=1}^{v_2} \bar{\phi}_j^z \bar{q}_j \right) \right] \underline{a}_3 \\
 & + \left[\psi_2 x_3 - \psi_3 x_2 + u_1 \psi_1 x_3 - u_1^2 \left(x_1 + \sum_{j=1}^{v_2} \bar{\phi}_j^x \bar{q}_j \right) - \psi_3 u_1 x_1 + \right. \\
 & \left. \sum_{j=1}^{v_2} \bar{\phi}_j^x \dot{u}_{1+v_1+j} \right] \underline{a}_1 + \left[-\psi_1 x_3 + \psi_3 x_1 + u_1 \psi_2 x_3 - u_1^2 \left(x_2 + \sum_{j=1}^{v_2} \bar{\phi}_j^y \bar{q}_j \right) \right. \\
 & \left. - \psi_3 u_1 x_2 + \sum_{j=1}^{v_2} \bar{\phi}_j^y \dot{u}_{1+v_1+j} \right] \underline{a}_2 + \left[\psi_1 x_2 - \psi_2 x_1 - u_1^2 \left(x_3 + \sum_{j=1}^{v_2} \bar{\phi}_j^z \bar{q}_j \right) \right. \\
 & \left. - \psi_3 u_1 x_3 + \sum_{j=1}^{v_2} \bar{\phi}_j^z \dot{u}_{1+v_1+j} \right] \underline{a}_3 + \left[\dot{u}_1 \left(x_1 + \sum_{j=1}^{v_2} \bar{\phi}_j^x \bar{q}_j \right) \right. \\
 & \left. + u_1 \psi_2 x_3 - u_1 \psi_3 x_2 + 2u_1 \sum_{j=1}^{v_2} \bar{\phi}_j^x \dot{u}_{1+v_1+j} \right] \underline{a}_1 +
 \end{aligned}$$

$$\left[\dot{u}_1 \left(x_2 + \sum_{j=1}^{v_2} \bar{\phi}_j^y \bar{q}_j \right) - u_1 \psi_1 x_3 + u_1 \psi_3 x_1 \right) + 2u_1 \sum_{j=1}^{v_2} \bar{\phi}_j^z \dot{u}_{1+v_1+j} \right] d_2 + \left[\dot{u}_1 \left(x_3 + \sum_{j=1}^{v_2} \bar{\phi}_j^z \bar{q}_j \right) + u_1 \psi_1 x_2 - u_1 \psi_2 x_1 + 2u_1 \sum_{j=1}^{v_2} \bar{\phi}_j^z \dot{u}_{1+v_1+j} \right) \right] d_3$$

5. Partial Velocities

The generalized partial velocities and angular velocities are assembled in Table 2.1 and Table 2.2. These values and the acceleration equations are the basis of the formulation for the generalized inertia forces.

TABLE 2.1
PARTIAL VELOCITIES OF BODY A AND BODY B

	r	ω _r ^A	v _r ^{A*}	v _r ^B
1	a ₃	-ba ₂	- [P ₂ + ∑ _{i=1} ^{v₁} φ _i ^y q _i]	[P ₁ + ∑ _{i=1} ^{v₁} φ _i ^x q _i]
1 + j	0.	0.	φ _j ^x a ₁ + φ _j ^y a ₂ + φ _j ^z a ₃	
j=1, ..., v ₁				

TABLE 2.2

PARTIAL VELOCITIES OF BODY C

r	ω_r^c	v_r^c
1	a_3	$- \left[H_2 + \sum_{i=1}^{v_1} \phi_i^y(H) q_i \right] a_1 + \left[H_1 + \sum_{i=1}^{v_1} \phi_i^x(H) q_i \right] a_2 +$ $\left(x_1 + \sum_{j=1}^{v_2} \bar{\phi}_j^x \bar{q}_j \right) a_1$
1 + j	$\psi_j^1(H) \Omega_1 +$	$\phi_j^x(H) a_1 + \phi_j^y(H) a_2 + \phi_j^z(H) a_3 +$ $\left[\psi_j^2 \left(x_3 + \sum_{k=1}^{v_2} \bar{\phi}_k^z \bar{q}_k \right) - \psi_j^3 \left(x_2 + \sum_{k=1}^{v_2} \bar{\phi}_k^y \bar{q}_k \right) \right] \Omega_1$ $+ \left[\psi_j^3 \left(x_1 + \sum_{k=1}^{v_2} \bar{\phi}_k^x \bar{q}_k \right) - \psi_j^1 \left(x_3 + \sum_{k=1}^{v_2} \bar{\phi}_k^z \bar{q}_k \right) \right] \Omega_2$ $+ \left[\psi_j^1 \left(x_2 + \sum_{k=1}^{v_2} \bar{\phi}_k^y \bar{q}_k \right) - \psi_j^2 \left(x_1 + \sum_{k=1}^{v_2} \bar{\phi}_k^x \bar{q}_k \right) \right] \Omega_3$
1 + v ₁ + k	0.	$\phi_k^x \Omega_1 + \phi_k^y \Omega_2 + \phi_k^z \Omega_3$
k=1, ..., v ₂		

6. Generalized Inertia Forces

a. Generalized Inertia Force of Body A

The generalized inertia force for body A is comprised of two parts. the first is due to the moment of inertia of body A's mass center about the a_3 axis. The second is due to the inertial force of body A's mass center.

$$(Eqn. 2.25) \quad {}^A F_1^* = \underline{\omega}_r^A \cdot \begin{pmatrix} -J_3 \dot{\alpha} \\ \alpha \end{pmatrix} - m_A \underline{v}_r^{A*} \cdot \underline{\ddot{a}}^{NA*}$$

where J_3 is the moment of inertia of A^* and m_A is the mass of body A.

Using the values of $\underline{\omega}_r^A$ and \underline{v}_r^{A*} from Table 2.1, the generalized inertia

force of body A is

$$(Eqn. 2.26) \quad {}^A F_1^* = J_3 \dot{u}_1 - m_A b^2 \dot{u}_1$$

There is only one equation since body A is rigid and displays only rotational motion.

b. Generalized Inertia Forces of Body B

Body B is a continuous elastic beam with a mass per unit length of p . Thus, the generalized inertia equations are an integration along the length of the beam

$$(Eqn. 2.27) \quad {}^B F_r^* = - \int_0^H (\underline{v}_r^B \cdot \underline{N}^P) p dx$$

The result is an equation for the large motion and one equation for each deformable degree of freedom of body B.

The large motion equation incorporates only first-order terms, while the small motion equation neglects third-order or higher terms.

$$\begin{aligned}
\text{(Eqn. 2.28) } B_{F_1}^* &= - \int_0^H \dot{u}_1 \left\{ P_1^2 + P_2^2 + 2P_1 \sum_{i=1}^{V_1} \phi_i^x q_i + 2P_2 \sum_{i=1}^{V_1} \phi_i^y q_i \right\} \\
&+ \sum_{i=1}^{V_1} \dot{u}_{1+i} \left\{ P_1 \phi_i^y - P_2 \phi_i^x \right\} + 2u_1 \sum_{i=1}^{V_1} u_{1+i} \left\{ P_1 \phi_i^x + P_2 \phi_i^y \right\} p dx \\
B_{F_{1+j}}^* &= - \int_0^H \dot{u}_1 \left\{ \phi_j^y \left(P_1 + \sum_{i=1}^{V_1} \phi_i^x q_i \right) - \phi_j^x \left(P_2 + \sum_{i=1}^{V_1} \phi_i^y q_i \right) \right\} \\
&+ \sum_{i=1}^{V_1} \dot{u}_{1+i} \left\{ \phi_j^x \phi_i^x + \phi_j^y \phi_i^y + \phi_j^z \phi_i^z \right\} - u_1^2 \left\{ P_1 \phi_j^x + P_2 \phi_j^y + \sum_{i=1}^{V_1} q_i \right. \\
&\left. \left(\phi_j^x \phi_i^x + \phi_j^y \phi_i^y \right) \right\} + 2u_1 \sum_{i=1}^{V_1} \dot{u}_{1+i} \left\{ \left(\phi_j^y \phi_i^x - \phi_j^x \phi_i^y \right) \right\} p dx
\end{aligned}$$

c. Generalized Inertia Forces of Body C

Body C was modelled with lumped masses at 63 grid points. Therefore, the generalized inertia equations consist of a summation of the acceleration dotted with the generalized partial velocity times the mass

$$\text{(Eqn. 2.29) } c_{F_r}^* = \sum_{x=0}^{L_2} \left(\underline{v}_r^c \cdot \underline{a}^{NX} \right) m_x^c$$

There are $1 + \nu_1 + \nu_2$ equations of motion for body C. Again, the large motion equation has only first-order terms and the subsequent small motion equations neglect third-order and higher terms.

(Eqn. 2.30)

$$\begin{aligned}
 {}^C F_1^* = & \sum_{x=0}^{L_2} \dot{u}_1 \left\{ H_1^2 + H_2^2 + x_1^2 + x_2^2 + 2(H_1 + x_1) \left(\sum_{i=1}^{\nu_1} \phi_i^x(H) q_i \right) + \sum_{j=1}^{\nu_2} \bar{\phi}_j^x \bar{q}_j \right. \\
 & + 2(H_2 + x_2) \left(\sum_{i=1}^{\nu_1} \phi_i^y(H) q_i + \sum_{j=1}^{\nu_2} \bar{\phi}_j^y \bar{q}_j \right) + 2x_1 H_1 + 2x_2 H_2 - \\
 & \left. 2\psi_1 x_3 (H_2 + x_2) + 2\psi_2 x_3 (H_1 + x_1) + 2\psi_3 (H_2 x_1 - H_1 x_2) \right\} + \\
 & \sum_{i=1}^{\nu_1} \dot{u}_{1+i} \left\{ -\phi_i^x(H)(H_2 + x_2) + \phi_i^y(H)(H_1 + x_1) - \psi_i^1 x_3 (H_1 + x_1) - \right. \\
 & \left. \psi_i^2 (H_2 + x_2) + \psi_i^3 [x_1(x_1 + H_1) + x_2(x_2 + H_2)] \right\} + \\
 & \sum_{j=1}^{\nu_2} \dot{u}_{1+i\nu_1+j} \left\{ -\bar{\phi}_j^x(H_2 + x_2) + \bar{\phi}_j^y(H_1 + x_1) \right\} - 2u_1 \left\{ \sum_{i=1}^{\nu_1} \dot{u}_{1+i} \right. \\
 & \left[\phi_i^x(H)(H_1 + x_1) + \phi_i^y(H)(H_2 + x_2) + x_3 \psi_i^1 (H_2 + x_2) - \right. \\
 & \left. \left. x_3 \psi_i^2 (H_1 + x_1) + \psi_i^3 (H_1 x_2 - x_1 H_2) \right] \right\} +
 \end{aligned}$$

$$\left. \sum_{j=1}^{V_2} \dot{u}_{1+V_1+j} \left[-\bar{\phi}_j^x (H_1+x_1) - \bar{\phi}_j^y (H_2+x_2) \right] \right\} m_x^c$$

$$\begin{aligned} c_{F_{1+j}}^* = & - \sum_{x=0}^{L_2} \dot{u}_1 \left\{ \phi_j^x(H) \left(\psi_1 x_3 - \psi_3 x_1 - H_2 - x_2 - \sum_{i=1}^{V_1} \phi_i^y(H) q_i - \sum_{k=1}^{V_2} \bar{\phi}_k^y \bar{q}_k \right) \right. \\ & + \phi_j^y(H) \left(\psi_2 x_3 - \psi_3 x_2 + H_1 + x_1 + \sum_{i=1}^{V_1} \phi_i^x(H) q_i + \sum_{k=1}^{V_2} \bar{\phi}_k^x \bar{q}_k \right) \\ & + \left(\psi_j^3 x_2 - \psi_j^2 x_3 \right) \left(-\psi_3 H_1 - \psi_1 x_3 + H_2 + x_2 + \sum_{i=1}^{V_1} \phi_i^y(H) q_i + \sum_{k=1}^{V_2} \bar{\phi}_k^y \bar{q}_k \right) \\ & + \left(\psi_j^3 x_1 - \psi_j^1 x_3 \right) \left(-\psi_3 H_2 + \psi_2 x_3 + H_1 + x_1 + \sum_{i=1}^{V_1} \phi_i^x(H) q_i + \sum_{k=1}^{V_2} \bar{\phi}_k^x \bar{q}_k \right) \\ & + \left(\psi_j^2 x_1 - \psi_j^1 x_2 \right) (\psi_1 (H_1 + x_1) + \psi_2 (H_2 + x_2)) \\ & + \left(\psi_j^3 \sum_{k=1}^{V_2} \bar{\phi}_k^y \bar{q}_k - \psi_j^2 \sum_{k=1}^{V_2} \bar{\phi}_k^z \bar{q}_k \right) (H_2 + x_2) + \left(\psi_j^3 \sum_{k=1}^{V_2} \bar{\phi}_k^x \bar{q}_k \right) \end{aligned}$$

$$\begin{aligned}
& (H_1 + x_1) \left\{ + \sum_{i=1}^{v_1} \dot{u}_{1+i} \left\{ \phi_j^x(H) \left(\phi_i^x(H) + \psi_i^2 x_3 - \psi_i^3 x_2 \right) \right. \right. \\
& + \phi_j^y(H) \left(\phi_i^y(H) - \psi_i^1 x_3 + \psi_i^3 x_1 \right) + \phi_j^z(H) \left(\phi_i^z(H) + \psi_i^1 x_2 - \psi_i^2 x_1 \right) \\
& + \left(\psi_j^2 x_3 - \psi_j^3 x_2 \right) \left(\phi_i^x(H) + x_3 \psi_i^2 - x_2 \psi_i^3 \right) + \left(\psi_j^3 x_1 - \psi_j^1 x_3 \right) \\
& \left. \left. \left(\phi_i^y(H) - \psi_i^1 x_3 + \psi_i^3 x_1 \right) \right\} \left(\psi_j^1 x_2 + \psi_j^2 x_1 \right) \left(\phi_i^z(H) + \psi_i^1 x_2 - \psi_i^2 x_1 \right) \right\} \\
& + \sum_{k=1}^{v_2} \dot{u}_{1+v_1+k} \left\{ \bar{\phi}_k^x \left(\phi_j^x(H) + \psi_j^2 x_3 - \psi_j^3 x_2 \right) \right. \\
& \left. + \bar{\phi}_k^y \left(\phi_j^y(H) + \psi_j^3 x_1 - \psi_j^1 x_3 \right) + \bar{\phi}_k^z \left(\phi_j^z(H) + \psi_j^1 x_2 - \psi_j^2 x_1 \right) \right\}
\end{aligned}$$

$$\begin{aligned}
& -u_1^2 \left\{ \phi_j^x(H) \left[H_1 + x_1 + \sum_{i=1}^{v_1} \phi_i^x(H) q_i + \sum_{k=1}^{v_2} \bar{\phi}_k^x(H) \bar{q}_k - \psi_3 x_2 + \psi_2 x_3 \right] \right. \\
& \phi_j^y(H) \left[H_2 + x_2 + \sum_{i=1}^{v_1} \phi_i^y(H) q_i + \sum_{k=1}^{v_2} \bar{\phi}_k^y \bar{q}_k - \psi_1 x_3 + \psi_3 x_1 \right] \\
& \left. + \left[\psi_j^2 x_3 - \psi_j^3 x_2 \right] \left[H_1 + x_1 + \sum_{i=1}^{v_1} \phi_i^x(H) q_i + \sum_{k=1}^{v_2} \bar{\phi}_k^x \bar{q}_k + H_2 \psi_3 + x_3 \psi_2 \right] \right\}
\end{aligned}$$

$$+ \left[\psi_j^3 x_1 - \psi_j^1 x_3 \right] \left[H_2 + x_2 + \sum_{i=1}^{v_1} \phi_i^y(H) q_i + \sum_{k=1}^{v_2} \bar{\phi}_k^y \bar{q}_k + \psi_1 x_3 - H_1 \psi_3 \right]$$

$$+ \left[\psi_j^1 x_2 - \psi_j^2 x_1 \right] [\psi_2(H_1 + x_1) - \psi_1(H_2 + x_2)] + \left[\psi_j^2 \sum_{k=1}^{v_2} \bar{\phi}_k^z \bar{q}_k - \right.$$

$$\left. \psi_j^3 \sum_{k=1}^{v_2} \bar{\phi}_k^y \bar{q}_k \right] [H_1 + x_1] + \left[\psi_j^3 \sum_{k=1}^{v_2} \bar{\phi}_k^x \bar{q}_k - \psi_j^1 \sum_{k=1}^{v_2} \bar{\phi}_k^z \bar{q}_k \right] [H_2 + x_2] \left. \right\}$$

$$- 2u_1 \left\{ \sum_{i=1}^{v_1} u_{1+i} \left\langle \phi_j^x(H) \left(\phi_i^y(H) + \psi_i^3 x_1 - \psi_i^1 x_3 \right) \right\rangle \phi_j^y(H) \right.$$

$$\left(\phi_i^x(H) + \psi_i^2 x_3 - \psi_i^3 x_2 \right) + \phi_j^z(H) \left(.5 \psi_i^3 x_3 \right) + \left(\psi_j^2 x_3 - \psi_j^3 x_2 \right)$$

$$\left(\phi_i^y(H) - \psi_i^1 x_3 + \psi_i^3 x_1 \right) + \left(\psi_j^1 x_3 - \psi_j^3 x_1 \right) \left(\phi_i^x(H) + \psi_i^2 x_3 + \psi_i^3 x_2 \right) +$$

$$\left(\psi_j^2 x_1 - \psi_j^1 x_2 \right) \left(.5 \psi_i^3 x_3 \right) \left. \right\rangle + \sum_{k=1}^{v_2} u_{1+v_1+k} \left\langle -\bar{\phi}_k^x \left(\phi_j^y(H) + \psi_j^3 x_1 - \psi_j^1 x_3 \right) \right.$$

$$\left. + \bar{\phi}_k^y \left(\phi_j^x + \psi_j^2 x_3 - \psi_j^3 x_2 \right) \right\rangle \left. \right\}$$

(Eqn. 2.31)

$$\begin{aligned}
 C_{F_{1+v_1+k}}^* &= \sum_{x=0}^{L_2} \dot{u}_1 \left\{ \bar{\phi}_k^x \left[\psi_3 H_1 + \psi_1 x_3 - H_2 - x_2 - \sum_{i=1}^{v_1} \phi_i^y(H) q_i - \sum_{j=1}^{v_2} \bar{\phi}_j^y \bar{q}_j \right] \right. \\
 &+ \bar{\phi}_k^y \left[\psi_3 H_2 + \psi_2 x_3 + H_1 + x_1 + \sum_{i=1}^{v_1} \phi_i^x(H) q_i + \sum_{j=1}^{v_2} \bar{\phi}_j^x \bar{q}_j \right] \\
 &- \bar{\phi}_k^z [\psi_1(x_1 + H_1) + \psi_2(x_2 + H_2)] \left. \right\} + \sum_{i=1}^{v_1} \dot{u}_{1+i} \left\{ \bar{\phi}_k^x \left[\psi_i^2 x_3 - \psi_i^3 x_2 + \phi_i^x(H) \right] \right. \\
 &+ \bar{\phi}_k^y \left[\phi_i^y(H) - \psi_i^1 x_3 + \psi_i^3 x_1 \right] + \bar{\phi}_k^z \left[\phi_i^z(H) + \psi_i^1 x_2 - \psi_i^2 x_1 \right] \left. \right\} + \\
 &\sum_{j=1}^{v_2} \dot{u}_{1+v_1+k} \left[\bar{\phi}_j^x \bar{\phi}_k^x + \bar{\phi}_j^y \bar{\phi}_k^y + \bar{\phi}_j^z \bar{\phi}_k^z \right] - u_1^2 \left\{ \bar{\phi}_k^x \left[H_1 + \sum_{i=1}^{v_1} \phi_i^x(H) q_i \right. \right. \\
 &+ \psi_3 H_2 + \psi_2 x_3 + x_1 + \sum_{j=1}^{v_2} \bar{\phi}_j^x \bar{q}_j \left. \right] + \bar{\phi}_k^y \left[H_2 + \sum_{i=1}^{v_1} \phi_i^y(H) q_i - \psi_3 H_1 - \right. \\
 &\left. \psi_1 x_3 + x_2 + \sum_{j=1}^{v_2} \bar{\phi}_j^y \bar{q}_j \right] \bar{\phi}_k^z [-\psi_1(H_2 + x_2) + \psi_2(H_1 + x_1)] \left. \right\} \\
 &- 2u_1 \left\{ \sum_{i=1}^{v_1} u_{1+i} \left[\phi_i^y(H) \bar{\phi}_k^x - \phi_i^x(H) \bar{\phi}_k^y + \bar{\phi}_k^x (\psi_i^3 x_1 - \psi_i^1 x_3) \right] \right. +
 \end{aligned}$$

$$\bar{\phi}_k^y \left(\psi_i^3 x_2 - \psi_i^2 x_3 \right) \cdot 5 \bar{\phi}_k^z \psi_i^3 x_3 \left] + \sum_{j=1}^{v_2} \dot{u}_{1+v_1+j} \left[\bar{\phi}_k^x \bar{\phi}_k^y - \bar{\phi}_k^y \bar{\phi}_k^x \right] \right\} m_x^c$$

7. Generalized Active Forces

The generalized active forces are derived from the forces exerted on the differential elements. Only the internal elastic forces and the external forces were considered in this formulation. Rotation of the individual beam elements was neglected.

The equation for the generalized internal forces is of the form

$$(Eqn. 2.32) \quad F_r^I = \int_0^H v_r^B \cdot df^B + \sum_{x=0}^{L_2} v_r^C \cdot df^C$$

where df consists of internal axial and shear forces.

The shear force portion of df for the beam is

$$(Eqn. 2.33) \quad df_{shear} = \frac{a^2}{ax^2} \left(EI \frac{a^2 y}{ax^2} \right) dx \ a_2$$

$$\text{where } y = \sum_{j=1}^{v_1} \phi_j^y q_j$$

The axial force portion of df for the beam is

$$df_{axial} = AE \frac{a^2 u}{ax^2} dx \ a_1$$

$$\text{where } u = \sum_{j=1}^{v_1} \phi_j^x q_j$$

When these differential forces are dotted with the generalized partial velocity and then integrated by parts, the remaining terms are simply the forces due to strain energy.

The generalized internal forces are reduced to

$$(Eqn. 2.34) \quad F_{1+j}^I = -B\omega_j^Z M_j^B q_j$$

The external force on the boom was the torque applied about a_3 axis at point Q, the fixed end of the boom. This torque was dotted with the generalied partial angular velocity to produce

$$(Eqn. 2.35) \quad F_1^E = T_A$$

For the reflector dish, it was assumed that the strain energy would account for the internal forces and no external forces were applied to the reflector.

Thus, the generalized active forces for the reflector are

$$(Eqn. 2.36) \quad F_{1+v_1+k}^I = -C\omega_j^2 M_k^C \bar{q}_k$$

8. Final Equations

The equations of Sections B.6 and B.7 were gathered to obtain the following equations:

$$(Eqn. 2.37) \quad AF_1^* + BF_1^* + CF_1^* + F\xi = 0$$

$$(Eqn. 2.38) \quad BF_{1+j}^* + BF_{1+j}^* + CF_{1+j}^* = 0 \quad j = 1, \dots, v_1$$

$$(Eqn. 2.39) \quad CF_{1+v_1+k}^* + BF_{1+v_1+k}^* = 0 \quad k = 1, \dots, v_2$$

The orthogonality condition for the boom is:

$$(Eqn. 2.40) \quad \int_0^H \phi_i^x \phi_j^x + \phi_i^y \phi_j^y + \phi_i^z \phi_j^z \rho dx +$$

$$\sum_{x=0}^{L_2} \left[\phi_i^x(H) \phi_j^x(H) + \phi_i^y(H) \phi_j^y(H) + \phi_i^z(H) \phi_j^z(H) \right] m_x^c$$

$$\begin{aligned}
 &= B M_j & i = j \\
 &= 0 & i \neq j
 \end{aligned}$$

and for the reflector:

$$\begin{aligned}
 \text{(Eqn. 2.41)} \quad \sum_{x=0}^{L_2} \left[\bar{\phi}_i^x \bar{\phi}_j^x + \bar{\phi}_i^y \bar{\phi}_j^y + \bar{\phi}_i^z \bar{\phi}_j^z \right] m_x^C &= c m_j & i = j \\
 &= 0 & i \neq j
 \end{aligned}$$

These conditions were incorporated into the final equations to reduce the number of terms in the final equations.

III. COMPUTER IMPLEMENTATION

A. INTRODUCTION

Computer implementation to solve these equations of motion involved three stages. Modal analysis was conducted using the NASA Structural Analysis (NASTRAN). NASTRAN is a general-purpose digital computer program for the analysis of various structures [Ref. 7]. NASTRAN provided values for the natural frequencies, mode shapes, and generalized modal masses for the two flexible bodies.

The data was transferred and read into an IBM/VS FORTRAN program. Constants were calculated in this program, which then were inserted into the initial stage of a Dynamic Simulation Language (DSL) program. DSL is a digital simulation for continuous systems [Ref. 8]. DSL was used to solve the simultaneous differential equations.

B. MODAL ANALYSIS

A multibody dynamic analysis requires special consideration of the boundary conditions. For the boom, one end was fixed and the other end was free with a tip mass attached. The tip mass was equal to the total mass of the reflector. The mode shapes, natural frequencies, and generalized masses were calculated using 17 grid points (Figure A.6). Figures A.7, A.8, A.9, and A.10 depict the first four modes of the boom.

The reflector was represented by 63 grid points (Figure A.1). Various links between grid points were constrained from rotating and the hinge point (Grid 63) was fixed. Figures A.2, A.3, A.4, and A.5 depict the first four modes of the reflection.

Ten modes were generated by NASTRAN for each body. A preliminary analysis between two, three, four, and five modes for each body was conducted. Four modes was

chosen for the final analysis because minimal changes occurred between the four- and five-mode cases.

Modified Given's method (MGIV) was used to conduct the modal analysis of the boom and the reflector. The generalized mass was normalized to equal one simplifying the equations.

The natural frequencies for the boom and two cases of the reflector are tabulated in Table 3.1. In the results section, the effects of reflector flexibility are discussed. The NASTRAN programs are shown in Appendix E.

TABLE 3.1
REAL EIGENVALUES

Mode	Boom Natural Frequency (cycles)	Reflector 1 Natural Frequency (cycles)	Reflector 2 Natural Frequency (cycles)
1	.71674	2.0937	1.1635
2	.78059	12.469	6.9084
3	2.624	15.929	14.32
4	4.723	15.929	14.342

C. EVALUATION OF TIME CONSTANTS

Two files were transferred to the IBM/VS computer. Both files contained ten modes of data for one of the bodies. All ten modes are read into a FORTRAN program, but the number of modes used to calculate constants was varied by a parameter statement in the beginning of the program. This strategy provided easier formatting to read in the data,

while still generalizing the program and making the computations more efficient. The program is shown in Appendix E.

The equations of motion were systematically evaluated to identify terms that depended on position alone and were repeated several times. These terms were isolated from the time-dependent terms. Subroutines were written to calculate these position terms and were called immediately after reading in the mode shape data. The main program consisted of multiplications and additions between system constants and the subroutine outputs, since the subroutines carried out the required position integrations or summations.

The reason for having separate programs is that all the position calculations can be completed beforehand. Thus, the DSL program need only be concerned with time step calculations. The number of constants and their dimensions depended on the DSL implementation and will be discussed in that section.

D. DSL IMPLEMENTATION

With the separate FORTRAN program to evaluate the time constants, the DSL program is relatively simple. The equations of motion are put in the form

$$[A] \dot{\underline{u}} = \underline{B}$$

where $[A]$ is a matrix of the coefficients of the acceleration terms (the left-hand side of the equations of motion), while \underline{B} is a vector of all other terms (the right-hand side of the equations of motion).

These coefficients were supplied by the FORTRAN program. The A matrix and B vector were assembled in the derivative section of the DSL program. Two subroutines from LINPACK were called to decompose the A matrix and solve the matrix equation. DGEFA uses gaussian elimination to decompose A and DGESL solves the matrix equation.

DSL provided many alternatives to solve a time-stepping problem for simultaneous differential equations. A Runge-Kutta fifth-order method with variable step size was selected because it was self-starting, stable, and accurate. Although other methods may have been more efficient computationally, accuracy was a primary selection criterion. The program is shown in Appendix E.

The results were printed out in a file and plotted using the TEK618. Plotting was accomplished via the GRAFAEL command, which is a particularly powerful accessory of the DSL program.

IV. RESULTS

Three parameters of the LFMR system were varied in the computer simulation to investigate the effects of these parameters on pointing error of the LFMR system during a spin-up procedure. Deflections and slope changes at the boom tip (grid point 63) and grid points 1 and 4 of the reflector were compared for this purpose. The locations of these grid points are shown in Figure 4.1. The first analysis compared the effects of changing the reflector flexibility, while the boom properties remained the same. The second analysis compared vibrational amplitudes of three cases with different in-plane orientation of the reflector. These orientations were accomplished by lining up the a_1, a_2, a_3 coordinate system with the C_1, C_2, C_3 coordinate system and rotating the C_1 and C_3 axes about the a_2 axis to the desired angle. The third analysis compared the case of a particular in-plane orientation (-155° case) with the case of the same in-plane orientation plus slight out-of-plane tilt ($+5^\circ$). The out-of-plane orientation was achieved by rotating the reflector about the a_3 axis.

The same spin-up procedure was used in all computer simulation runs and the torque applied to the LFMR system during the spin-up procedure is shown in Figure 4.2.

A. MATERIAL PROPERTIES AND PARAMETERS

The material used to model the boom and reflector is Isotropic Graphite-Epoxy Composite (T300/5208 (0/90/45/-45)_s) [Ref. 9]. The inertia property of the electronics box was obtained, assuming it to be a uniform two-foot cubic body. The properties of the boom and reflectors are presented in Table 4.1. Reflector 1 is the baseline design of the reflector used throughout the analyses. Reflector 2 is a more flexible model of the reflector

and was used in the reflector flexibility analysis. The geometric parameters for the boom and two models of the reflectors are given in Table 4.2.

TABLE 4.1
BOOM AND REFLECTOR PROPERTIES

Property	Boom	Reflector 1	Reflector 2
Modulus of elasticity (E)	10.1E + 6 psi	10.1E + 6 psi	10.1E + 6 psi
Poisson's Ratio (ν)	.25	.25	.25
x-sectional area (A)	1.1868 in ²	.1425 in ²	.1425 in
Inner diameter Rod element (d_1)	2.5 in	1.04859 in	.8177 in
Outer diameter rod element (d_2)	3.0 in	1 in	.75 in
Thickness of rod element	.5 in	.04859 in	.0677 in
Mass per unit length (ρ)	1.522 E-4 slugs/in ³	1.522 E-4 slugs/in ³	1.522 E-4 slugs/in ³
Area moment of inertia (A)	1.2231 in ⁴	.0165 in ⁴	.00853 in ⁴

TABLE 4.2
GEOMETRIC PARAMETERS

Parameter	
l_1 : length of lower boom	162 in
l_2 : length of upper boom	126 in
α : angle between l_1 and a_3 axis	34.5°
β : angle between l_1 and l_2	98.76°
M_A : weight of electronics box	50 lb
M_C : weight of reflector	37.5 lb

B. EFFECTS OF THE REFLECTOR FLEXIBILITY

Two cases of reflector flexibility were chosen for comparison. As shown in Table 4.1, Reflector 1 was stiffer than Reflector 2. The difference in the angular velocity is shown in Figures B.1 and B.2. Greater amplitude oscillations occur after the applied torque is removed for the more flexible reflector. This effect is due to larger vibrations of the more flexible reflector (Reflector 2).

The fourth generalized coordinate ($Q_4(t)$) of the boom was chosen to represent the reflector flexibility effects on the boom's generalized coordinates. Figures B.3 and B.4 depict this boom generalized coordinate for the two cases. They show a definite dynamic interaction between the boom and reflector. The more flexible reflector displayed greater

fluctuations in the boom generalized coordinate, which translated into greater vibrations at the boom tip. The vertical deflections of the boom tip are shown in Figures B.7 and B.8.

The third reflector generalized coordinate ($Q_3(t)$) was chosen to represent the effects of reflector flexibility on the reflector's generalized coordinates. Comparison of Figures B.5 and B.6 shows a negative shift in the graph of the more flexible reflector. The amplitude of the reflector generalized coordinate is unchanged.

The rotational vibrations about the vertical axis are compared in Figures B.9 and B.10. The more flexible reflector caused greater amplitude rotational vibration at the boom tip.

C. EFFECTS OF IN-PLANE ORIENTATION CHANGES

As mentioned previously, cases of different in-plane orientations between the reflector and the boom were analyzed: Three cases of angle rotations about the a_2 axis were compared: -135° , -145° , and -155° . The angular displacement for these three orientations is shown in Figures C.1-3. The angular displacements oscillated after the applied torque was set to zero. An increasing amplitude trend in angular displacements was apparent as the orientation was a less negative angle.

The horizontal deflection at the boom tip represents the effects of reflector orientation on the boom. Figures C.4-6 show that greater amplitude vibration occurred for the case of -135° reflector orientation in the horizontal direction.

The rotations at the boom tip about the horizontal axis are shown in Figures C.7-9. Greater fluctuations occurred for the -135° orientation. The larger amplitude results for the case of -135° orientation is due to the location of the center of mass of the reflector. The radius of rotation is larger for the -135° orientation. Thus, the moment of inertia is increased.

The reflector orientation also affects the reflector vibration. Figures 3.10-12 show the horizontal displacement of grid point 1. Higher frequency components appear in the -155° case, but the greater amplitude vibrations occur in the -135° case.

D. EFFECT OF OUT-OF-PLANE ORIENTATION OF REFLECTOR

The case of -155° in-plane orientation of the reflector is compared to the case with the same 155° in-plane rotation plus a 5° tilt out of plane. The first boom generalized coordinate ($Q_1(t)$) was the only boom coordinate affected by the tilt out of plane. The tilt produced a positive shift in ($Q_1(t)$) value as shown in Figures D.1 and D.2. The oscillations were same in amplitude.

The fourth reflector generalized coordinate ($Q_4(t)$) was chosen to represent the effect of the out-of-plane orientation on the reflector generalized coordinates. Figures D.3 and D.4 show that vibrations with larger amplitude appeared for the out-of-plane orientation.

The out-of-plane orientation deflections for the boom and reflector were the most affected by the out-of-plane tilt of the reflector. Figures D.5 and D.6 show the effects at the boom tip. The first boom generalized coordinate was the predominant component resulting in a positive shift in the out-of-plane displacement of the boom. Figures D.7 and D.8 show the effects at grid point 4 with the first boom generalized coordinate producing a positive shift. The reflector generalized coordinates produced a larger amplitude vibration for the out-of-plane rotation.

V. CONCLUSIONS AND RECOMMENDATIONS

A. CONCLUSIONS

The purpose of this research was to develop a realistic model of the LFMR sensor system. This goal was successfully met by applying Kane's method to a multibody model. Efficient computer simulation was achieved. The programs were general enough to use up to ten modes for each body, but the results indicate that superimposition of four modes for each body was sufficient.

The flexibility of the reflector did affect the vibration of the boom and was related to pointing error. The multibody system allowed the effects of reflector flexibility to be investigated without reanalyzing the entire system.

The program also applied easily to different orientations of the reflector. Modal analysis did not have to be repeated as in the case of a single-body model.

B. RECOMMENDATIONS

Application of this research could include a study of the effects of a full range of different configurations on the system dynamics. Also, damping effects can easily be incorporated in this work to study the dynamic interaction of each subsystem. Extension of this research could include a study of the effects of a flexible body connected to the spacecraft's main body on three-dimensional motion and control.

APPENDIX A

MODAL ANALYSIS OF REFLECTOR AND BOOM

Figures A.1 through A.10 show the undeformed as well as the first four mode shapes of the reflector and boom. The figures are on pages 84-93.

APPENDIX B

REPRESENTATIVE EFFECT OF REFLECTOR FLEXIBILITY

Figures B.1 through B.10 show representative effects of two different reflector flexibilities on the dynamic response of the system. The figures are on pages 96-105.

APPENDIX C

REPRESENTATIVE EFFECT OF IN-PLANE REFLECTOR ROTATION

Figures C.1 through C.12 show representative effects of three different in-plane orientations of the reflector on the dynamic response of the system. The figures are on pages 106-117.

APPENDIX D

REPRESENTATIVE EFFECT OF OUT-OF-PLANE REFLECTOR ROTATION

Figures D.1 through D.8 show representative effects of an out-of-plane orientation of the reflector on the dynamic response of the system. The figures are on pages 118-125.

APPENDIX E

PROGRAMS

```
id nastran Natalie
sol 3
time 500
cend
title=Nomal Mode Analysis of LFMR Boom
subtitle=Research on N-ROSS DYNAMICS
method=10
displacement=all
spc=100
output(plot)
set 1 = all
origin 5,0.,0.
axes y,z,x
view -30.,20.,0.
ptitle=Undeformed Boom
find scale,origin 5,set 1
plot set 1,label grid
ptitle=Mode Shape
maximum deformation 15
find scale,origin 5,set 1
plot modal,deformation,0,1 THRU 10,set 1,pen 4,shape
begin bulk
$
$EIGR,sid,METHOD,f1,f2,ne,nd,,+,
$  +,NORM,g,c
$
eigr,10,MGIV,0.0,100.0,,10
$
$CORD2C,cid,rid,a1,a2,a3,b1,b2,b3,+
$  +,c1,c2,c3
$
cord2r,1,,0.,0.,0.,0.,0.,1.,+2r
+2r,1.,0.,1.
$
$GRID,id,cp,x1,x2,x3,cd,ps,seid
$
grid,1,1,0.,0.,0.
=,*(1),=,*(10.1953),=,*(14.83427),== $
=7
grid,10,1,91.75781,0.,133.5084
=,*(1),=,*(-13.1085),=,*(12.3356),== $
=6
grid,18,1,0.,0.,100.
$
$CBEAM,eid,pid,ga,gb,g0/x1,x2,x3
$
cbeam,1,3,1,2,18
=,*(1),=,*(1),*(1),== $
#14
```

```
$
$
$PBEAM,pid,mid1,A,I1,I2,J,nsm
$
pbeam,3,1,1.1868,1.2231,1.2231,,2.4462

$MAT1,mid,E,G,Nu,Rho,A,Tref,Ge
$
$ A = Thermal Expan. Coef.
$ Tref = Ref. Temp.
$ Ge = Damping Coef. (= 2 x C/Co )
$
mat1,1,101.+5,,0.25,1522.-7
$
$CONM2,eid,g,cid,m,x1,x2,x3,,+
$ +,I11,I21,I31,I32,I33
$
conm2,50,17,1.9.4502-2
$
spc1,100,123456,1,18
$
enddata
```

```

id nastran Natalie
sol 3
time 500
cend
title=Nomal Mode Analysis of LFMR Reflector
subtitle=Research on N-ROSS DYNAMICS
method=10
displacement=all
spc=100
output(plot)
set 1 = all
origin 5,0.,0.
axes z,x,y
view 34.27,-23.17,0.
ptitle=Undeformed Reflector
find scale,origin 5,set 1
plot set 1,label grid
ptitle=Mode Shape
maximum deformation 15
find scale,origin 5,set 1
plot modal,deformation,1 THRU 10,set 1,pen 4,shape
begin bulk
$
$EIGR,sid,METHOD,f1,f2,ne,nd,,+,
$   +,NORM,g,c
$
eigr,10,MGIV,0.0,100.0,,10
$
SCORD2C,cid,rid,a1,a2,a3,b1,b2,b3,+
$   +,c1,c2,c3
$
cord2r,1,,0.,0.,0.,0.,0.,1.,+2r
+2r,1.,0.,1.
cord2c,2,1,0.,0.,0.,0.,0.,1.,+ab
+ab,10.,0.,10.
$
$GRID,id,cp,x1,x2,x3,cd,ps,seid
$
grid,1,2,116.81,15.,40.83
=,*(1),=,*(30.),== $
=10
grid,13,2,89.26,15.,36.71
=,*(1),=,*(30.),== $
=10
grid,25,2,60.86,15.,32.45
=,*(1),=,*(30.),== $
=10
grid,37,2,31.5,15.,30.13
=,*(1),=,*(30.),== $
=10
grid,49,2,63.8,15.,4.72
=,*(1),=,*(30.),== $
=10
grid,61,1,0.,0.,31.67

```

```

grid,62,1,0.,0.,27.65
grid,63,1,0.,0.,0.
grid,64,1,0.,0.,50.
grid,65,2,50.,0.,0.
$
$CBEAM,eid,pid,ga,gb,g0/x1,x2,x3
$
cbeam,1,1,1,13,64
=,*(1),=,*(1),*(1),== $
=10
cbeam,13,1,13,25,64
=,*(1),=,*(1),*(1),== $
=10
cbeam,25,1,25,37,64
=,*(1),=,*(1),*(1),== $
=10
cbeam,37,1,37,62,64
=,*(1),=,*(1),== $
=10
cbeam,49,2,63,62,65
cbeam,50,2,62,61,65
$
crod,1,10,25,49
=,*(1),=,*(1),*(1),== $
=10
crod,13,11,1,49
=,*(1),=,*(1),*(1),== $
=10
crod,25,11,25,63
=,*(1),=,*(1),== $
=10
crod,37,11,49,63
=,*(1),=,*(1),== $
=10
crod,49,11,1,2
=,*(1),=,*(1),*(1),== $
=9
crod,60,11,12,1
crod,61,11,13,14
=,*(1),=,*(1),*(1),== $
=9
crod,72,11,24,13
crod,73,11,25,26
=,*(1),=,*(1),*(1),== $
=9
crod,84,11,36,25
crod,85,11,37,38
=,*(1),=,*(1),*(1),== $
=9
crod,96,11,48,37
crod,97,11,25,50
=,*(1),=,*(1),*(1),== $
=9
crod,108,11,36,49

```

```

crod,109,11,49,26
=,*(1),=,*(1),*(1),== $
=9
crod,120,11,60,25
$
$PBEAM,pid,mid1,A,I1,I2,J,nsm
$
pbeam,1,,C,0.1452,0.01647,0.01647,,0.03295
pbeam,2,1,3.927,3.1907,3.1907,,6.3814
prod,10,1,0.03286,1.882-3,1.0
prod,11,1,0.01094,1.911-5,1.0
$
$MAT1,mid,E,G,Nu,Rho,A,Tref,Ge
$
$ A = Thermal Expan. Coef.
$ Tref = Ref. Temp.
$ Ge = Damping Coef. (= 2 x C/Co )
$
mat1,1,101,+5,,0.25,1522,-7
$
$CONM2,eid,g,cid,m,x1,x2,x3,,+
$ +,I11,I21,I31,I32,I33
$
conm2,1,1,2,0.4562-3
=,*(1),*(1),== $
=10
conm2,13,13,2,0.5432-3
=,*(1),*(1),== $
=10
conm2,25,25,2,0.4122-3
=,*(1),*(1),== $
=10
conm2,37,37,2,0.4438-3
=,*(1),*(1),== $
=10
conm2,49,62,1,0.626-2
conm2,50,63,1,0.649-2
$
spc1,100,123456,63 thru 65
$
enddata

```

```

*****
*
*   THIS PROGRAM IS DESIGN TO READ IN MODAL INFORMATION FROM
*   A NASTRAN DATA FILE AND CALCULATE TIME CONSTANTS FOR A DSL
*   PROGRAM. TWO FILES ARE READ CONTAINING THE DATA FOR THE LFMR
*   BOOM AND REFLECTOR. A PARAMETER STATEMENT IS USED TO DEFINE
*   THE NUMBER OF GRID POINTS AND MODES FOR BOTH BODIES IN THE
*   BEGINNING FOR A MORE GENERAL PROGRAM.
*
*   THE FOLLOWING PARAMETERS ARE USED IN THIS PROGRAM :
*
*   NPT,NPTC      : THE NUMBER OF GRID POINTS FOR BODY B AND C
*                  RESPECTIVELY
*
*   M,MC          : THE NUMBER OF MODES FOR BODY B AND C
*                  RESPECTIVELY TO BE USED TO CALCULATE CONSTANTS
*
*   J3            : THE MOMENT OF INERTIA OF BODY A ABOUT THE
*                  SPIN AXIS
*
*   B2MA          : THE INERTIA DUE TO THE DISPLACEMENT OF
*                  BODY A'S CENTER OF MASS FROM THE SPIN AXIS
*
*   P1,P2,P3      : THE COORDINATES OF THE GRID POINTS ON
*                  BODY B
*
*   X1,X2,X3      : THE COORDINATES OF THE GRID POINTS ON
*                  BODY C
*
*   AMASS         : THE TOTAL MASS OF BODY A
*
*   CMASS         : AN ARRAY OF THE MASS AT EACH GRID POINT OF
*                  BODY C
*
*   BMASS         : A DUMMY ARRAY TO READ IN MODAL DATA
*
*   RHO           : THE MASS PER UNIT LENGTH OF BODY B
*
*   DX            : THE INTERVAL DISTANCE BETWEEN GRID POINTS ON
*                  BODY B
*
*   FIBX,FIBY,FIBZ : MATRICES OF BODY B'S TRANSLATIONAL MODE
*                  SHAPES (ROWS ARE DOFS, COLUMNS ARE MODES)
*
*   FICK,FICY,FICZ : MATRICES OF BODY B'S TRANSLATIONAL MODE
*                  SHAPES (SAME FORMAT AS FIBX,FIBY,FIBZ )
*
*   PSI1,PSI2,PSI3 : ARRAYS OF THE ROTATIONAL MODES OF THE HINGE
*                  POINT BETWEEN BODY B AND BODY C
*
*   OMGAB,OMGAC   : THE ANGULAR FREQUENCY OF BODIES B AND C
*
*   P1P2IN        : INTEGRAL OF  $P1^{**2}+P2^{**2}*RHO*DX$ 
*
*   PSFSIN        : INTEGRAL OF  $(P1*FIBX + P2*FIBY)*RHO*DX$ 
*
*   BIN1I         : INTEGRAL OF  $(P1*FIBY + P2*FIBX)*RHO*DX$ 
*
*   PHBXY         : INTEGRAL OF  $(FIBX(I,J)*FIBY(I,K)*RHO*DX$ 
*
*   PHZS          : INTEGRAL OF  $FIBZ(I,J)*FIBZ(I,K)*RHO*DX$ 
*
*   CMS           : SUMMATION OF GRID POINT MASSES OF BODY C
*
*   X1SMS         : SUMMATION OF  $X1^{**2} * CMASS$ 
*
*   X2SMS         : SUMMATION OF  $X2^{**2} * CMASS$ 
*
*   X3SMS         : SUMMATION OF  $X3^{**2} * CMASS$ 
*
*   X1CM          : SUMMATION OF  $X1 * CMASS$ 
*
*   X2CM          : SUMMATION OF  $X2 * CMASS$ 
*
*   X3CM          : SUMMATION OF  $X3 * CMASS$ 
*
*   X12MS         : SUMMATION OF  $X1*X2*CMASS$ 
*
*   X23MS         : SUMMATION OF  $X2*X3*CMASS$ 
*
*   X13MS         : SUMMATION OF  $X1*X3*CMASS$ 
*
*   PBX,PBY,PBZ   : SUMMATION OF FICK,Y,Z * CMASS
*
*   PBXS,PBYS,PBZS : SUMMATION OF FICK,Y,Z(I,J)*FICK,Y,Z(I,K)*CMASS*
*
*   PBXY          : SUMMATION OF FICK(I,J)*FICY(I,K)*CMASS
*

```

```

*      X1PBX,Y,Z      : SUMMATION OF X1*FICK,Y,Z*CMASS      *
*      X2PBX,Y,Z      : SUMMATION OF X2*FICK,Y,Z*CMASS      *
*      X3PBX,Y,Z      : SUMMATION OF X3*FICK,Y,Z*CMASS      *
*      UID11           : A(1,1) CONSTANT TERM              *
*      UID12           : A(1,1) COEFFICIENTS OF BODY B GENERALIZED *
*                      COORDINATES                          *
*      UID13           : A(1,1) COEFFICIENTS OF BODY C GENERALIZED *
*                      COORDINATES                          *
*      UJD11           : A(1,J+1)                          *
*      UID21           : A(1+J,1) COEFFICIENTS OF BODY B GENERALIZED *
*                      COORDINATES                          *
*      UID22           : A(1+J,1) COEFFICIENTS OF BODY C GENERALIZED *
*                      COORDINATES                          *
*      UKD11           : A(1,1+M+K)                        *
*      UID31           : A(1+M+K,1) COEFFICIENTS OF BODY B GENERALIZED *
*                      COORDINATES                          *
*      UID32           : A(1+M+K,1) COEFFICIENTS OF BODY C GENERALIZED *
*      UJD21           : A(1+I,1+J)                      *
*      UKD21           : A(1+J,1+M+K)                    *
*      B12UUJ          : B(1) COEFFICIENTS OF 2U1 TIMES BODY B'S *
*                      GENERALIZED SPEEDS                  *
*      B12UUK          : B(1) COEFFICIENTS OF 2*U1 TIMES BODY C'S *
*                      GENERALIZED SPEEDS                  *
*      BU221           : B(1+J) U1**2 CONSTANT TERM       *
*      BU222           : B(1+J) COEFFICIENTS OF U1**2 TIMES BODY B'S *
*                      GENERALIZED COORDINATES             *
*      BU223           : B(1+J) COEFFICIENTS OF U1**2 TIMES BODY C'S *
*                      GENERALIZED COORDINATES             *
*                      : ALSO B(1+M+K) COEFFICIENTS OF U1**2 TIMES *
*                      BODY B'S GENERALIZED COORDINATES    *
*      B22UUJ          : B(1+J) COEFFICIENTS OF 2*U1 TIMES BODY B'S *
*                      GENERALIZED SPEEDS                  *
*      B22UUK          : B(1+J) COEFFICIENTS OF 2*U1 TIMES BODY C'S *
*                      GENERALIZED SPEEDS                  *
*      B3U211          : B(1+M+K) CONSTANT COEFFICIENTS OF U1**2 *
*      B3U213          : B(1+M+K) COEFFICIENTS OF U1**2 TIMES BODY C'S *
*                      GENERALIZED COORDINATES             *
*      B32UUJ          : B(1+M+K) COEFFICIENTS OF 2*U1 TIMES BODY B'S *
*                      GENERALIZED SPEEDS                  *
*      B32UUK          : B(1+M+K) COEFFICIENTS OF 2*U1 TIMES BODY C'S *
*                      GENERALIZED SPEEDS                  *

```

```

IMPLICIT REAL*8(A-H,O-Z)
INTEGER NPT,NPTC,M,MC,I,J,K
PARAMETER (NPT=17,NPTC=63 ,M=10,MC=10)
REAL*8 J3
DIMENSION P1(NPT),P2(NPT),P3(NPT),P1SQ(NPT),P2SQ(NPT),RPFMIX(NPT,M
+),P1SP2S(NPT),RPSSQ(NPT),CMASS(NPTC),X1(NPTC),
+X2(NPTC),X3(NPTC),FIBZ(NPT,M),PHI2C(NPTC),
+FIBX(NPT,M),FIBY(NPT,M),FICK(NPTC,MC),FICY(NPTC,MC),FICZ(NPTC
+,MC),P1FBX(NPT,M),P2N(NPT),P2FXN(NPT,M),P1FY(NPT,M),PFMIX(NPT,M)
+,P2FBY(NPT,M),P1P2FA(NPT,M),RPSFA(NPT,M),PSFSIN(M),PSI1(M),PSI2(M)
+,PSI3(M),FBX(MC),PBY(MC),X1PBX(MC),X2PBY(MC),X2PBX(MC),X1PBY(MC),
+X1PBZ(MC),X2PBZ(MC),X3PBX(MC),X3PBY(MC),X3PBZ(MC),

```

```

+UID12(M),UID13(MC),UJD11(M),UKD11(MC),B12UUJ(M),B12UUK(MC),
+BU221(M),B3U211(MC),UID21(M,M),UID22(M,MC),UJD21(M,M),UKD21(M,MC),
+BU222(M,M),BU223(M,MC),B22UUJ(M,M),B22UUK(M,MC),B32UUJ(M,MC),
+UID31(M,MC),B3U213(MC,MC),B32UUK(MC,MC),
+PHIPHI(NPT),PHEXY(M,M),PHZS(M,M),PBZ(MC),PBXS(MC,MC),
+PBYS(MC,MC),PBXY(MC,MC),BIN1I(M),UID32(MC,MC),PBZS(MC,MC),
+FREQB(M),OMGAB(M),FREQC(MC),OMGAC(MC),BMASS(NPT)
DATA J3,B,AMASS,DX,RHO/12.0,12.,.1295,18.,1.80631D-4/

```

* READ IN CONSTANTS

```

CALL MODATB(M,NPT,P1,P2,P3,FIBX,FIBY,FIBZ,PSI1,PSI2,PSI3,BMASS,
+FREQB,OMGAB)
CALL MODATC(MC,NPTC,X1,X2,X3,FICX,FICY,FICZ,CMASS,
+FREQC,OMGAC)

```

* CALL ALL CONSTANT SUBROUTINES

```

CALL BINT11(NPT,RHO,DX,P1,P2,P1SQ,P2SQ,P1SP2S,RPSSQ,P1P2IN)
CALL BINT12(NPT,M,P1,P2,FIBX,FIBY,P1FBX,P2FBY,P1P2FA,RPSFA,
+RHO,DX,PSFSIN)
CALL BINT1I(NPT,M,P1,P2,FIBX,FIBY,RHO,DX,P2N,P2FXN,P1FY,
+FFIMIX,RPFMIX,BIN1I)
CALL CALPKY(NPT,M,FIBX,FIBY,RHO,DX,PHIPHI,PHEXY)
CALL FIBZSQ(NPT,M,FIBZ,PHIPHI,DX,RHO,PHZS)
CALL SUMASS(NPTC,CMASS,CMS)
CALL XSQCMS(NPTC,CMASS,X1,X1,X1SMS)
CALL XSQCMS(NPTC,CMASS,X2,X2,X2SMS)
CALL XSQCMS(NPTC,CMASS,X3,X3,X3SMS)
CALL SUMC(NPTC,X1,CMASS,X1CM)
CALL SUMC(NPTC,X2,CMASS,X2CM)
CALL SUMC(NPTC,X3,CMASS,X3CM)
CALL XSQCMS(NPTC,CMASS,X1,X2,X12MS)
CALL XSQCMS(NPTC,CMASS,X2,X3,X23MS)
CALL XSQCMS(NPTC,CMASS,X1,X3,X13MS)
CALL CALPBM(NPTC,MC,FICX,CMASS,PBX)
CALL CALPBI(NPTC,MC,FICY,CMASS,PBY)
CALL CALPBI(NPTC,MC,FICZ,CMASS,PBZ)
CALL PBSYMS(NPTC,MC,FICX,CMASS,PHI2C,PBXS)
CALL PBSYMS(NPTC,MC,FICY,CMASS,PHI2C,PBYS)
CALL PBSYMS(NPTC,MC,FICZ,CMASS,PHI2C,PBZS)
CALL CALPBS(NPTC,MC,FICX,FICY,CMASS,PHI2C,PBXY)
CALL CALXPB(NPTC,MC,X1,FICX,CMASS,X1PBX)
CALL CALXPB(NPTC,MC,X1,FICY,CMASS,X1PBY)
CALL CALXPB(NPTC,MC,X1,FICZ,CMASS,X1PBZ)
CALL CALXPB(NPTC,MC,X2,FICX,CMASS,X2PBX)
CALL CALXPB(NPTC,MC,X2,FICY,CMASS,X2PBY)
CALL CALXPB(NPTC,MC,X2,FICZ,CMASS,X2PBZ)
CALL CALXPB(NPTC,MC,X3,FICX,CMASS,X3PBX)
CALL CALXPB(NPTC,MC,X3,FICY,CMASS,X3PBY)
CALL CALXPB(NPTC,MC,X3,FICZ,CMASS,X3PBZ)
B2MA = B*B*AMASS
H1H2CM = (P1(NPT)*P1(NPT) + P2(NPT)*P2(NPT))*CMS
UID11 = J3+B2MA+P1P2IN+H1H2CM+X1SMS+X2SMS+2.*(P1(NPT)*X1CM+P2(NPT)
+ *X2CM)

```

*

```

DO 10 J =1,M

```

```

FXTER = FIBX(NPT,J)*(P1(NPT)*CMS + X1CM)
FYTER = FIBY(NPT,J)*(P2(NPT)*CMS + X2CM)
SI1TER = -PSI1(J)*(P2(NPT)*X3CM + X23MS)
SI2TER = PSI2(J)*(P1(NPT)*X3CM + X13MS)
SI3TER = PSI3(J)*(P2(NPT)*X1CM - P1(NPT)*X2CM)
BU221(J) = PSFSIN(J)+FXTER+FYTER+SI2TER+SI3TER+SI1TER
U1D12(J) = 2. * BU221(J)
10 CONTINUE
DO 11 K = 1,MC
U1D13(K)=2.*(P1(NPT)*PBX(K) +X1PBX(K) + P2(NPT)*PBY(K) + X2PBY(K))
11 CONTINUE
*
DO 12 J = 1,M
FXTER = FIBX(NPT,J)*(P2(NPT)*CMS + X2CM)
FYTER = FIBY(NPT,J)*(P1(NPT)*CMS + X1CM)
SI1TER = PSI1(J)*(P1(NPT)*X3CM + X13MS)
SI2TER = PSI2(J)*(P2(NPT)*X3CM + X23MS)
SI3TER = PSI3(J)*(P1(NPT)*X1CM+X15MS+X25MS+P2(NPT)*X2CM)
UJD11(J) = BIN11(J)-FXTER+FYTER-SI1TER-SI2TER+SI3TER
12 CONTINUE
*CALCULATES A(1,3) AND PART OF A(3,1)
DO 13 K = 1,MC
UKD11(K) = -PBX(K)*P2(NPT)-X2PBX(K)+PBY(K)*P1(NPT) + X1PBY(K)
13 CONTINUE
DO 14 J = 1,M
FXTER = FIBX(NPT,J)*(P1(NPT)*CMS + X1CM)
FYTER = FIBY(NPT,J)*(P2(NPT)*CMS + X2CM)
SI1TER = PSI1(J)*(P2(NPT)*X3CM + X23MS)
SI2TER = PSI2(J)*(P1(NPT)*X3CM + X13MS)
SI3TER = PSI3(J)*(P1(NPT)*X2CM + P2(NPT)*X1CM)
B12UUJ(J)=-PSFSIN(J)-FXTER-FYTER-SI1TER+SI2TER-SI3TER
14 CONTINUE
DO 15 K = 1,MC
B12UUK(K)=-P1(NPT)*PBX(K)-X1PBX(K)-P2(NPT)*PBY(K)-X2PBY(K)
B3U211(K) = -B12UUK(K)
15 CONTINUE
* 1+J EQUATION
*
DO 16 I = 1,M
DO 17 J=1,M

FXTER=FIBX(NPT,J)*(PSI1(I)*X3CM-PSI3(I)*X1CM-FIBY(NPT,I)*CMS)
FYTER=FIBY(NPT,J)*(PSI2(I)*X3CM-PSI3(I)*X2CM+FIBX(NPT,I)*CMS)
SI1TER=PSI1(J)*( (PSI3(I)*P2(NPT) + FIBX(NPT,I))*X3CM +
+(PSI1(I)*P1(NPT) + PSI2(I)*P2(NPT))*X2CM + PSI2(I)*(X3SMS+X2SMS)
++PSI1(I)*X12MS)
SI2TER=PSI2(J)*( (PSI3(I)*P1(NPT) - FIBY(NPT,I))*X3CM +
+(PSI1(I)*P1(NPT) + PSI2(I)*P2(NPT))*X1CM + PSI1(I)*(X3SMS+X1SMS)
++PSI2(I)*X12MS)
SI3TER=PSI3(J)*( (-PSI3(I)*P1(NPT) + FIBY(NPT,I))*X2CM +
+(PSI3(I)*P2(NPT)+FIBX(NPT,I))*X1CM-PSI1(I)*X23MS+PSI2(I)*X13MS)
U1D21(J,I)=PHBXY(I,J)-PHBXY(J,I)+FXTER+FYTER-SI1TER+SI2TER+SI3TER
17 CONTINUE
16 CONTINUE

```

```

*
DO 18 J =1,M
  DO 19 K = 1,MC
    FXTER=FIBX(NPT,J)*PBX(K)
    FYTER=FIBY(NPT,J)*PBY(K)
    SI1TER=-PSI1(J)*(X3PBX(K)+P1(NPT)*PBZ(K)+X1PBZ(K))
    SI2TER=-PSI2(J)*(X3PBY(K)+P2(NPT)*PBZ(K)+X2PBZ(K))
    SI3TER=PSI3(J)*(2.*(X2PBY(K)+X1PBX(K))+P2(NPT)*PBY(K)+P1(NPT)*
+      PBX(K))
    UID22(J,K)=-FXTER + FYTER + SI1TER + SI2TER + SI3TER
19  CONTINUE
18  CONTINUE
    DO 20 I= 1,M
      DO 21 J = I,M
        FXTER=FIBX(NPT,J)*(PSI2(I)*X3CM - PSI3(I)*X2CM)
+      +FIBX(NPT,I)*(PSI2(J)*X3CM - PSI3(J)*X2CM)
        FYTER=FIBY(NPT,J)*(-PSI1(I)*X3CM + PSI3(I)*X1CM)
+      +FIBY(NPT,I)*(-PSI1(J)*X3CM + PSI3(J)*X1CM)
        FZTER=FIBZ(NPT,J)*(PSI1(I)*X2CM - PSI2(I)*X1CM)
+      +FIBZ(NPT,I)*(PSI1(J)*X2CM - PSI2(J)*X1CM)
        SI1TER=PSI1(J)*(PSI1(I)*(X3SMS+X2SMS)-PSI2(I)*X12MS)
+      +PSI1(I)*(PSI1(J)*(X3SMS+X2SMS)-PSI2(J)*X12MS)
        SI2TER=PSI2(J)*(PSI2(I)*(X3SMS+X1SMS)-PSI3(I)*X23MS)
+      +PSI2(I)*(PSI2(J)*(X3SMS+X1SMS)-PSI3(J)*X23MS)
        SI3TER=PSI3(J)*(PSI3(I)*(X2SMS+X1SMS)-PSI1(I)*X13MS)
+      +PSI3(I)*(PSI3(J)*(X2SMS+X1SMS)-PSI1(J)*X13MS)
        IF(I .EQ. J)THEN
          UJD21(I,J)=1.+FXTER+FYTER+FZTER+SI1TER+SI2TER+SI3TER
        ELSE
          UJD21(I,J)=FXTER+FYTER+FZTER+SI1TER+SI2TER+SI3TER
          UJD21(J,I)=UJD21(I,J)
        ENDIF
21  CONTINUE
20  CONTINUE
* CALCULATES A(2,3) AND A(3,2)
    DO 22 K = 1,MC
      DO 23 J = 1,M
        FXTER=FIBX(NPT,J)*PBX(K)
        FYTER=FIBY(NPT,J)*PBY(K)
        FZTER=FIBZ(NPT,J)*PBZ(K)
        SI1TER=PSI1(J)*(X2PBZ(K)-X3PBY(K))
        SI2TER=PSI2(J)*(X3PBX(K)-X1PBZ(K))
        SI3TER=PSI3(J)*(X1PBY(K)-X2PBX(K))
        UKD21(J,K)= FXTER+FYTER+FZTER+SI1TER+SI2TER+SI3TER
23  CONTINUE
22  CONTINUE
*
    DO 24 J = 1,M
      DO 25 I = 1,M
        FXTER=FIBX(NPT,J)*(-PSI3(I)*X2CM+PSI2(I)*X3CM)
        FYTER=FIBY(NPT,J)*(-PSI1(I)*X3CM+PSI3(I)*X1CM)
        SI1TER=PSI1(J)*(-FIBY(NPT,I)*X3CM+PSI1(I)*(X3SMS-X2SMS-P2(NPT)
+X2CM)+PSI2(I)*(P1(NPT)*X2CM+X12MS)+PSI3(I)*P1(NPT)*X3CM)
        SI2TER=PSI2(J)*(FIBX(NPT,I)*X3CM+PSI2(I)*(X3SMS-X1SMS-P1(NPT)

```

```

+*X1CM)+PSI1(I)*(P2(NPT)*X1CM+X12MS)+PSI3(I)*P2(NPT)*X3CM)
      SI3TER=PSI3(J)*(-FIBX(NPT,I)*X2CM-PSI3(I)*(P2(NPT)*X2CM+P1(NPT)
+*X1CM)-PSI1(I)*(X13MS)-PSI2(I)*X23MS+FIBY(NPT,I)*X1CM)
      IF (I .EQ. J) THEN
      BU222(J,I)=1.-PHZS(J,I)-CMS*FIBZ(NPT,I)*FIBZ(NPT,J)+FXTER+FYTER
+
      +SI1TER+SI2TER+SI3TER
      ELSE
      BU222(J,I)=-PHZS(J,I)-CMS*FIBZ(NPT,I)*FIBZ(NPT,J)+FXTER+FYTER
+
      +SI1TER+SI2TER+SI3TER
      ENDIF
25      CONTINUE
24      CONTINUE
*
DO 26 K=1,MC
  DO 27 J = 1,M
    FXTER=FIBX(NPT,J)*PBX(K)
    FYTER=FIBY(NPT,J)*PBY(K)
    SI1TER=-PSI1(J)*(X3PBY(K)+P2(NPT)*PBZ(K)+X2PBZ(K))
    SI2TER=PSI2(J)*(X3PBX(K)+P1(NPT)*PBZ(K)+X1PBZ(K))
    SI3TER=PSI3(J)*(P2(NPT)*PBX(K)-P1(NPT)*PBY(K))
    BU223(J,K)=FXTER+FYTER+SI1TER+SI2TER+SI3TER
27      CONTINUE
26      CONTINUE
*
DO 28 J=1,M
  DO 29 I=1,M
    FXTER=FIBX(NPT,J)*(FIBY(NPT,I)*CMS+PSI3(I)*X1CM-PSI1(I)*X3CM)
    FYTER=-FIBY(NPT,J)*(FIBX(NPT,I)*CMS+PSI2(I)*X3CM-PSI3(I)*X2CM)
    FZTER=FIBZ(NPT,J)*( .5*PSI3(I)*X3CM)
    SI1TER=PSI1(J)*(FIBX(NPT,I)*X3CM+PSI2(I)*X3SMS-PSI3(I)*1.5*X23MS)
    SI2TER=PSI2(J)*(FIBY(NPT,I)*X3CM-PSI1(I)*X3SMS+PSI3(I)*1.5*X13MS)
    SI3TER=PSI3(J)*(-FIBY(NPT,I)*X2CM-PSI2(I)*X13MS+PSI1(I)*X23MS-
+
      FIBX(NPT,I)*X1CM)
    B22UUJ(J,I)=PHBXY(I,J)-PHBXY(J,I) + FXTER + FYTER + FZTER +
+
      SI1TER+SI2TER+SI3TER
29      CONTINUE
28      CONTINUE
*
DO 30 K = 1,MC
  DO 31 J = 1,M
    FXTER= FIBX(NPT,J)*PBY(K)
    FYTER= -FIBY(NPT,J)*PBX(K)
    SI1TER= PSI1(J)*X3PBX(K)
    SI1TRK= SI1TER -PSI1(J)*(P1(NPT)*PBZ(K)+X1PBZ(K))
    SI2TER= PSI2(J)*X3PBY(K)
    SI2TRK= SI2TER -PSI2(J)*(P2(NPT)*PBZ(K)+X2PBZ(K))
    SI3TER= -PSI3(J)*(X1PBX(K)+X2PBY(K))
    SI3TRK = PSI3(J)*(P1(NPT)*PBX(K)+P2(NPT)*PBY(K))
    B22UUK(J,K) = FXTER + FYTER + SI1TER + SI2TER + SI3TER
    B32UUJ(J,K) = -B22UUK(J,K)+.5*X3PBZ(K)*PSI3(J)
    UID31(J,K) = FXTER + FYTER + SI1TRK + SI2TRK + SI3TRK
31      CONTINUE
30      CONTINUE
* 1+N+K EQUATION (UKD11 IS 1RST TERM; UID31 IS 2ND; IDENTITY IS 3RD)

```

```

* B3 (B3U211 IS 1RST TERM;BU223 IS U2 Q(I) TERM;
* B32UUJ IS 2U *U(1+I)TERM
  DO 32 K = 1,MC
    DO 33 J =K,MC
      IF (K .EQ.J) THEN
        B3U213 (J,K) = 1. - PBZS(J,K)
      ELSE
        B3U213 (J,K) = -PBZS(J,K)
        B3U213(K,J) = B3U213(J,K)
      ENDIF
33    CONTINUE
32  CONTINUE
  DO 34 K = 1,MC
    DO 35 J = 1,MC
      B32UUK(J,K) = PBXY(K,J)-PBXY(J,K)
      UID32(J,K) = - B32UUK(J,K)
35  CONTINUE
34  CONTINUE
C PRINT OUT RESULTS IN FILE 25
  WRITE (25, '(10X, 'A11C' )')
  WRITE (25,100) UID11
100  FORMAT (D15.6)
  WRITE(25, '(10X, 'A11Q' ,9X, 'AJ1C' ,8X, 'B1Q' ,9X, 'BJU1C' ,9X,
+ 'OMGAB' )')
  DO 1 J= 1,M
  WRITE(25,200)J,UID12(J),UJD11(J),B12UUJ(J),BU221(J),OMGAB(J)
1  CONTINUE
200  FORMAT (I4,5D13.6)
  WRITE(25, '(10X, 'B1QB' ,9X, 'A11QB' ,8X, 'A1KC' ,9X, 'BKU1C' ,9X,
+ 'OMGAC' )')
  DO 2 K = 1,MC
  WRITE(25,200)K,B12UUK(K),UID13(K),UKD11(K),B3U211(K),OMGAC(K)
2  CONTINUE
  WRITE(25, '(14X, 'AJJC' ,11X, 'AJQ' ,12X, 'BJU1Q' ,13X, 'BJ2UQ' )')
  DO 3 I = 1,M
  DO 4 J = 1,M
  WRITE(25,500)J,I,UJD21(J,I),UID21(J,I),BU222(J,I),B22UUJ(J,I)
4  CONTINUE
3  CONTINUE
500  FORMAT (2I4,4D15.6)
  WRITE(25, '(12X, 'AK1QB' ,9X, 'BKU1QB' ,9X, 'BK2UQB' )')
  DO 5 K = 1,MC
  DO 6 I = 1,MC
  WRITE(25,300)I,K,UID32(I,K),B3U213(I,K),B32UUK(I,K)
6  CONTINUE
5  CONTINUE
300  FORMAT(2I4,3D15.6)
  WRITE(25, '(12X, 'AJ1QB' ,9X, 'AKJC' ,12X, 'BKU1Q' ,11X, 'BJ2UQB'
+ ')')
  DO 7 K =1,MC
  DO 8 J = 1,M
  WRITE(25,500)J,K,UID22(J,K),UKD21(J,K),BU223(J,K),B22UUK(J,K)
8  CONTINUE
7  CONTINUE

```

```

WRITE(25, '(12X, 'AK1Q', 9X, 'BK2UQ')')
DO 98 K = 1, MC
DO 99 J = 1, M
WRITE (25, 400) J, K, U1D31(J, K), B32UUJ(J, K)
99 CONTINUE
98 CONTINUE
400 FORMAT (2I4, 2D15.6)
DO 94 J = 1, M
DO 95 I = 1, NPT
WRITE(25, 900) FIBX(I, J), FIBY(I, J), FIBZ(I, J)
95 CONTINUE
94 CONTINUE
DO 96 J = 1, MC
DO 97 I = 1, NPTC
WRITE(25, 900) FICX(I, J), FICY(I, J), FICZ(I, J)
97 CONTINUE
96 CONTINUE
DO 93 J = 1, M
WRITE (25, 900) PSI1(J), PSI2(J), PSI3(J)
93 CONTINUE
DO 92 I = 1, NPTC
WRITE (25, 900) X1(I), X2(I), X3(I)
92 CONTINUE
900 FORMAT (3D20.6)
END

```

```

*****
*
* VECADD
* ( ADD TWO ARRAYS TO PRODUCE AN ARRAY )
*
*****

```

```

SUBROUTINE VECADD (NPT, A, B, ARG)
REAL*8 A(NPT), B(NPT), ARG(NPT)
DO 10 I = 1, NPT
ARG(I) = A(I) + B(I)
10 CONTINUE
RETURN
END

```

```

*****
*
* MULTSV
* ( MULTIPLIES A SCALAR TIMES A VECTOR )
*
*****

```

```

SUBROUTINE MULTSV (NPT, A, B, ARG)
REAL*8 A, B(NPT), ARG(NPT)
DO 10 I = 1, NPT
ARG(I) = A * B(I)
10 CONTINUE
RETURN
END

```

```

*****
*
* MATADD
* ( ADDS TWO MATRICES TO PRODUCE A MATRIX )
*
*****

```

```

*****
      SUBROUTINE MATADD(NPT,M,A,B,ARG)
      REAL*8 A(NPT,M),B(NPT,M),ARG(NPT,M)
      DO 10 J = 1,M
        DO 20 I = 1,NPT
          ARG(I,J) = A(I,J) + B(I,J)
20      CONTINUE
10      CONTINUE
      RETURN
      END
*****
*      SUBROUTINE MULT2S                                     *
*      ( CALCULATES A COLN TIMES A ROW VECTOR )           *
*****
      SUBROUTINE MULT2S ( NPT,A,B,ARG)
      REAL*8 A(NPT),B(NPT),ARG(NPT)
      DO 10 I = 1,NPT
        ARG(I) = A(I) * B(I)
10      CONTINUE
      RETURN
      END
*****
*      MULTSM                                               *
*      ( MULTIPLIES A SCALAR TIMES A MATRIX )             *
*****
      SUBROUTINE MULTSM (NPT,M,A,B,ARG)
      REAL*8 A,B(NPT,M),ARG(NPT,M)
      DO 10 J = 1,M
        DO 20 I = 1,NPT
          ARG(I,J) = A* B(I,J)
20      CONTINUE
10      CONTINUE
      RETURN
      END
*****
*      SUBROUTINE MULTVM                                     *
*      ( MULTIPLIES VECTOR AND MATRIX TO PRODUCE A MATRIX ) *
*****
      SUBROUTINE MULTVM (NPT,M,A,B,ARG)
      REAL*8 A(NPT),B(NPT,M),ARG(NPT,M)
      DO 10 I = 1,NPT
        DO 20 J =1,M
          ARG(I,J) = A(I) * B(I,J)
20      CONTINUE
10      CONTINUE
      RETURN
      END
*****
*      SUBROUTINE FIBZSQ                                     *
*      ( CALCULATES THE INTEGRAL OF PIBZ(I,J)*PIBZ(I,K)*RHO*DX ) *
*****
      SUBROUTINE FIBZSQ(NPT,M,FIBZ,PHIPHI,DX,RHO,PHZS)
      REAL*8 FIBZ(NPT,M),PHIPHI(NPT),PHZS(M,M),RHO,DX
      DO 10 K = 1,M

```

```

        DO 20 J = K,M
          DO 30 I = 1,NPT
            PHIPHI(I) = FIBZ(I,J)*FIBZ(I,K)*RHO
30      CONTINUE
        CALL TRAPZ(NPT,DX,PHIPHI,SUM)
        PHZS(J,K) = SUM
        PHZS(K,J)=PHZS(J,K)
20      CONTINUE
10     CONTINUE
        RETURN
        END
*****
*      TRAPZ
*      ( PERFORMS INTEGRATION APPROXIMATION USING TRAPEZOIDAL RULE) *
*****
        SUBROUTINE TRAPZ(NPT,DX,F,INT)
        REAL*8 DX,F(NPT),INT,SUM
        SUM = 0.
        DO 10 I= 1,8
          IF(I .EQ. 1 .OR. I .EQ. NPT) THEN
            FACTOR = 1.
          ELSE
            FACTOR = 2.
          ENDIF
          SUM = SUM + FACTOR*F(I)
10     CONTINUE
        INT = DX/2. * SUM
        RETURN
        END
*****
*      MATTRP
*      ( INTEGRATION APPROXIMATION OF A MATRIX USING TRAPEZOIDAL RULE) *
*****
        SUBROUTINE MATTRP(NPT,M,DX,F,INT)
        REAL*8 DX,F(NPT,M),INT(M),SUM
        DO 5 J = 1,2
          SUM = 0.
          DO 10 I= 1,8
            IF(I .EQ. 1 .OR. I .EQ. 8) THEN
              FACTOR = 1.
            ELSE
              FACTOR = 2.
            ENDIF
            SUM = SUM + FACTOR*F(I,J)
10     CONTINUE
          INT(J) = DX/2. * SUM
5      CONTINUE
        RETURN
        END
*****
*      SUMC
*      ( PERFORMS SUMMATION OF GRID POINT MASSES OF BODY C TIMES
*      AN ARBITRARY VECTOR OF EQUAL DIMENSION )
*****

```

```

SUBROUTINE SUMC(NPTC,F,CMASS,SUM)
REAL*8 F(NPTC),CMASS(NPTC),SUM
SUM = 0.
DO 10 I = 1,NPTC
    SUM = SUM + F(I)*CMASS(I)
10 CONTINUE
RETURN
END
*****
* MATSUM *
* ( PERFORMS SUMMATION OF THE GRID POINT MASES OF BODY C TIMES *
* AN ARBITRARY MATRIX OF EQUAL DOF ) *
*****
SUBROUTINE MATSUM (NPT,M,F,CMASS,SUM)
REAL*8 F(NPT,M),CMASS(NPT),SUM(M)
DO 10 J= 1,M
    DO 20 I = 1,NPT
        SUM(J) = SUM(J) + F(I,J)*CMASS(I)
20 CONTINUE
10 CONTINUE
RETURN
END
*****
* BINT11 *
* ( PERFORMS INTEGRATION OF (P1**2 + P2**2*RHO*DX) *
*****
SUBROUTINE BINT11(NPT,RHO,DX,P1,P2,P1SQ,P2SQ,P1SP2S,RPSSQ,P1P2IN)
REAL*8 P1(NPT),P2(NPT),P1P2IN,P1SQ(NPT),P2SQ(NPT),RPSSQ(NPT)
REAL*8 P1SP2S(NPT),RHO,DX
CALL MULT2S(NPT,P1,P1,P1SQ)
CALL MULT2S(NPT,P2,P2,P2SQ)
CALL VECADD(NPT,P1SQ,P2SQ,P1SP2S)
CALL MULTSV(NPT,RHO,P1SP2S,RPSSQ)
CALL TRAPZ(NPT,DX,RPSSQ,P1P2IN)
RETURN
END
*****
* BINT12 *
* ( PERFORMS INTEGRATION OF (P1*FIBX + P2*FIBY)*RHO*DX ) *
*****
SUBROUTINE BINT12 (NPT,M,P1,P2,FIBX,FIBY,P1FBX,P2FBY,P1P2FA,RPSFA,
+RHO,DX,PSFSIN)
REAL*8 P1(NPT),P2(NPT),FIBX(NPT,M),FIBY(NPT,M),P1FBX(NPT,M),
+P2FBY(NPT,M),P1P2FA(NPT,M),PSFSIN(M),RPSFA(NPT,M),RHO,DX
CALL MULTVM(NPT,P1,FIBX,P1FBX)
CALL MULTVM(NPT,P2,FIBY,P2FBY)
CALL MATADD(NPT,P1FBX,P2FBY,P1P2FA)
CALL MULTSM(NPT,M,RHO,P1P2FA,RPSFA)
CALL MATTRP(NPT,M,DX,RPSFA,PSFSIN)
RETURN
END
*****
* BINT11 *
* ( PERFORMS INTEGRATION OF (P1*FIBY - P2*FIBX)*RHO*DX ) *

```

```

*****
      SUBROUTINE BINT1I (NPT,M,P1,P2,FIBX,FIBY,RHO,DX,P2N,P2FXN,P1FY,
+PFIMIX,RPFMIX,BIN1I)
      REAL*8 P1(NPT),P2(NPT),FIBX(NPT,M),FIBY(NPT,M),P2N(NPT),BIN1I(M)
+ ,P2FXN(NPT,M),P1FY(NPT,M),PFIMIX(NPT,M),RPFMIX(NPT,M),RHO,DX
      DO 10 I = 1,NPT
          P2N(I) = -P2(I)
10      CONTINUE
          CALL MULTVM (NPT,M,P2N,FIBX,P2FXN)
          CALL MULTVM (NPT,M,P1,FIBY,P1FY)
          CALL MATADD (NPT,M,P2FXN,P1FY,PFIMIX)
          CALL MULTSM (NPT,M,RHO,PFIMIX,RPFMIX)
          CALL MATTRP (NPT,M,DX,RPFMIX,BIN1I)
          RETURN
      END
*****
*      CALPX
*      INTEGRAL OF ( FIBX(I,J)*FIBY(I,K)*RHO*DX)
*****
      SUBROUTINE CALPX ( NPT,M,FIBX,FIBY,RHO,DX,PHIPHI,PHBXY)
      REAL*8 FIBX(NPT,M),FIBY(NPT,M),PHBXY(M,M),PHIPHI(NPT),RHO,SUM
+ ,DX
      DO 10 K = 1,M
          DO 20 J = 1,M
              DO 30 I = 1,NPT
                  PHIPHI(I) = FIBX(I,J)*FIBY(I,K)*RHO
30          CONTINUE
              CALL TRAPZ(NPT,DX,PHIPHI,SUM)
              PHBXY(J,K) = SUM
20          CONTINUE
10      CONTINUE
          RETURN
      END
*****
*      SUMASS
*      (SUMMATION OF THE GRID POINT MASSES OF BODY C )
*****
      SUBROUTINE SUMASS (NPTC,CMASS,CMS)
      REAL*8 CMASS(NPTC),CMS
      CMS = 0.
      DO 10 I =1,NPTC
          CMS = CMS + CMASS(I)
10      CONTINUE
          RETURN
      END
*****
*      XSQCMS
*      ( SUMMATION OF THE MULTIPLICATION OF TWO ARBITRARY X'S TIMES
*      THE GRID POINT MASSES OF BODY C )
*****
      SUBROUTINE XSQCMS (NPTC,CMASS,XA,XB,XSMS)
      REAL*8 XA(NPTC),XB(NPTC),CMASS(NPTC),XSMS
      XSMS = 0.
      DO 10 I =1,NPTC

```

```

      XSMS = XSMS + XA(I)*XB(I)*CMASS(I)
10  CONTINUE
    RETURN
    END
*****
*    CALPBM
*    (SUMMATION OF AN ARBITRARY MODE SHAPE MATRIX TIMES THE GRID
*    POINT MASSES OF BODY C )
*****
SUBROUTINE CALPBM (NPTC,MC,FIC,CMASS,PB)
REAL*8 FIC(NPTC,MC),CMASS(NPTC),PB(MC),SUM
DO 10 J = 1,MC
  SUM = 0.
  DO 20 I = 1,NPTC
    SUM = SUM + FIC(I,J)*CMASS(I)
20  CONTINUE
  PB(J) = SUM
10  CONTINUE
    RETURN
    END
*****
*    CALPBS
*    ( SUMMATION OF THE MULTIPLICATION OF TWO ARBITRARY MODE SHAPES
*    TIMES THE GRID POINT MASSES OF BODY C )
*****
SUBROUTINE CALPBS (NPTC,MC,FICA,FICB,CMASS,PHI2C,PBS)
REAL*8 FICA(NPTC,MC),FICB(NPTC,MC),CMASS(NPTC),PBS(MC,MC)
REAL*8 PHI2C(NPTC),SUM
DO 10 K = 1,MC
  DO 20 J = 1,MC
    DO 30 I = 1,NPTC
      PHI2C(I) = FICA(I,J)*FICB(I,K)
30  CONTINUE
    CALL SUMC(NPTC,PHI2C,CMASS,SUM)
    FBS (J,K) = SUM
20  CONTINUE
10  CONTINUE
    RETURN
    END
*****
*    PBSYMS
*    (SUMMATION A MODE SHAPE MATRIX TRANSPOSED TIMES THE MODE SHAPE
*    MATRIX TIMES THE GRID POINT MASSES OF BODY C)- A SYMMETRIC MATRIX
*****
SUBROUTINE PBSYMS (NPTC,MC,FICA,CMASS,PHI2C,PBS)
REAL*8 FICA(NPTC,MC),CMASS(NPTC),PBS(MC,MC)
REAL*8 PHI2C(NPTC),SUM
DO 10 K = 1,MC
  DO 20 J = K,MC
    DO 30 I = 1,NPTC
      PHI2C(I) = FICA(I,J)*FICA(I,K)
30  CONTINUE
    CALL SUMC(NPTC,PHI2C,CMASS,SUM)
    FBS (J,K) = SUM

```

```

          FBS (K,J) = FBS (J,K)
20      CONTINUE
10      CONTINUE
        RETURN
        END
*****
*      CALXPB
*      ( SUMMATION OF ANY X*ANY MODE SHAPE MATRIX*THE GRID POINT MASSES *
*      OF BODY C )
*****
        SUBROUTINE CALXPB (NPTC,MC,X,FIC,CMASS,XPB)
        REAL*8 FIC(NPTC,MC),CMASS(NPTC),XPB(MC),SUM,X(NPTC)
        DO 10 J = 1,MC
          SUM = 0.
          DO 20 I = 1,NPTC
            SUM = X(I)*FIC(I,J)*CMASS(I) + SUM
20      CONTINUE
        XPB(J) = SUM
10      CONTINUE
        RETURN
        END
*****
*      MODATB: READ AND TAYLOR MODAL DATA OF BODY B *
*****
        SUBROUTINE MODATB (M,NPT,X1,X2,X3,FIBX,FIBY,FIBZ,
+          PS1,PS2,PS3,CMASS,FREQ,OMEGA)
C
        IMPLICIT REAL*8(A-H,O-Z)
        DIMENSION FREQ(M),OMEGA(M),CMASS(NPT)
        DIMENSION X1(NPT),X2(NPT),X3(NPT)
        DIMENSION FIBX(NPT,M),FIBY(NPT,M),FIBZ(NPT,M)
        DIMENSION PS1(M),PS2(M),PS3(M)
        DIMENSION PSI1(100,30),PSI2(100,30),PSI3(100,30)
        DIMENSION VB(3),VC(3),VO(3),VN(3),C(3,3)
C
        REWIND 8
        REWIND 21
C
        PI = 4.0 * ATAN(1.DO)
        TPI = 2.0 * PI
        FRAD = PI/180.0
C
        READ(8,100) ICOR,IMAS,ICMOD,ICTR,NGRID,NMOD
C
        IF(ICTR .LE. 1) GO TO 3
        IF(ICTR .GE. 3) GO TO 2
        READ(8,104) ALP
        GO TO 3
2      READ(8,106) VB(1),VB(2),VB(3),
+          VC(1),VC(2),VC(3)
C
3      IF(IMAS .EQ. 0) GOTO 9
C
        DO 5 I=1,IMAS

```

```

      READ(8,150) J1,J2,BMAS
      DO 4 J=J1,J2
4      CMASS(J) = BMAS
5      CONTINUE
C
9      DO 10 I=1,NGRID
10     READ(8,200) X1(I),X2(I),X3(I)
C
      IF(ICOR .EQ. 0) GO TO 30
C
      DO 20 I=1,NGRID
      R = X1(I)
      THTA = X2(I) * FRAD
      X1(I) = R * COS(THTA)
20     X2(I) = R * SIN(THTA)
C
30     DO 50 I=1,NMOD
      READ(8,300) IMOD
      READ(8,400) FREQ(IMOD)
      OMEGA(IMOD) = TPI * FREQ(IMOD)
C
      DO 40 J=1,NGRID
      READ(8,500) FIBX(J,IMOD),FIBY(J,IMOD),FIBZ(J,IMOD),
+      PSI1(J,IMOD),PSI2(J,IMOD),PSI3(J,IMOD)
40     CONTINUE
      PS1(I) = PSI1(NPT,I)
      PS2(I) = PSI2(NPT,I)
      PS3(I) = PSI3(NPT,I)
50     CONTINUE
C
      IF(ICTR .LE. 1) GO TO 80
      IF(ICTR .GE. 3) GO TO 75
C
C      2-DIMENSIONAL COORDNATE TRANSFORM
C
      ALP = ALP * FRAD
      CP = COS(ALP)
      SP = SIN(ALP)
      DO 60 I=1,NGRID
      X = X1(I)
      Z = X3(I)
      X1(I) = X * CP + Z * SP
60     X3(I) = - X * SP + Z * CP
C
      DO 70 I=1,NMOD
      DO 65 J=1,NGRID
      X = FIBX(J,I)
      Z = FIBZ(J,I)
      FIBX(J,I) = X * CP + Z * SP
65     FIBZ(J,I) = - X * SP + Z * CP
70     CONTINUE
      GO TO 80
C
C      3-DIMENSIONAL COORDINATE TRANSFORM

```

```

C
75 CALL CTRN3(VB,VC,C)
C
DO 76 I=1,NGRID
VO(1) = X1(I)
VO(2) = X2(I)
VO(3) = X3(I)
CALL TRN3(VO,VN,C)
X1(I) = VN(1)
X2(I) = VN(2)
76 X3(I) = VN(3)
DO 78 I=1,NMOD
DO 77 J=1,NGRID
VO(1) = FIBX(J,I)
VO(2) = FIBY(J,I)
VO(3) = FIBZ(J,I)
CALL TRN3(VO,VN,C)
FIBX(J,I) = VN(1)
FIBY(J,I) = VN(2)
77 FIBZ(J,I) = VN(3)
78 CONTINUE
C
C WRITE OUTPUT FILE
C
80 WRITE(21,110) NGRID,NMOD
IF(IMAS .EQ. 0) GO TO 85
DO 83 I=1,NGRID
83 WRITE(21,160) I, CMASS(I)
85 DO 87 I=1,NGRID
87 WRITE(21,210) I, X1(I),X2(I),X3(I)
C
DO 95 I=1,NMOD
WRITE(21,410) I, FREQ(I), OMEGA(I)
DO 90 J=1,NGRID
90 WRITE(21,550) J, FIBX(J,I), FIBY(J,I), FIBZ(J,I)
IF(ICMOD .EQ. 0) GO TO 95
DO 93 J=1,NGRID
93 WRITE(21,550) J, PSI1(J,I), PSI2(J,I), PSI3(J,I)
95 CONTINUE
C
C FORMAT
C
100 FORMAT(10X,6I5)
104 FORMAT(F10.4)
106 FORMAT(10X,3F10.4/10X,3F10.4)
110 FORMAT(/'NUMBER OF GRIDS =' ,I5/'NUMBER OF MODES =' ,I5)
150 FORMAT(10X,2I5.D15.4)
160 FORMAT(I4,D15.6)
200 FORMAT(20X,3F10.3)
210 FORMAT(3X,I4,3X,3D15.6)
300 FORMAT(8X,I4)
400 FORMAT(8X,D14.6)
410 FORMAT(/'MODE =' ,I5/'FREQUENCY =' ,F10.3,2X,'HZ'/'OMEGA =' ,D15.6)
500 FORMAT(2X,6D13.6)

```

```

550  FORMAT(3X,I4,3X,3D15.6)
C
      RETURN
      END

*****
*   MODATC: READ AND TAYLOR MODAL DATA OF BODY C   *
*****
      SUBROUTINE MODATC (M,NPT,X1,X2,X3,FIBX,FIBY,FIBZ,
+          CMASS,FREQ,OMEGA)
C
      IMPLICIT REAL*8(A-H,O-Z)
      DIMENSION FREQ(M),OMEGA(M),CMASS(NPT)
      DIMENSION X1(NPT),X2(NPT),X3(NPT)
      DIMENSION FIBX(NPT,M),FIBY(NPT,M),FIBZ(NPT,M)
      DIMENSION VB(3),VC(3),VO(3),VN(3),C(3,3)
C
      REWIND 9
C
      PI = 4.0 * ATAN(1.D0)
      TPI = 2.0 * PI
      FRAD = PI/180.0
C
      READ(9,100) ICOR,IMAS,ICMOD,ICTR,NGRID,NMOD
C
      IF(ICTR .LE. 1) GO TO 3
      IF(ICTR .GE. 3) GO TO 2
      READ(9,104) ALP
      GO TO 3
2     READ(9,106) VB(1),VB(2),VB(3),
+         VC(1),VC(2),VC(3)
C
3     IF(IMAS .EQ. 0) GOTO 9
C
      DO 5 I=1,IMAS
      READ(9,150) J1,J2,BMAS
        DO 4 J=J1,J2
4         CMASS(J) = BMAS
5     CONTINUE
C
9     DO 10 I=1,NGRID
10    READ(9,200) X1(I),X2(I),X3(I)
C
      IF(ICOR .EQ. 0) GO TO 30
C
      DO 20 I=1,NGRID
      R = X1(I)
      THTA = X2(I) * FRAD
      X1(I) = R * COS(THTA)
20    X2(I) = R * SIN(THTA)
C
30    DO 50 I=1,NMOD
      READ(9,300) IMOD
      READ(9,400) FREQ(IMOD)

```

```

      OMEGA(IMOD) = TPI * FREQ(IMOD)
C
      DO 40 J=1,NGRID
      READ(9,500) FIBX(J,IMOD),FIBY(J,IMOD),FIBZ(J,IMOD)
40    CONTINUE
50    CONTINUE
C
      IF(ICTR .LE. 1) GO TO 80
      IF(ICTR .GE. 3) GO TO 75
C
C    2-DIMENSIONAL COORDNATE TRANSFORM
C
      ALP = ALP * FRAD
      CP = COS(ALP)
      SP = SIN(ALP)
      DO 60 I=1,NGRID
      X = X1(I)
      Z = X3(I)
      X1(I) = X * CP + Z * SP
60    X3(I) = - X * SP + Z * CP
C
      DO 70 I=1,NMOD
      DO 65 J=1,NGRID
      X = FIBX(J,I)
      Z = FIBZ(J,I)
      FIBX(J,I) = X * CP + Z * SP
65    FIBZ(J,I) = - X * SP + Z * CP
70    CONTINUE
      GO TO 80
C
C    3-DIMENSIONAL COORDINATE TRANSFORM
C
75    CALL CTRN3(VB,VC,C)
C
      DO 76 I=1,NGRID
      VO(1) = X1(I)
      VO(2) = X2(I)
      VO(3) = X3(I)
      CALL TRN3(VO,VN,C)
      X1(I) = VN(1)
      X2(I) = VN(2)
76    X3(I) = VN(3)
      DO 78 I=1,NMOD
      DO 77 J=1,NGRID
      VO(1) = FIBX(J,I)
      VO(2) = FIBY(J,I)
      VO(3) = FIBZ(J,I)
      CALL TRN3(VO,VN,C)
      FIBX(J,I) = VN(1)
      FIBY(J,I) = VN(2)
77    FIBZ(J,I) = VN(3)
78    CONTINUE
C
C    WRITE OUTPUT FILE

```

```

C
80  WRITE(21,110) NGRID,NMOD
    IF(IMAS .EQ. 0) GO TO 85
    DO 83 I=1,NGRID
83  WRITE(21,160) I, CMASS(I)
85  DO 87 I=1,NGRID
87  WRITE(21,210) I, X1(I),X2(I),X3(I)
C
    DO 95 I=1,NMOD
    WRITE(21,410) I, FREQ(I), OMEGA(I)
        DO 90 J=1,NGRID
90  WRITE(21,550) J, FIBX(J,I), FIBY(J,I), FIBZ(J,I)
95  CONTINUE
C
C  FORMAT
C
100 FORMAT(10X,6I5)
104 FORMAT(F10.4)
106 FORMAT(10X,3F10.4/10X,3F10.4)
110 FORMAT(/'NUMBER OF GRIDS =' ,I5/'NUMBER OF MODES =' ,I5)
150 FORMAT(10X,2I5,D15.4)
160 FORMAT(I4,D15.6)
200 FORMAT(20X,F10.2,F10.4,F10.7)
210 FORMAT(3X,I4,3X,3D15.6)
300 FORMAT(8X,I4)
400 FORMAT(8X,D14.6)
410 FORMAT(/'MODE =' ,I5/'FREQUENCY =' ,F10.3,2X,'HZ'/'OMEGA =' ,D15.6)
500 FORMAT(24X,3D15.6)
550 FORMAT(3X,I4,3X,3D15.6)
C
    RETURN
    END
*****
*  SUBROUTINE CTRN3  *
*****
    SUBROUTINE CTRN3 (VB,VC,C)
    IMPLICIT REAL*8(A-H,O-Z)
    INTEGER I,I2,I3,IP2,IP3,J,K
    DIMENSION VB(3),VC(3),C(3,3)
    DIMENSION IP2(3),IP3(3)
    DIMENSION XN(3),YN(3),ZN(3)
    DATA IP2 /2,3,1/
    DATA IP3 /3,1,2/
C
    BL = 0.
    DO 10 I=1,3
10  BL = BL + VB(I) * VB(I)
    BL = DSQRT(BL)
    DO 20 I=1,3
20  ZN(I) = VB(I)/BL
    C(I,3) = ZN(I)
C
    DO 30 I=1,3
30  I2 = IP2(I)

```

```

      I3 = IP3(I)
30  YN(I) = ZN(I2) * VC(I3) - ZN(I3) * VC(I2)
      YL = 0.
      DO 40 I=1,3
40  YL = YL + YN(I) * YN(I)
      YL = DSQRT(YL)
      DO 50 I=1,3
      YN(I) = YN(I)/YL
50  C(I,2) = YN(I)
C
      DO 60 I=1,3
      I2 = IP2(I)
      I3 = IP3(I)
      XN(I) = YN(I2) * ZN(I3) - YN(I3) * ZN(I2)
60  C(I,1) = XN(I)
      RETURN
      END

```

```

*****
*      SUBROUTINE TRN3      *
*****
      SUBROUTINE TRN3 (VO,VN,C)
      IMPLICIT REAL*8(A-H,O-Z)
      INTEGER I,J,K
      DIMENSION VO(3),VN(3),C(3,3)
C
      DO 10 I=1,3
      VN(I) = 0.
          DO 10 J=1,3
10  VN(I) = VN(I) + C(I,J) * VO(J)
      RETURN
      END

```

```

C      CALCULATE A MATRIX ( UDOT COEFFICIENTS)
FIXED IER,IPVT,NPT,M,N,NPTC,MC
PARAM NPT=17 ,NPTC =63,M=4,MC=4
D      DIMENSION A(9,9)
D      DIMENSION UID21(10,10),UID22(10,10),UID32(10,10)
D      DIMENSION UJD21(10,10),UKD21(10,10),BU222(10,10),BU223(10,10)
D      DIMENSION B22UUJ(10,10),B22UUK(10,10),B32UUJ(10,10),UID31(10,10)
D      DIMENSION B3U213(10,10),B32UUK(10,10)
D      DIMENSION FIBX(17,10),FIBY(17,10),FIBZ(17,10),PSI1(10)
D      DIMENSION FICX(63,10),FICY(63,10),FICZ(63,10),PSI2(10)
D      DIMENSION PSI3(10),X1(63),X2(63),X3(63)
ARRAY IFVT(20)
ARRAY UID12(10),BU221(10),UID13(10),UJD11(10),UKD11(10)
ARRAY B12UUJ(10),B12UUK(10),B3U211(10)
ARRAY STRNB(10),STRNC(10),OMGAB(10),OMGAC(10)
INTEGER I,J,K,L
PARAM C1=.4,C2=10.,C3=24.65,DELT=.010
INITIAL
*      READ IN VALUES OF CONSTANTS
      READ (25,107)IDUM
      READ (25,102) UID11
      READ (25,107)IDUM1
      DO 1 J= 1,10
      READ(25,103)L,UID12(J),UJD11(J),B12UUJ(J),BU221(J),OMGAB(J)
1      CONTINUE
      READ (25,107)IDUM
      DO 2 K = 1,10
      READ(25,103)L,B12UUK(K),UID13(K),UKD11(K),B3U211(K),OMGAC(K)
2      CONTINUE
      READ (25,107)IDUM
      DO 3 I = 1,10
      DO 4 J = 1,10
      READ(25,106)L,L,UJD21(J,I),UID21(J,I),BU222(J,I),B22UUJ(J,I)
4      CONTINUE
3      CONTINUE
      READ (25,107)IDUM
      DO 5 K = 1,10
      DO 6 I = 1,10
      READ(25,104)L,L,UID32(I,K),B3U213(I,K),B32UUK(I,K)
6      CONTINUE
5      CONTINUE
      READ (25,107)IDUM
      DO 7 K =1,10
      DO 8 J = 1,10
      READ(25,106)L,L,UID22(J,K),UKD21(J,K),BU223(J,K),B22UUK(J,K)
8      CONTINUE
7      CONTINUE
      READ (25,107)IDUM
      DO 98 K = 1,10
      DO 99 J = 1,10
      READ (25,105) L,L,UID31(J,K),B32UUJ(J,K)
99      CONTINUE
93      CONTINUE
102     FORMAT (D15.6)

```

```

103  FORMAT (I4,5D13.6)
104  FORMAT(2I4,3D15.6)
105  FORMAT (2I4,2D15.6)
106  FORMAT (2I4,4D15.6)
107  FORMAT (I5)
      DO 94 J = 1,10
      DO 95 I =1,NPT
          READ(25,900)FIBX(I,J),FIBY(I,J),FIBZ(I,J)
95   CONTINUE
94   CONTINUE
      DO 96 J = 1,10
      DO 97 I = 1,NPTC
          READ (25,900) FICK(I,J),FICY(I,J),FICZ(I,J)
97   CONTINUE
96   CONTINUE
      DO 93 J = 1,10
      READ (25,900) PSI1(J),PSI2(J),PSI3(J)
93   CONTINUE
      DO 92 I =1,NFTC
          READ (25,900) X1(I),X2(I),X3(I)
92   CONTINUE
900  FORMAT (3D20.6)
      CALL STRNEG (M,CMGAB,STRNB)
      CALL STRNEG (MC,OMGAC,STRNC)
      DO 91 J =1,M
          WRITE (21,900) PSI1(J),PSI2(J),PSI3(J)
91   CONTINUE
DERIVATIVE
NOSORT
*   TA = 10.-10.*STEP(6.85)
      T1 = 2.
      TAO1 = 80.*TIME**2
      TAO2 = 320.*(1.-STEP(5.))
      TA = SWITCH(TIME .LE. T1,TAO1,TAO2)
*   TA = 5.
*   TA + 10.-10.*STEP(6.85)
      A11QB = 0.
      B12UJ = 0.
      DO 40 J = 1,M
          A11QB = Q(J+1) * U1D12(J) + A11QB
          B12UJ = B12UUJ(J) * U(1+J)+ B12UJ
          DO 10 I =J,M
              A(1+J,1+I) = UJD21(J,I)
              A(1+I,1+J) = A(1+J,1+I)
10   CONTINUE
      A1J1QB = 0.
      BJU2QB = 0.
      BJ2UUJ = 0.
      DO 20 I = 1,M
          A1J1QB =U1D21(J,I)*Q(1+I) + A1J1QB
          BJU2QB= BU222(J,I)*Q(1+I) + BJU2QB
          BJ2UUJ=B22UUJ(J,I)*U(1+I) + BJ2UUJ
20   CONTINUE
      A1J1QC = 0.

```

```

      BJU2QC = 0.
      BJ2UUK = 0.
      DO 30 K = 1,MC
        A1J1QC= UID22(J,K) *Q(1+M+K) + A1J1QC
        A(1+M+K,1+J)=UKD21(J,K)
        A(1+J,1+M+K) = A(1+M+K,1+J)
        BJU2QC= BU223(J,K)*Q(1+M+K) + BJU2QC
        BJ2UUK = B22UUK(J,K) *U(1+M+K)
30    CONTINUE
      A(1+J,1) = UJD11(J) + A1J1QB + A1J1QC
      A(1,1+J) = A(1+J,1)
      B(1+J)=U(1)*U(1)*(BU221(J)+BJU2QB+BJU2QC)...
          +2*U(1)*(BJ2UUJ + BJ2UUK)- STRNB(J)*Q(1+J)
40    CONTINUE
      A11QC = 0.
      B12UK = 0.
      DO 60 K = 1,MC
        B12UK = B12UUK(K)*U(1+M+K) + B12UK
        A1K1QC = 0.
        A1K1QB = 0.
        BKU2QC = 0.
        BK2UUK = 0.
        DO 50 I = 1,MC
          A1K1QC = Q(1+M+I) * UID32(I,K) + A1K1QC
          BKU2QC = B3U213(I,K)*Q(1+M+I) + BKU2QC
          BK2UUK =B32UUK(I,K)*U(1+M+I) + BK2UUK
          A(1+M+I,1+M+K) = 0.
50    CONTINUE
        BKU2QB = 0.
        BK2UUJ = 0.
        DO 55 J = 1,M
          A1K1QB = Q(1+J)* UID31(J,K) + A1K1QB
          BKU2QB = BU223(J,K) *Q(1+J) + BKU2QB
          BK2UUJ =B32UUJ(J,K)*U(1+J) + BK2UUJ
55    CONTINUE
        A11QC = Q(1+M+K) * UID13(K) + A11QC
        A(1+M+K,1+M+K) = 1.
        A(1+M+K,1) = UKD11(K) + A1K1QB + A1K1QC
        A(1,1+M+K) = A(1+M+K,1)
        B(1+M+K) = U(1)*U(1)*(B3U211(K)+BKU2QB+BKU2QC)+ ...
          2*U(1)*(BK2UUJ+B12UUK) -STRNB(K)*Q(1+M+K)
60    CONTINUE
      A(1,1)= UID11 + A11QB + A11QC
      B(1) = 2*U(1)*( B12UUJ + B12UK )+ TA
      WRITE(22,200)((A(I,J),J=1,1+M+MC),I=1,1+M+MC)
200  FORMAT(3E14.6)
      *
      CALL DGEFA(A,9,9,IPVT,IER)
      *
      WRITE(8,300) IER
300  FORMAT (I20)
      IF (IER.NE. 0) GO TO 100
      CALL DGESL (A,9,9,IPVT,B,D)
      *
      WRITE(4,200) (B(I),I=1,1+M+MC)
      U =INTEGR(D.,B.?)

```

```

      Q = INTGRL(0.,U,9)
*CALCULATE VARIOUS DISPLACEMENTS AT THREE LOCATIONS AND ROTATIONS AT TIF
      XHDISP = 0.
      YHDISP = 0.
      ZHDISP = 0.
      XHROT = 0.
      YHROT = 0.
      ZHROT = 0.
      DO 70 I = 1,M
          XHDISP = XHDISP + Q(I+1)*FIBX(NPT,I)
          YHDISP = YHDISP + Q(I+1)*FIBY(NPT,I)
          ZHDISP = ZHDISP + Q(I+1)*FIBZ(NPT,I)
          XHROT = XHROT + Q(I+1)*PSI1(I)
          YHROT = YHROT + Q(I+1)*PSI2(I)
          ZHROT = ZHROT + Q(I+1)*PSI3(I)
70    CONTINUE
      X1REL = 0.
      Y1REL = 0.
      Z1REL = 0.
      X4REL = 0.
      Y4REL = 0.
      Z4REL = 0.
      DO 80 I = 1,MC
          X1REL = X1REL + Q(I+1+M)*FICK(1,I)
          Y1REL = Y1REL + Q(I+1+M)*FICY(1,I)
          Z1REL = Z1REL + Q(I+1+M)*FICZ(1,I)
          X4REL = X4REL + Q(I+1+M)*FICK(4,I)
          Y4REL = Y4REL + Q(I+1+M)*FICY(4,I)
          Z4REL = Z4REL + Q(I+1+M)*FICZ(4,I)
80    CONTINUE
      X1DISP = XHDISP + X1REL + (YHROT*X3(1) - ZHROT*X2(1))
      Y1DISP = YHDISP + Y1REL + (ZHROT*X1(1) - XHROT*X3(1))
      Z1DISP = ZHDISP + Z1REL + (XHROT*X2(1) - YHROT*X1(1))
      X4DISP = XHDISP + X4REL + (YHROT*X3(4) - ZHROT*X2(4))
      Y4DISP = YHDISP + Y4REL + (ZHROT*X1(4) - XHROT*X3(4))
      Z4DISP = ZHDISP + Z4REL + (XHROT*X2(4) - YHROT*X1(4))
      RETURN
100   WRITE(6,101) TIME, IER
101   FORMAT('0 IER =',I7)
      CALL ENDOJOB
      PRINT TA,Q(1-5),U(1-5)
      CONTRL FINTIM=10.,DELPRT = .1
      SAVE .015,TA,Q(1),Q(2),Q(3),Q(4),Q(5),Q(6),Q(7),Q(8),Q(9),...
          U(1),XHDISP,YHDISP,ZHDISP,XHROT,YHROT,ZHROT,X1DISP,...
          Y1DISP,Z1DISP,X4DISP,Y4DISP,Z4DISP
*PAFH (G1,NI=7,DE=TEK618) TIME(NI=5,LE=10.,UN= ...
+      'SEC'), TA(UN='LB-IN')
*PAFH (G2,NI=7,DE=TEK618) TIME(NI=5,LE=10.,UN='SEC') ...
+      Q(1)(UN='RAD')
*PAFH (G3,NI=7,DE=TEK618) TIME(NI=5,LE=10.,UN='SEC') ...
+      U(1)(UN='RAD/SEC')
*PAFH (G4,NI=7,DE=TEK618) TIME(NI=5,LE=10.,UN='SEC') ...
+      Q(2)(UN='IN')
*PAFH (G5,NI=7,DE=TEK618) TIME(NI=5,LE=10.,UN='SEC') ...

```

```

*      , Q(3)(UN='IN')
*RAFH (G6,NI=7,DE=TEK618) TIME(NI=5,LE=10.,UN='SEC') ...
*      , Q(4)(UN='IN')
*RAFH (G7,NI=7,DE=TEK618) TIME(NI=5,LE=10.,UN='SEC') ...
*      , Q(5)(UN='IN')
*RAFH (G7A,NI=7,DE=TEK618) TIME(NI=5,LE=10.,UN='SEC') ...
*      , Q(6)(UN='IN')
*RAFH (G7B,NI=7,DE=TEK618) TIME(NI=5,LE=10.,UN='SEC') ...
*      , Q(7)(UN='IN')
*RAFH (G7C,NI=7,DE=TEK618) TIME(NI=5,LE=10.,UN='SEC') ...
*      , Q(8)(UN='IN')
*RAFH (G7D,NI=7,DE=TEK618) TIME(NI=5,LE=10.,UN='SEC') ...
*      , Q(9)(UN='IN')
*RAFH (G8,NI=7,DE=TEK618) TIME(NI=5,LE=10.,UN='SEC') ...
*      ,XHDISP(UN='IN',LI=5,LO=-10.,SC=2.)
GRAPH (G9,NI=7,DE=TEK618) TIME(NI=5,LE=10.,UN='SEC') ...
      ,YHDISP(UN='IN',LI=4,LO=-2.,SC=1.)
*RAFH (GA,NI=7,DE=TEK618) TIME(NI=5,LE=10.,UN='SEC') ...
*      ,ZHDISP(UN='IN',LI=4)
GRAPH (GR3,NI=7,DE=TEK618) TIME(NI=5,LE=10.,UN='SEC') ...
      ,XHROT(UN='RAD',LI=4,LO=-.020,SC=.005)
*RAFH (GR9,NI=7,DE=TEK618) TIME(NI=5,LE=10.,UN='SEC') ...
*      ,YHROT(UN='RAD')
*RAFH (GRA,NI=7,DE=TEK618) TIME(NI=5,LE=10.,UN='SEC') ...
*      ,ZHROT(UN='RAD')
*RAFH (GB,NI=7,DE=TEK618) TIME(NI=5,LE=10.,UN='SEC') ...
*      ,XIDISP(UN='IN',LI=5,LO=-20.,SC=5.)
GRAPH (GC,NI=7,DE=TEK618) TIME(NI=5,LE=10.,UN='SEC') ...
      ,YIDISP(UN='IN',LI=4,LO=-3.,SC=2.)
*GRAPH (GD,NI=7,DE=TEK618) TIME(NI=5,LE=10.,UN='SEC') ...
*      ,ZIDISP(UN='IN')
*GRAPH (GE,NI=7,DE=TEK618) TIME(NI=5,LE=10.,UN='SEC') ...
*      ,X4DISP(UN='IN',LI=5,LO=-3.,SC=2.)
GRAPH (GF,NI=7,DE=TEK618) TIME(NI=5,LE=10.,UN='SEC') ...
      ,Y4DISP(UN='IN',LI=4,LO=-1.,SC=1.)
*GRAPH (GG,NI=7,DE=TEK618) TIME(NI=5,LE=10.,UN='SEC') ...
*      ,Z4DISP(UN='IN')
LABEL (G1) APPLIED TORQUE
LABEL (G2) ANGULAR DISPLACEMENT
LABEL (G3) ANGULAR VELOCITY
LABEL (G4) GENERALIZED DISPLACEMENT Q1
LABEL (G5) GENERALIZED DISPLACEMENT Q2
LABEL (G6) GENERALIZED DISPLACEMENT Q3
LABEL (G7) GENERALIZED DISPLACEMENT Q4
LABEL (G7A) GENERALIZED DISPLACEMENT Q5
LABEL (G7B) GENERALIZED DISPLACEMENT Q6
LABEL (G7C) GENERALIZED DISPLACEMENT Q7
LABEL (G7D) GENERALIZED DISPLACEMENT Q8
LABEL (G8) X REFLECTION AT BUSH TIP
LABEL (G9) Y REFLECTION AT BUSH TIP
LABEL (GA) Z REFLECTION AT BUSH TIP
LABEL (GB) X ROTATION AT BUSH TIP
LABEL (GC) Y ROTATION AT BUSH TIP
LABEL (GD) Z ROTATION AT BUSH TIP

```

```
LABEL (GB) X DEFLECTION AT DISH POINT 1
LABEL (GC) Y DEFLECTION AT DISH POINT 1
LABEL (GD) Z DEFLECTION AT DISH POINT 1
LABEL (GE) X DEFLECTION AT DISH POINT 4
LABEL (GF) Y DEFLECTION AT DISH POINT 4
LABEL (GG) Z DEFLECTION AT DISH POINT 4
```

```
END
```

```
STOP
```

```
FORTRAN
```

```
*****
*      STRAIN ENERGY      *
*****
```

```
      SUBROUTINE STRNEG (M,OMEGA,STRAIN)
      REAL*8 OMEGA(10),STRAIN(10)
      DO 10 I = 1,M
         STRAIN(I) = OMEGA(I)**2
10     CONTINUE
      RETURN
      END
```

APPENDIX F

FIGURES

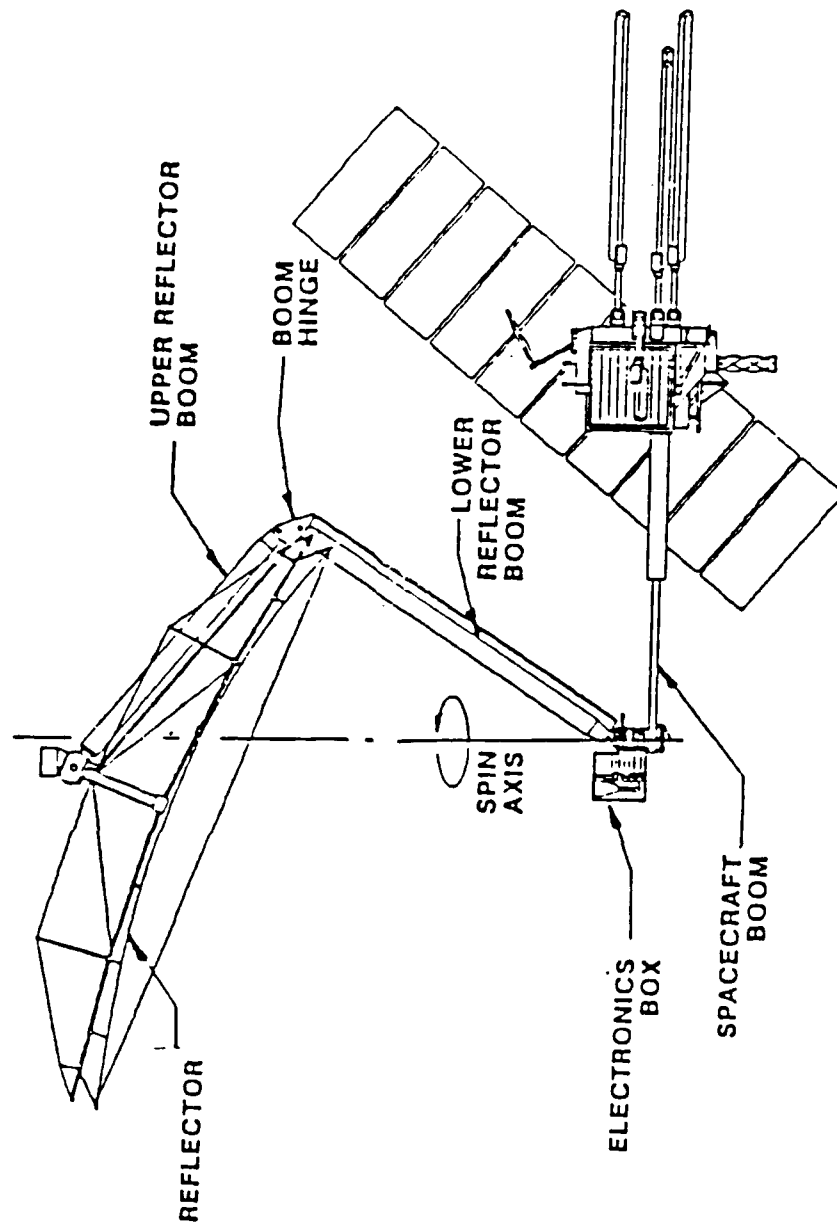


Figure 2.1
NROSS Baseline Configuration

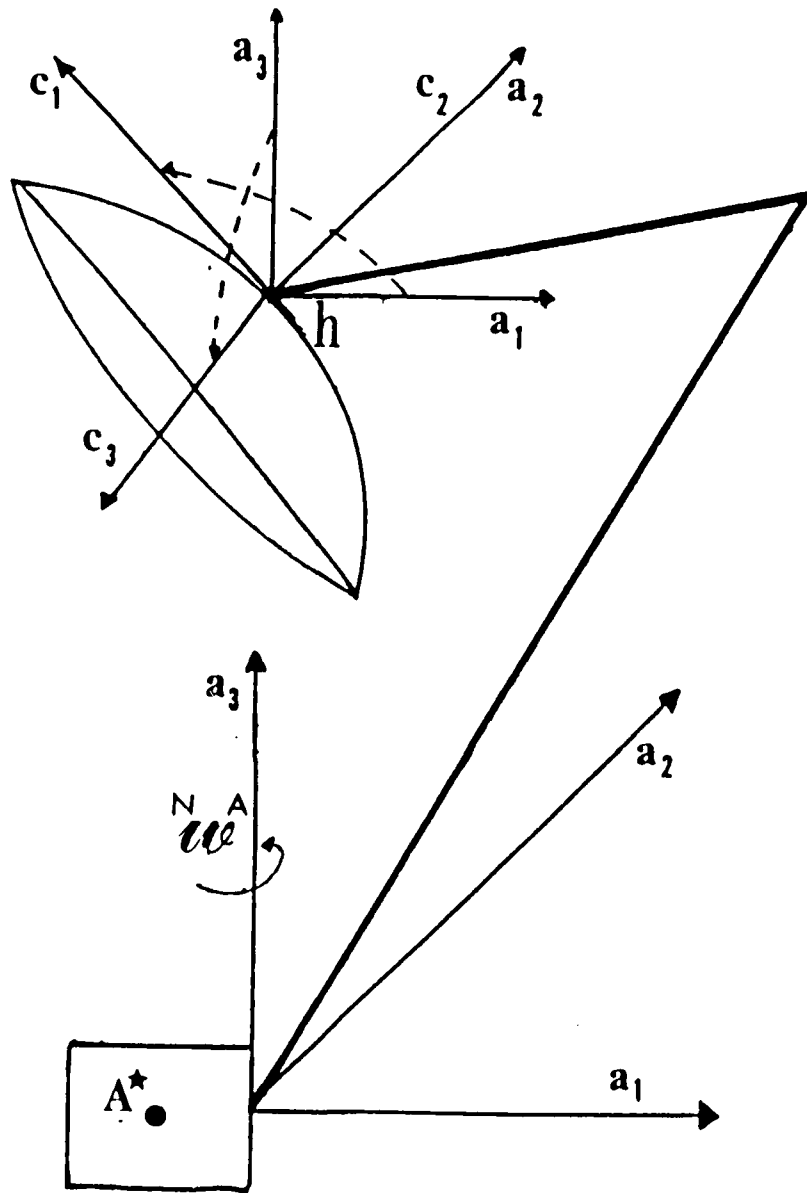


Figure 2.2
LFMR Model

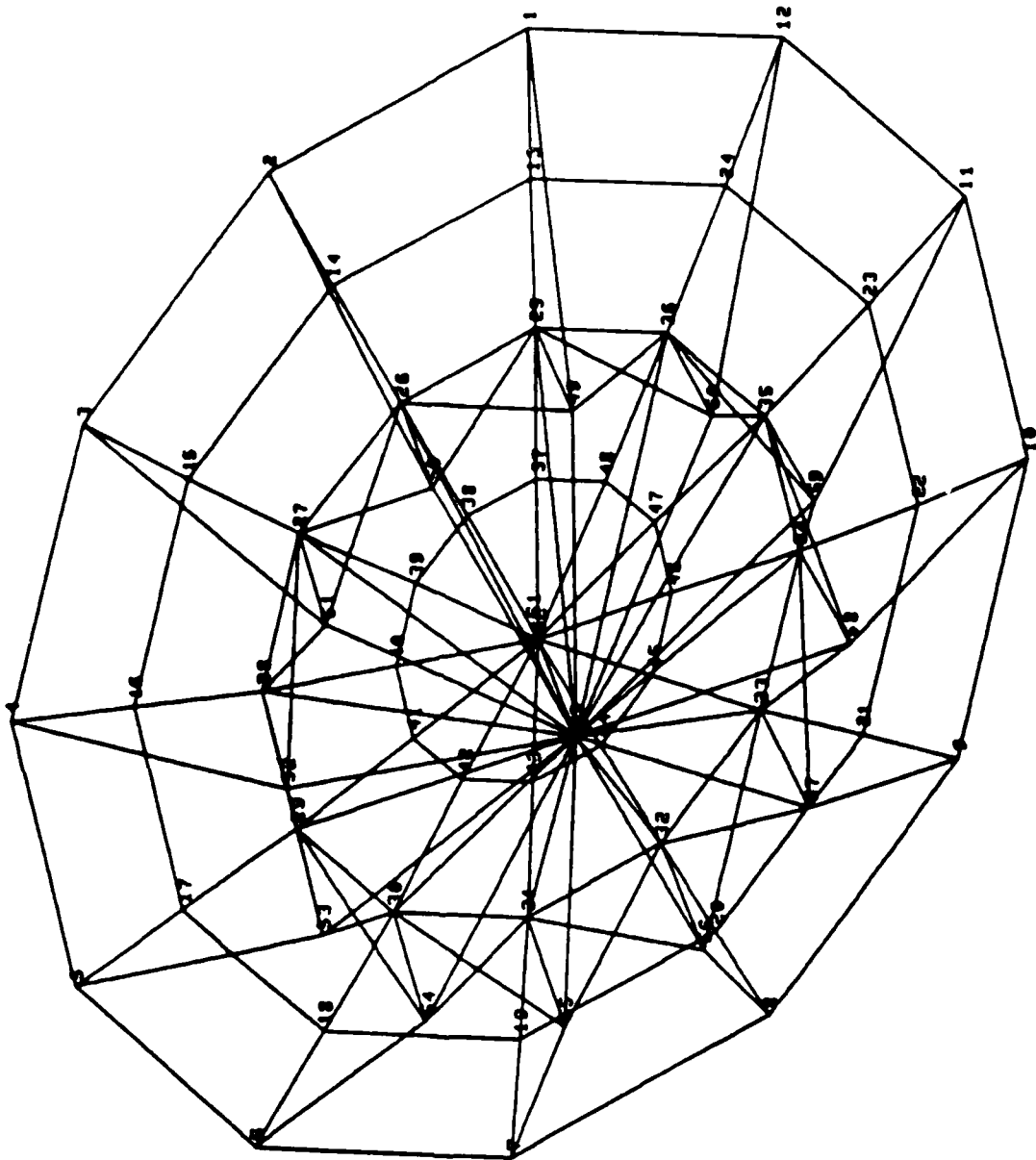


Figure A.1
Undeformed Reflector

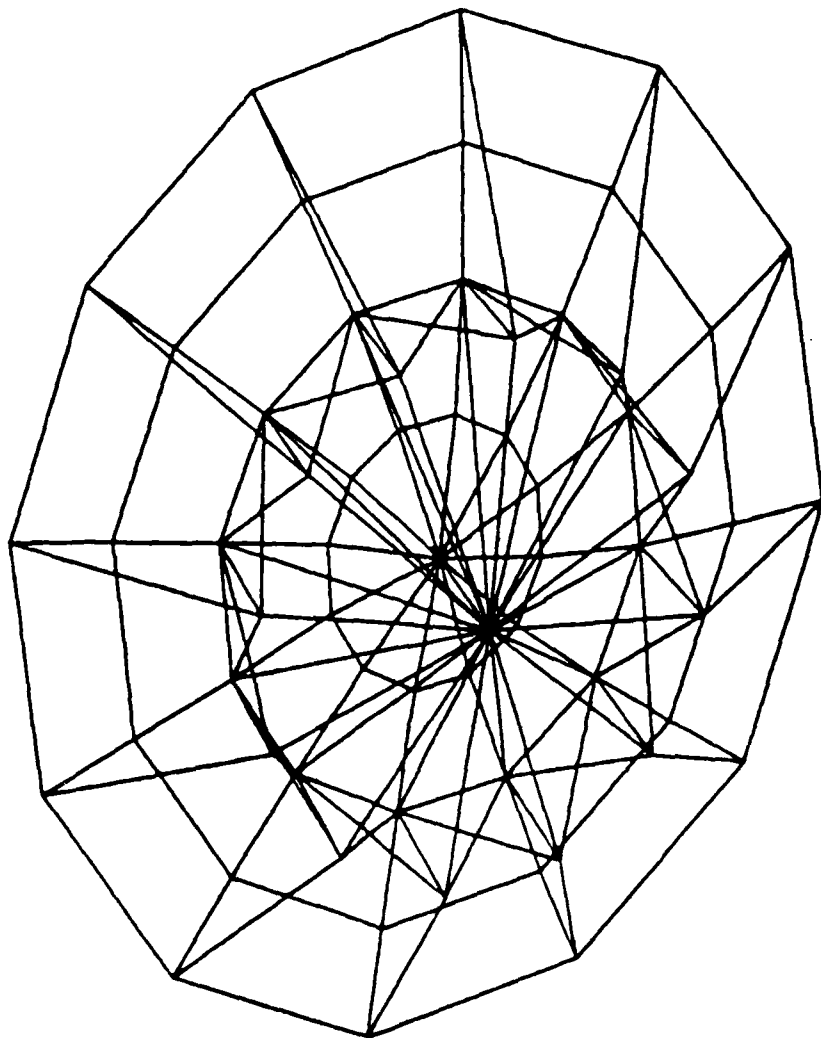


Figure A.2
First Mode of Reflector

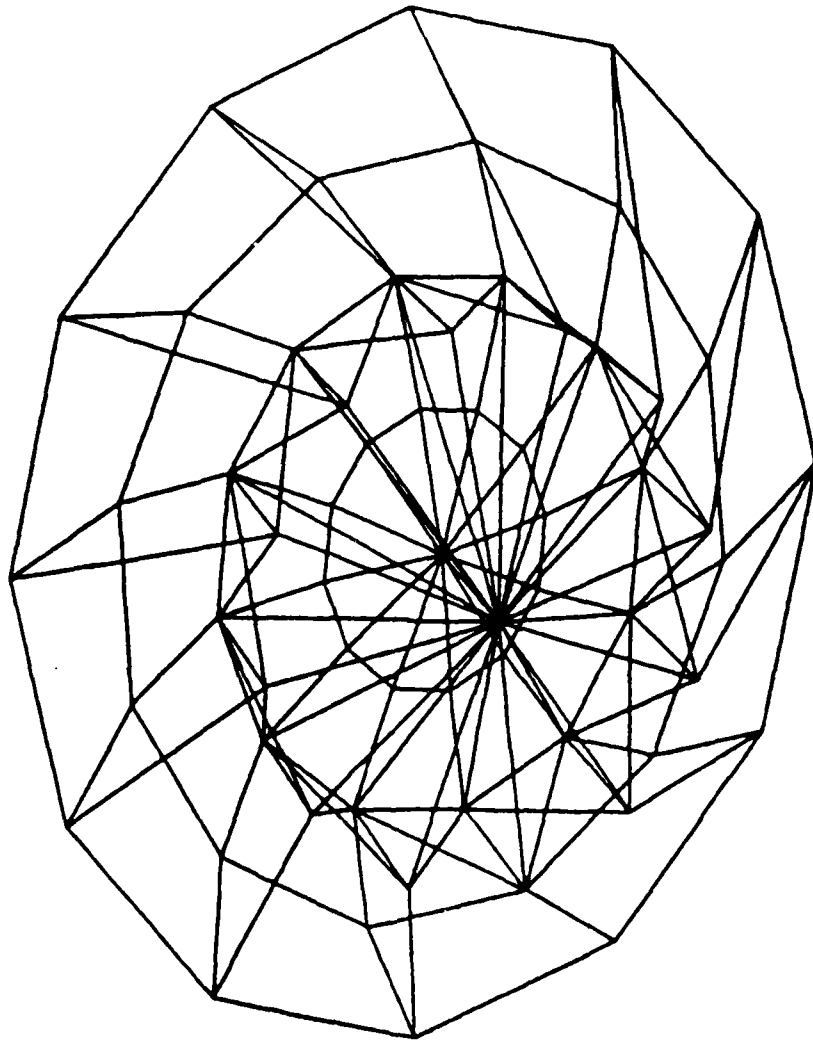


Figure A.3

Second Mode of Reflector

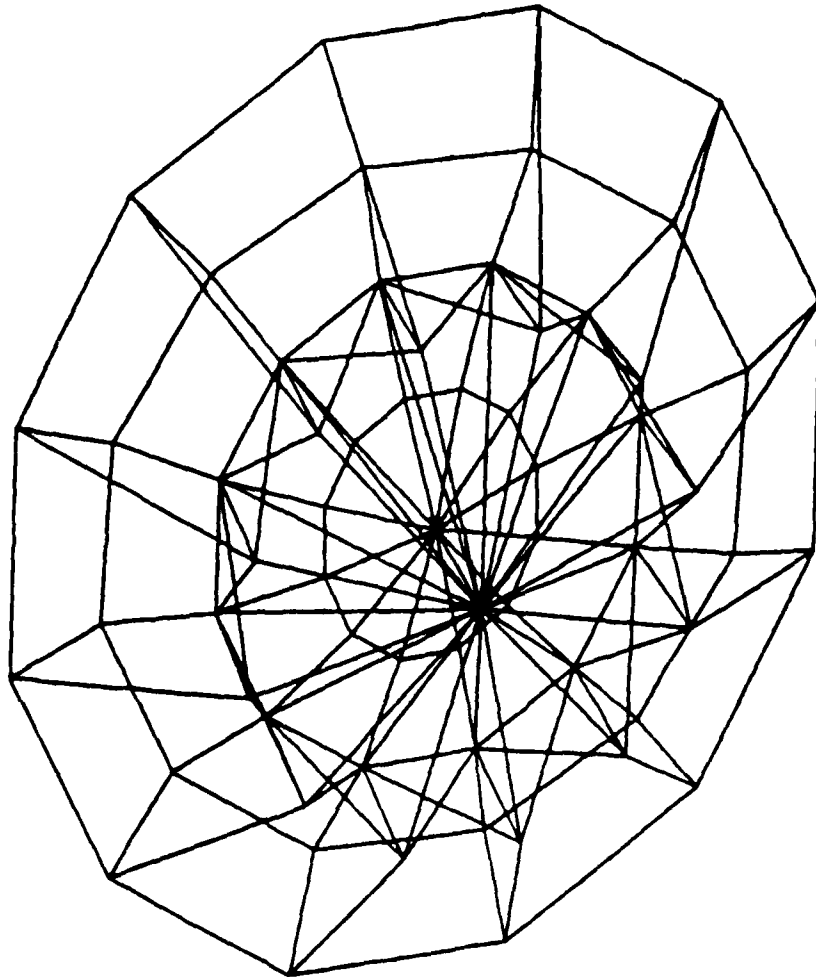


Figure A.4
Third Mode of Reflector

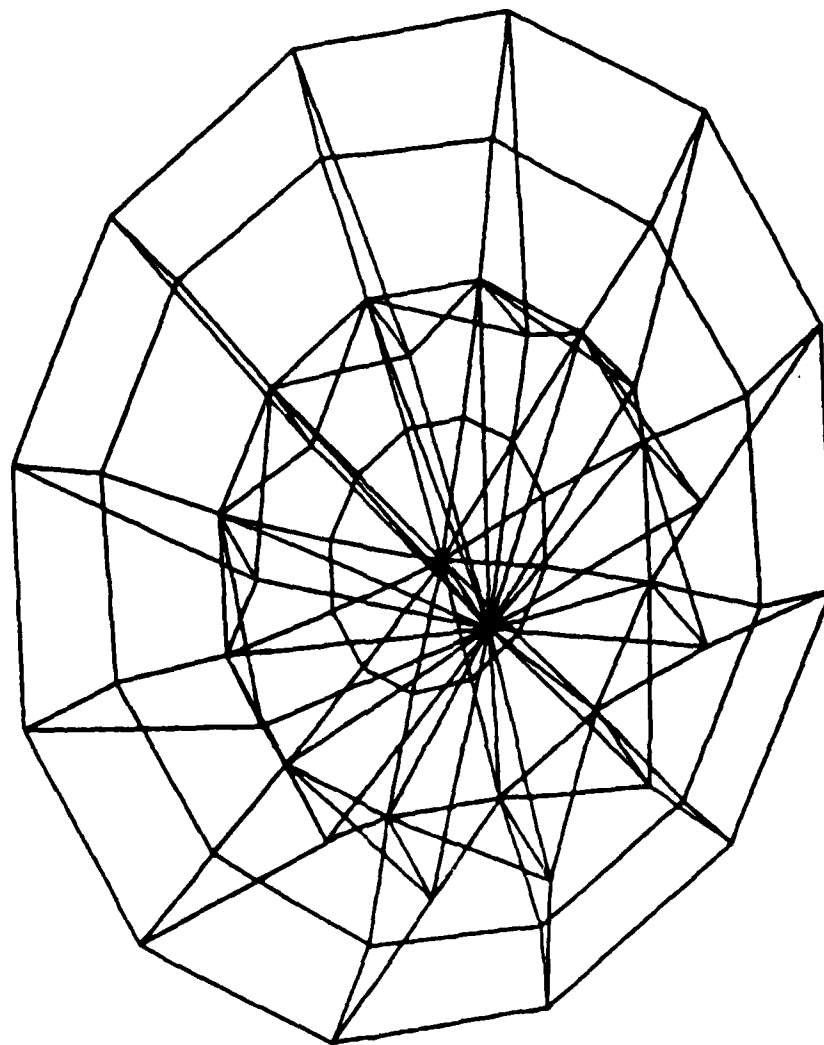


Figure A.5

Fourth Mode of Reflector

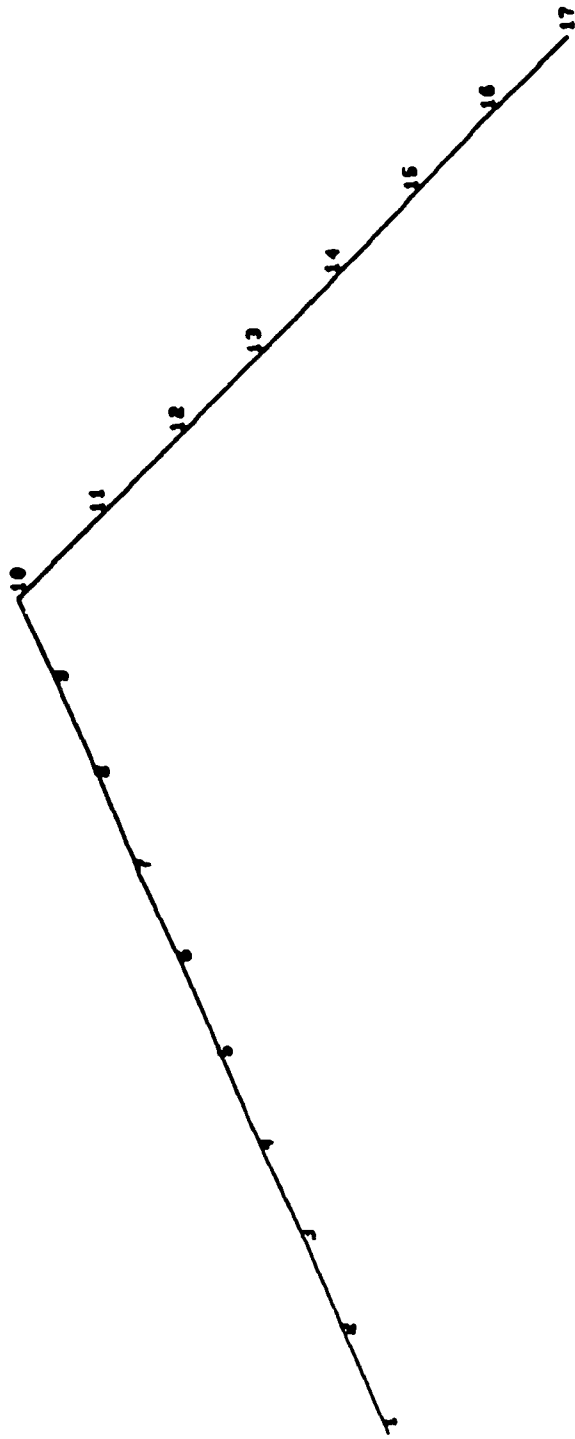


Figure A.6
Undeformed Boom

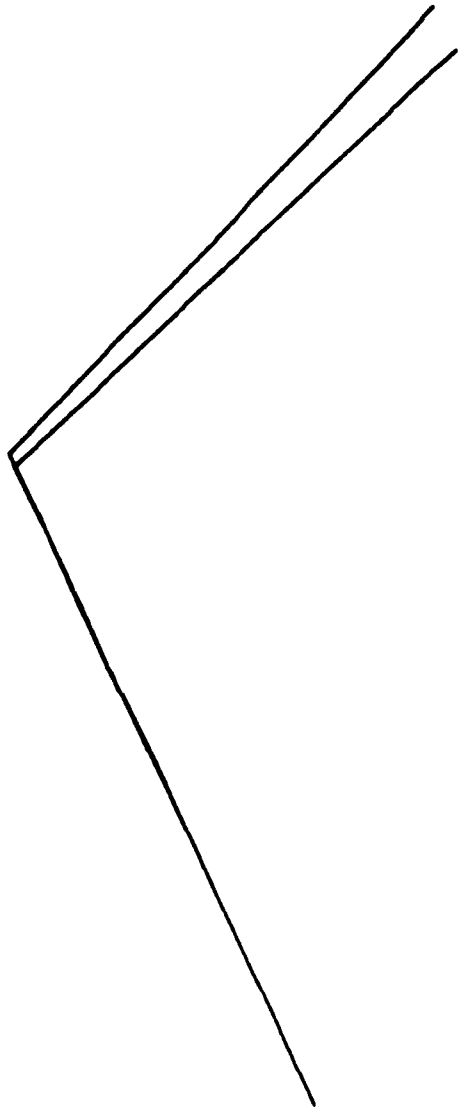


Figure A.7
First Mode of Boom

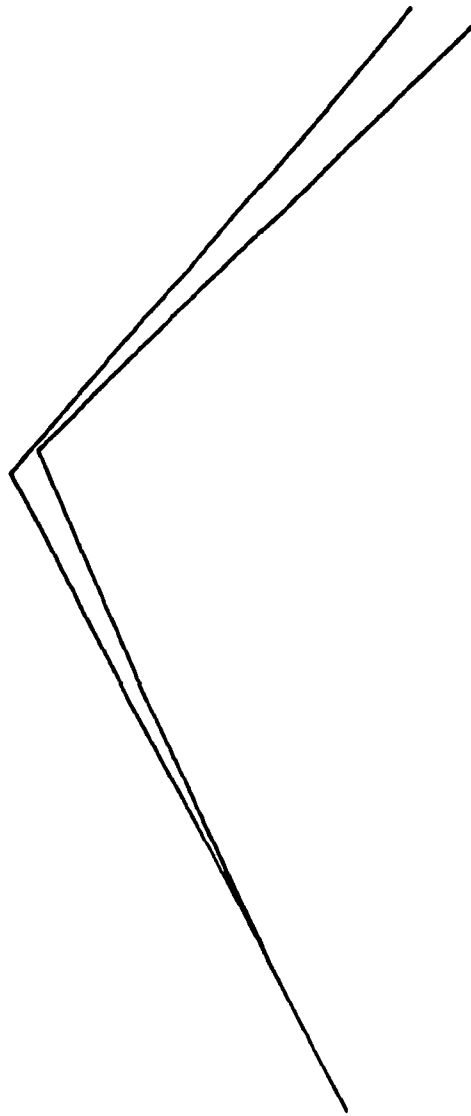


Figure A.8
Second Mode of Boom

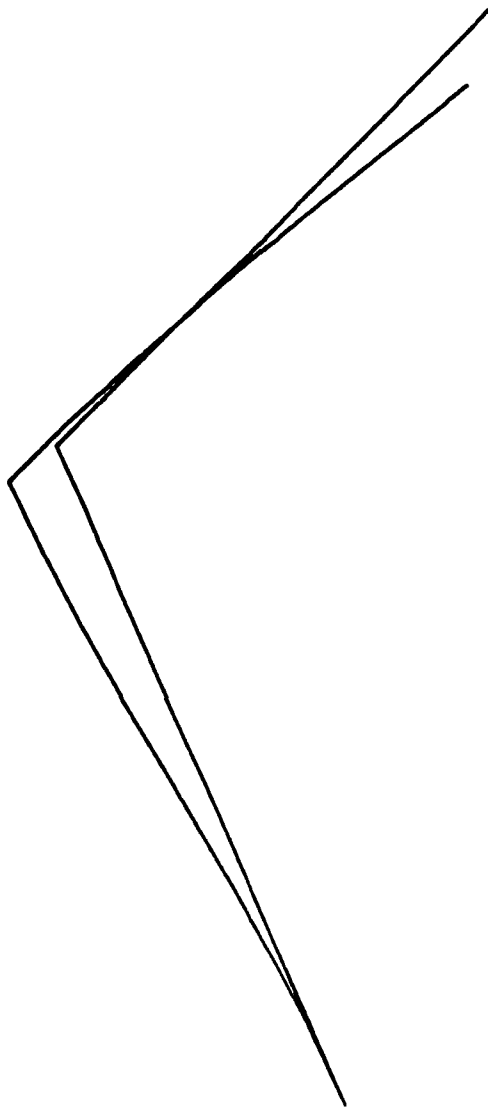


Figure A.9
Third Mode of Boom

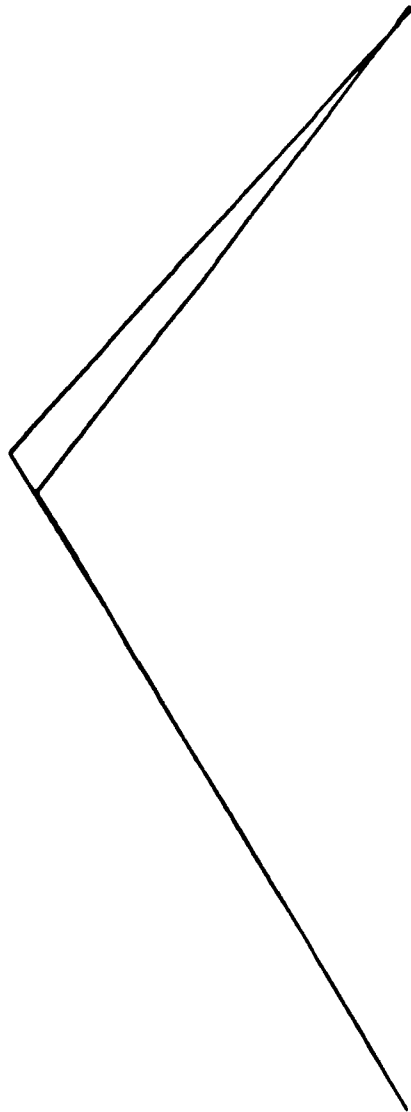


Figure A.10
Fourth Mode of Boom

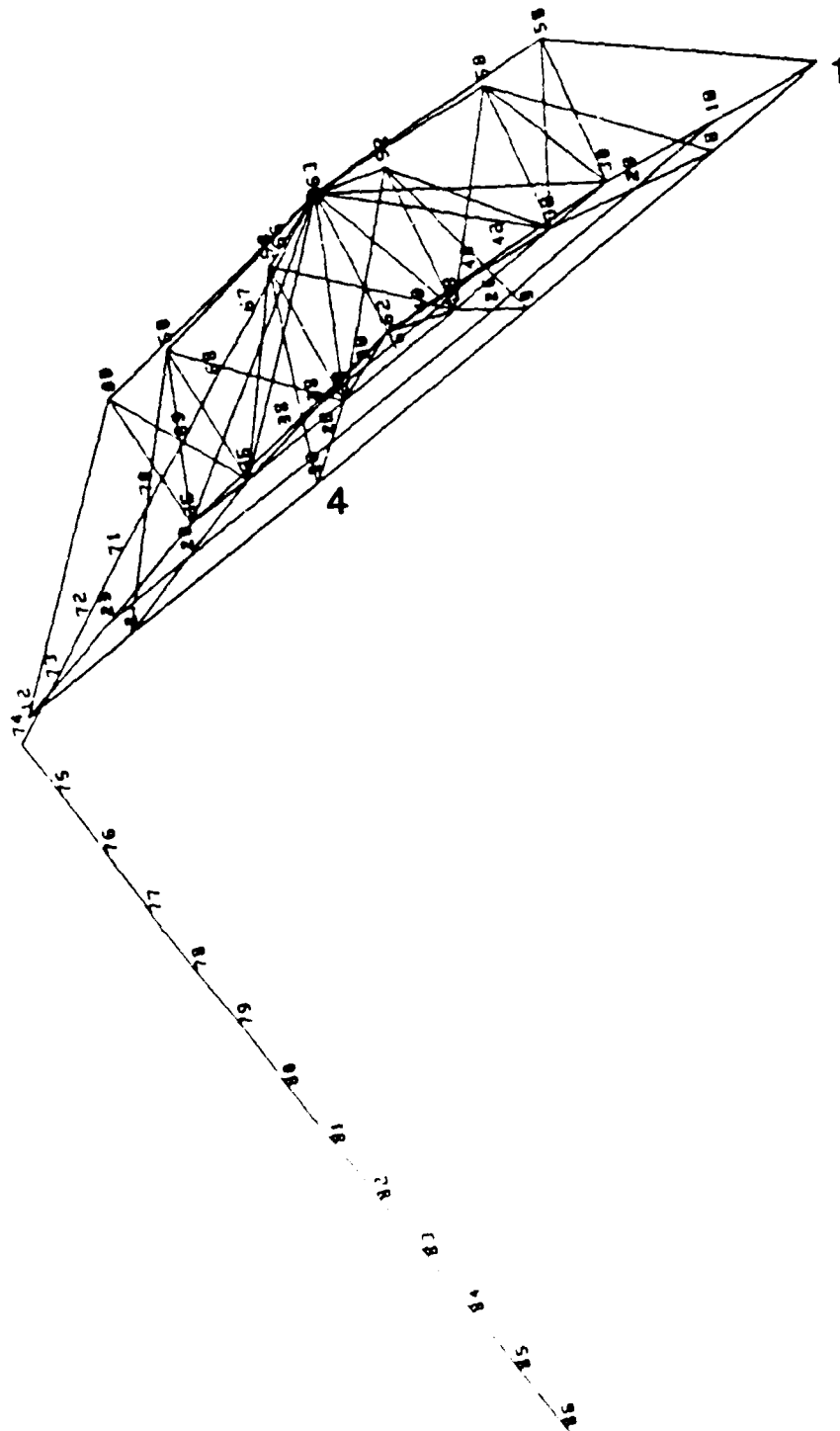


Figure 4.1

Finite Element Model of LFMR System

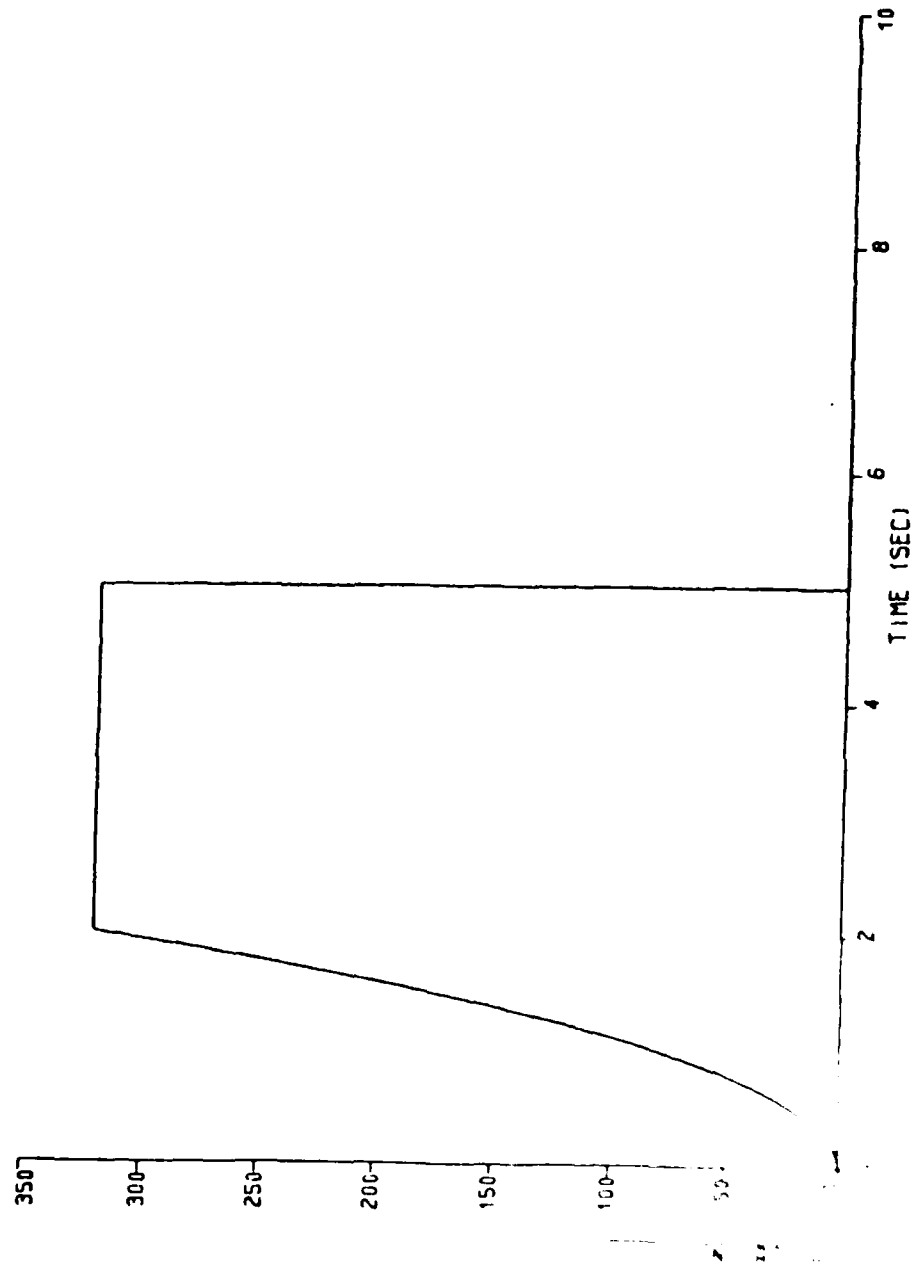


Figure 4.2
Applied Torque History During the Spin

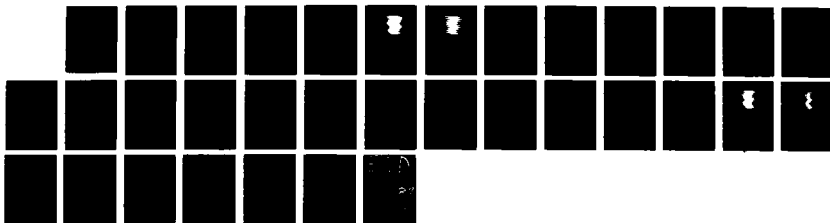
AD-A184 452

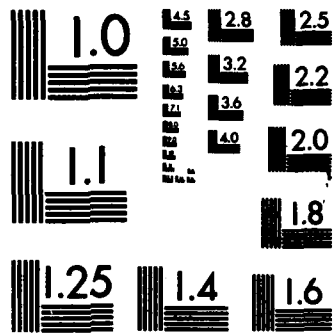
A MULTIBODY DYNAMIC ANALYSIS OF THE N-ROSS (NAVY REMOTE
OCEAN SENSING SYS (U) NAVAL POSTGRADUATE SCHOOL 2/2
MONTEREY CA N F HEFFERNAN JUN 87

UNCLASSIFIED

F/G 22/2

NL





MICROCOPY RESOLUTION TEST CHART
NATIONAL BUREAU OF STANDARDS-1963-A

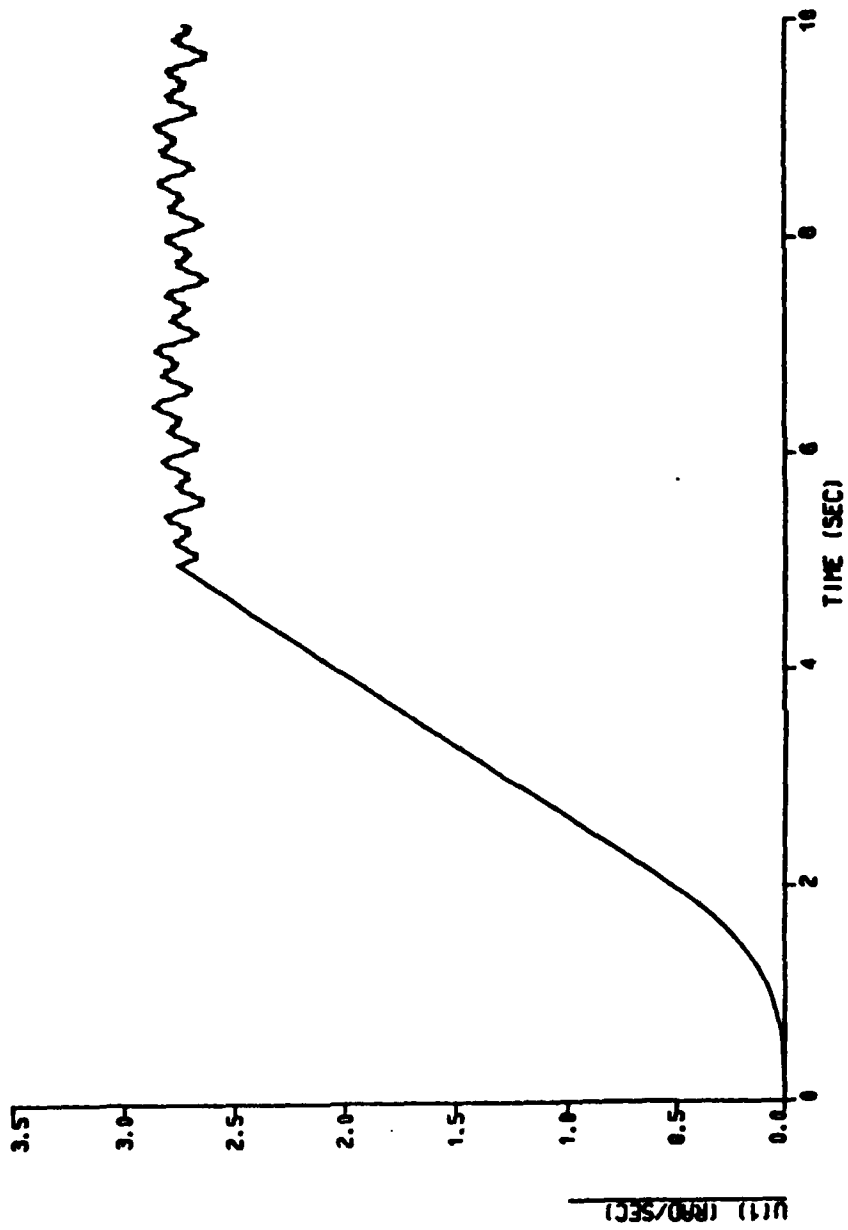


Figure B.1

Angular Velocity of Stiffer Reflector at -155°

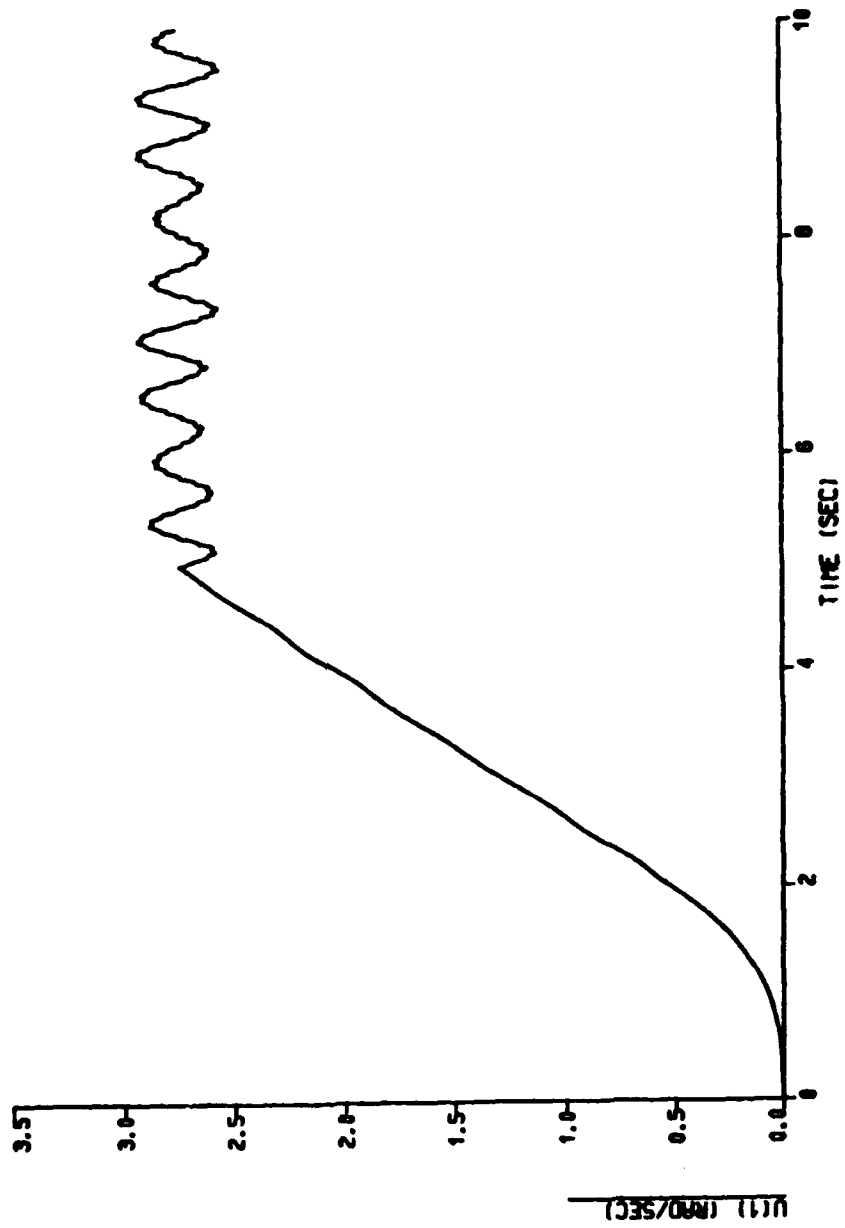


Figure B.2

Angular Velocity of More Flexible Reflector at -155°

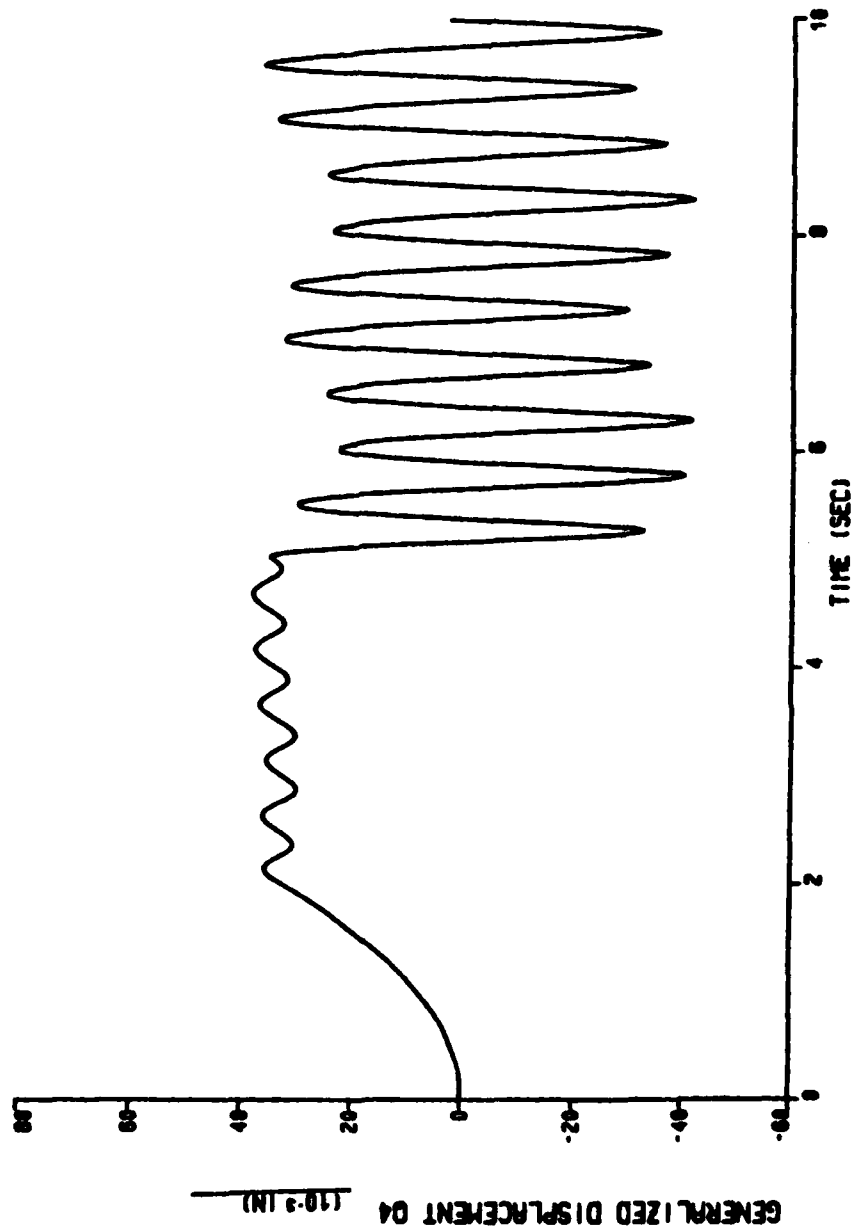


Figure B.3

Fourth Boom Generalized Coordinate of Stiffer Reflector at -155°

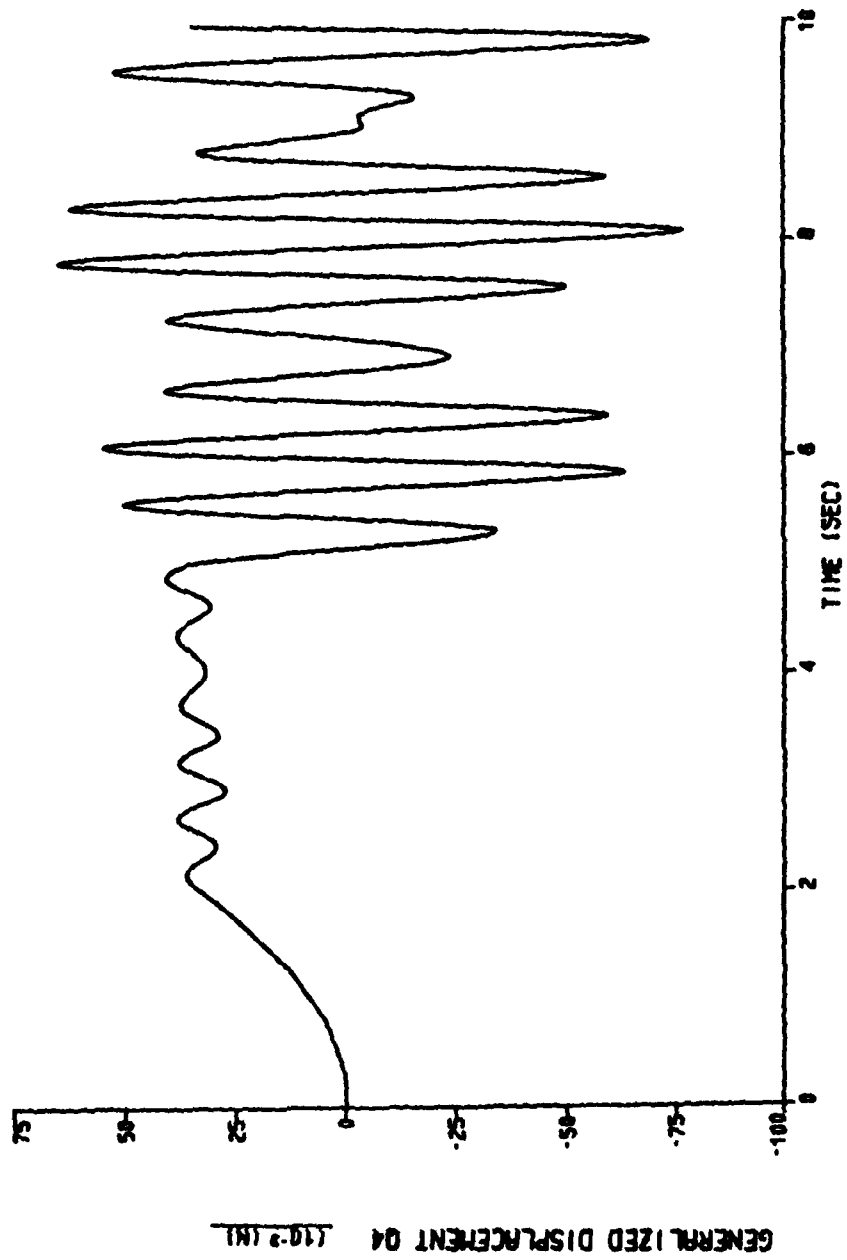


Figure B.4

**Fourth Boom Generalized Coordinate of
More Flexible Reflector at -155°**

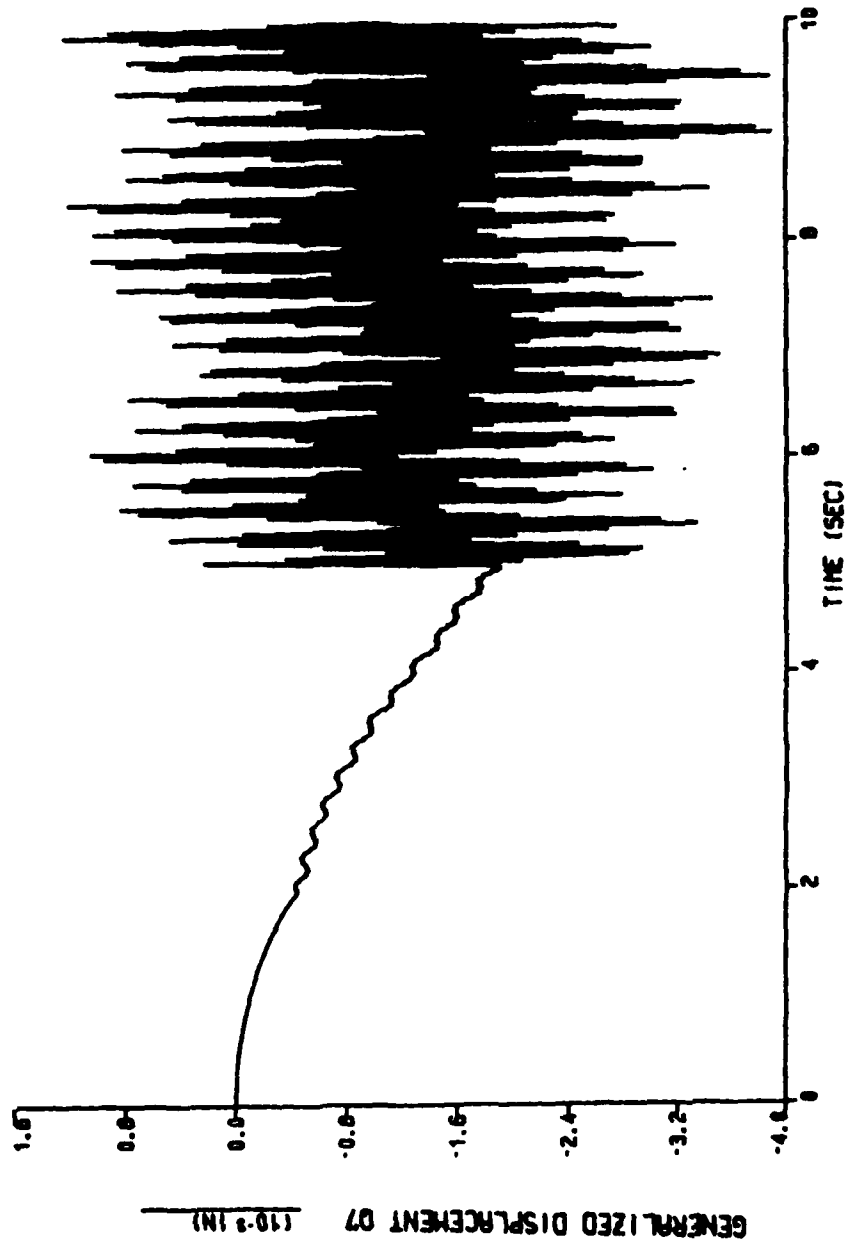


Figure B.5

**Third Reflector Generalized Coordinate of
Stiffer Reflector at -155°**

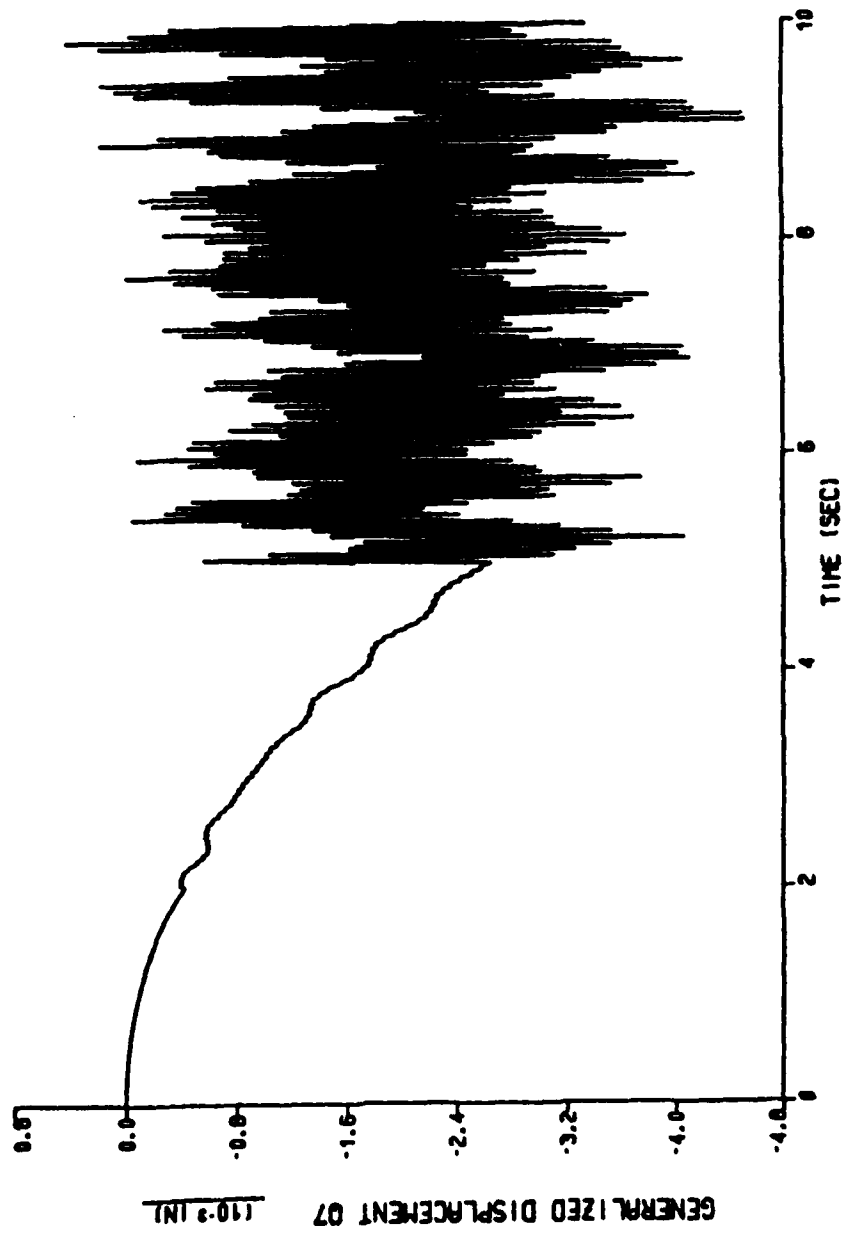


Figure B.6

**Third Reflector Generalized Coordinate of
More Flexible Reflector at -155°**

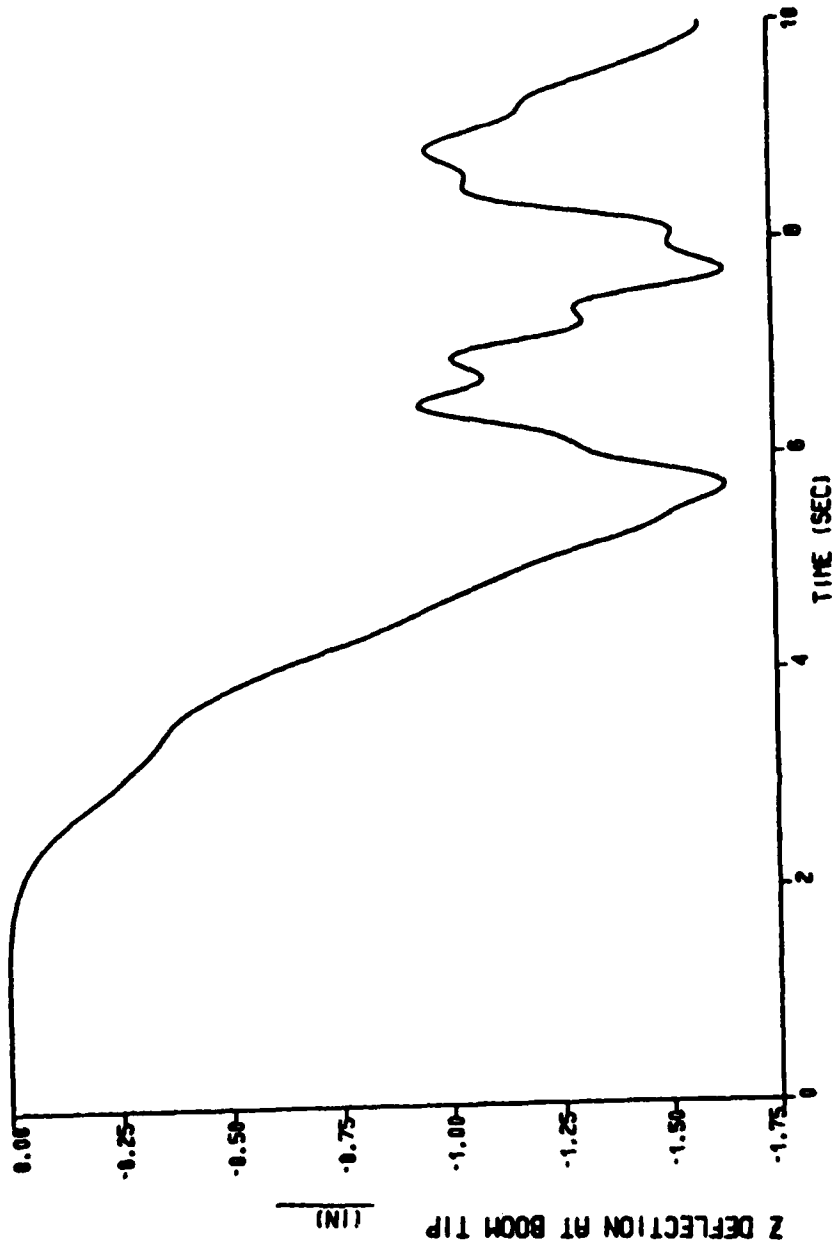


Figure B.7
 Vertical Deflection at Boom Tip of Stiffer Reflector at -155°

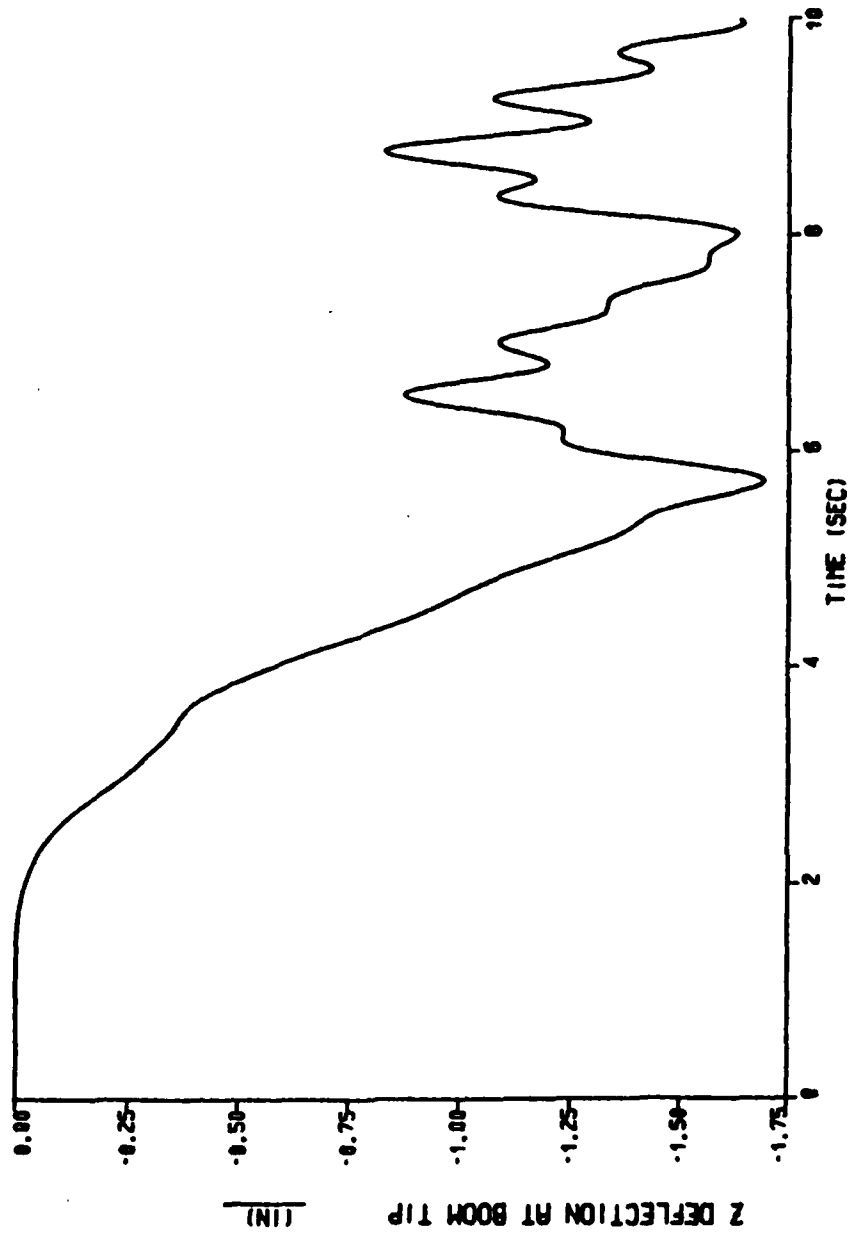


Figure B.8

Vertical Deflection at Boom Tip of
More Flexible Reflector at -155°

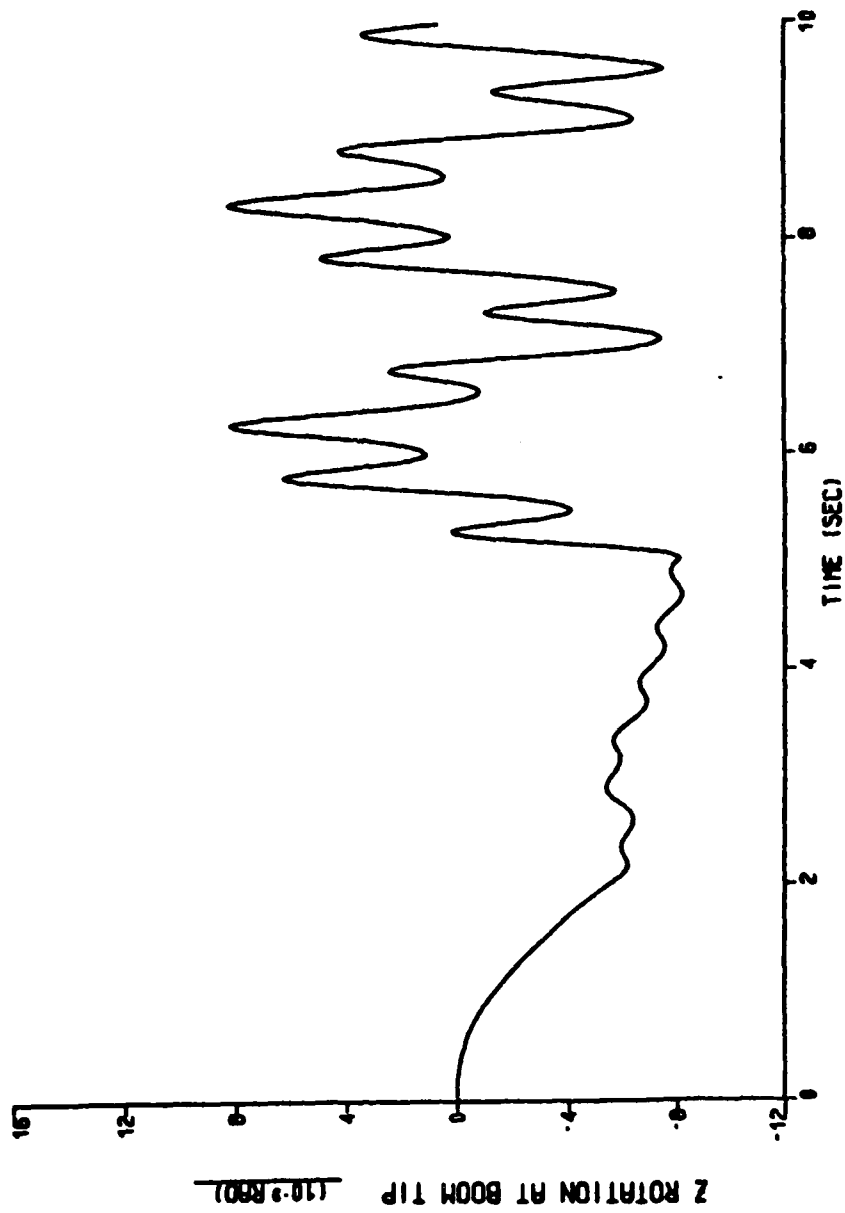


Figure B.9

**Rotation of Boom Tip About Vertical Axis
of Stiffer Reflector at -155°**

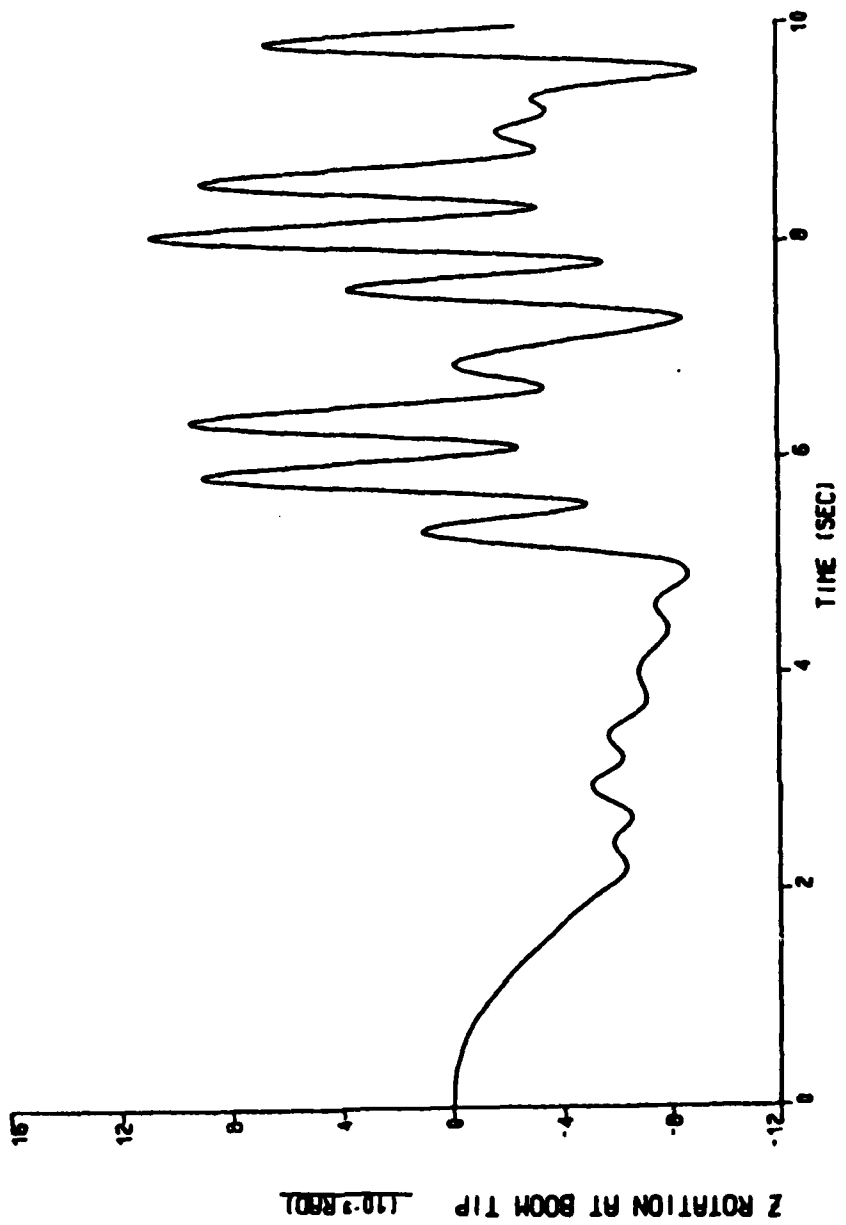


Figure B.10
**Rotation of Boom Tip About Vertical Axis
of More Flexible Reflector at -155°**

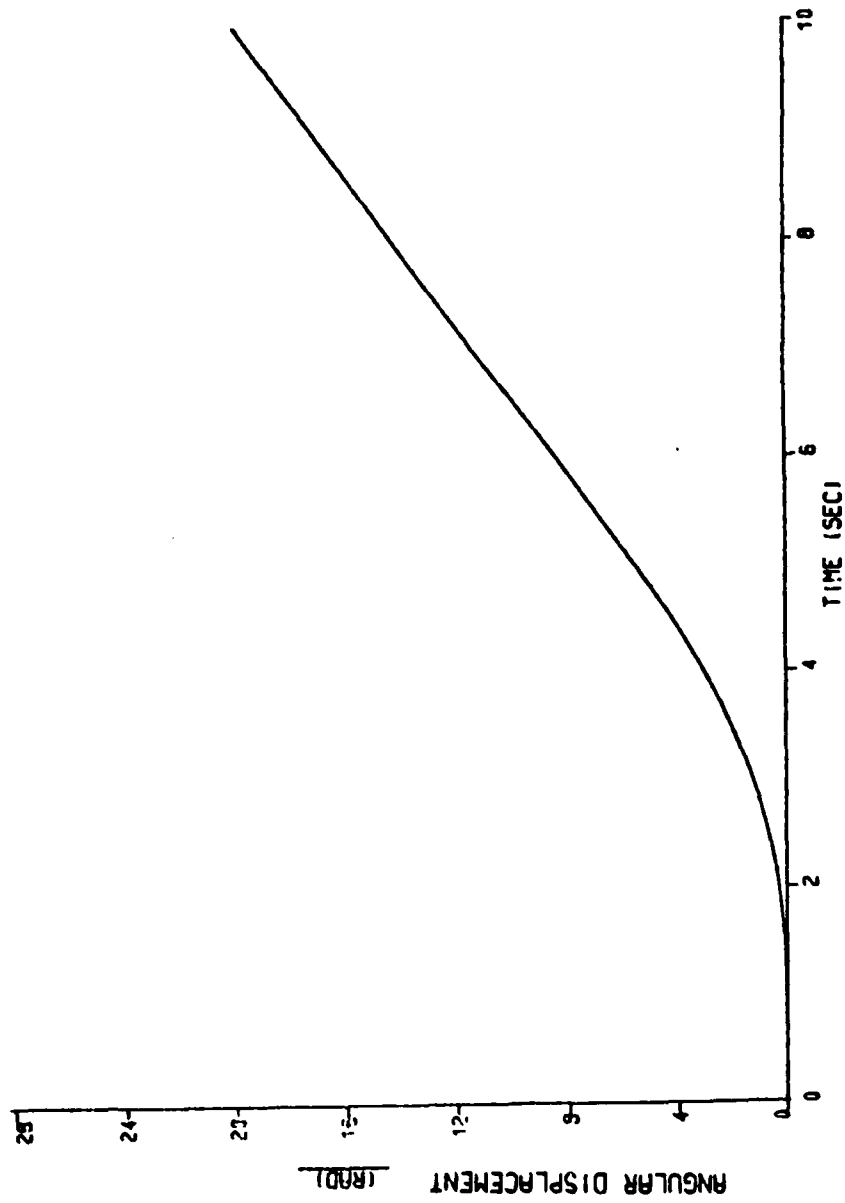


Figure C.1
Angular Displacement of Stiffer Reflector at -135°

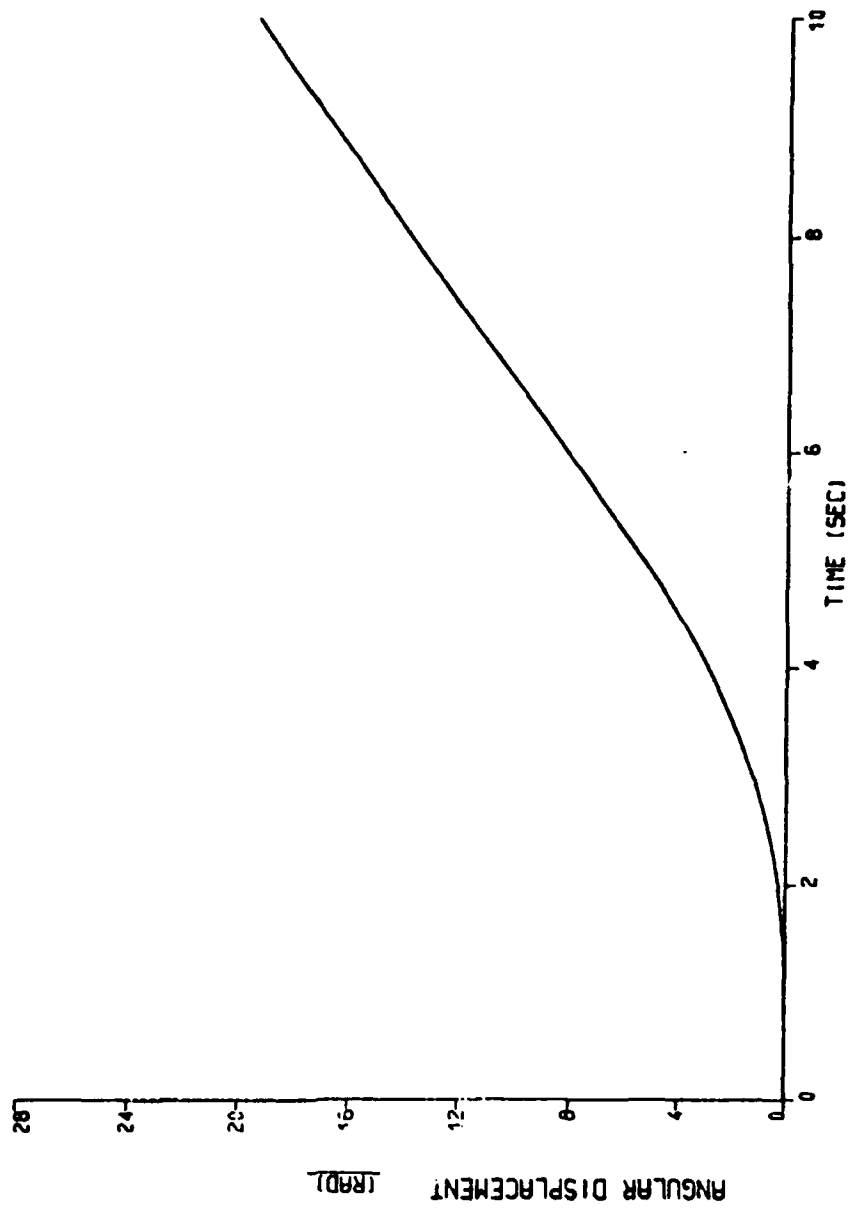


Figure C.2
Angular Displacement of Stiffer Reflector at -145°

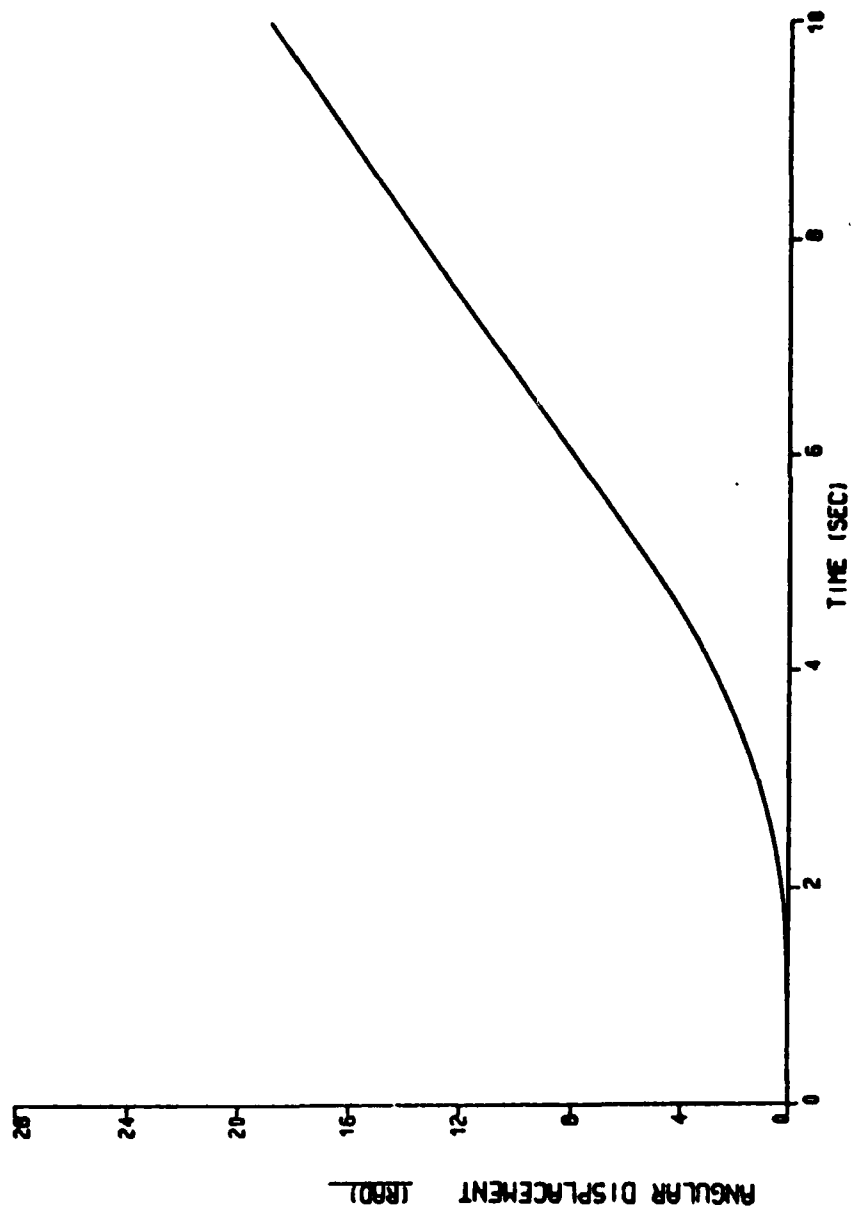


Figure C.3
Angular Displacement of Stiffer Reflector at -155°

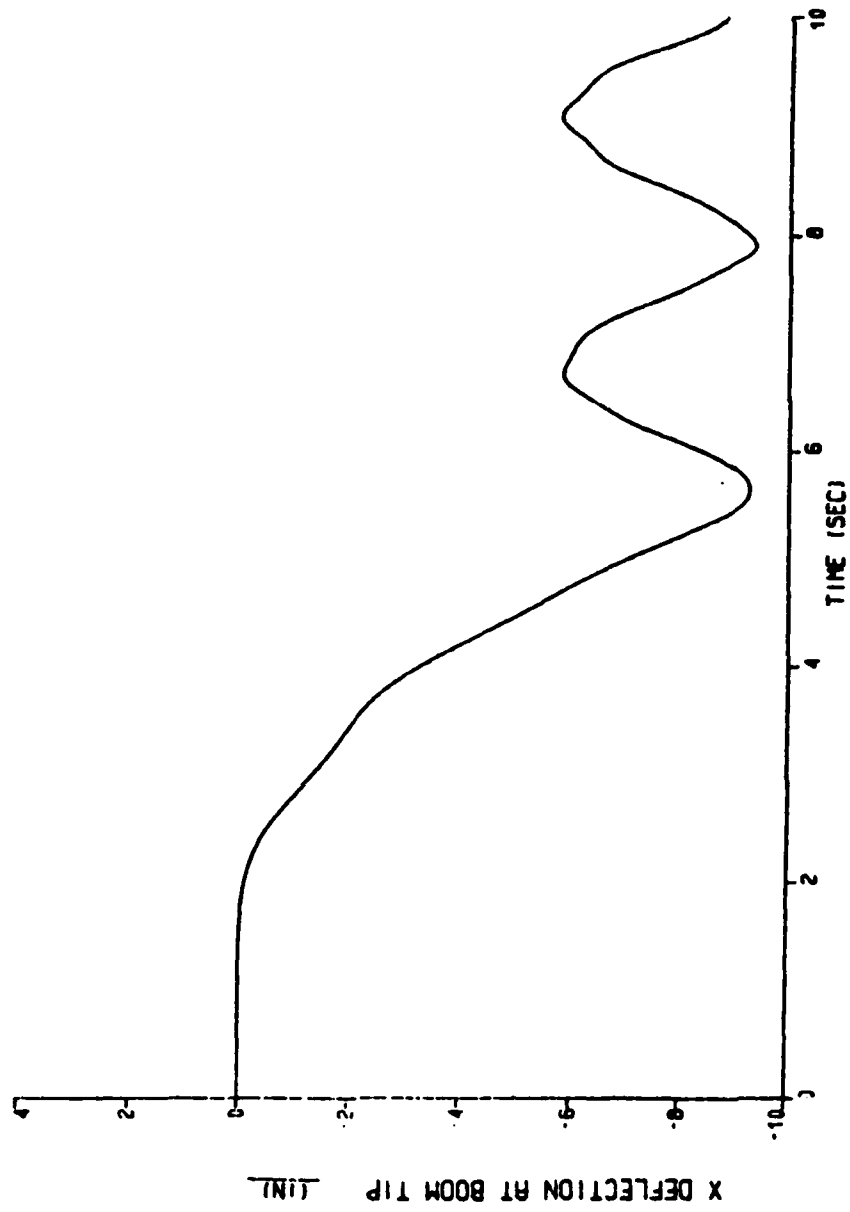


Figure C.4
Horizontal Deflection of Boom Tip of Stiffer Reflector at -135°

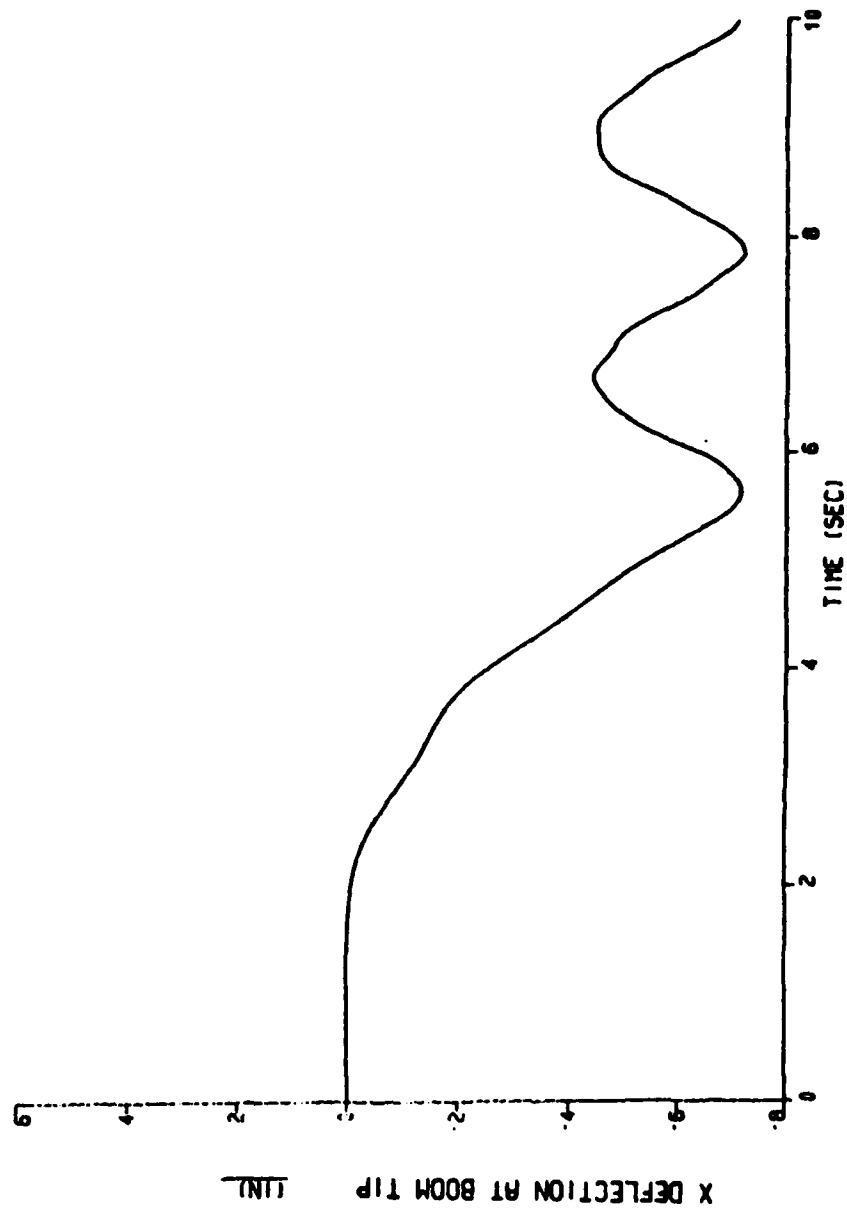


Figure C.5
Horizontal Deflection of Boom Tip of Stiffer Reflector at -145°

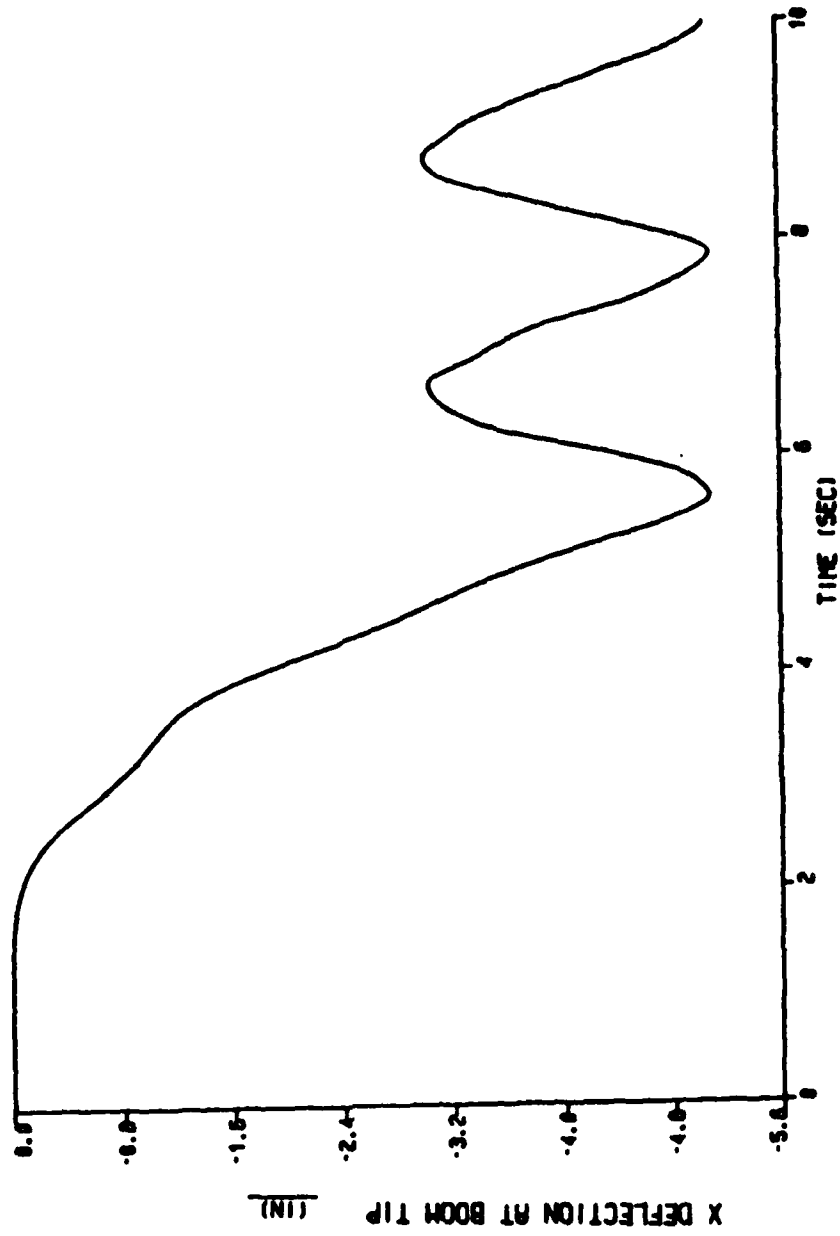


Figure C.6
 Horizontal Deflection of Boom Tip of Stiffer Reflector at -155°

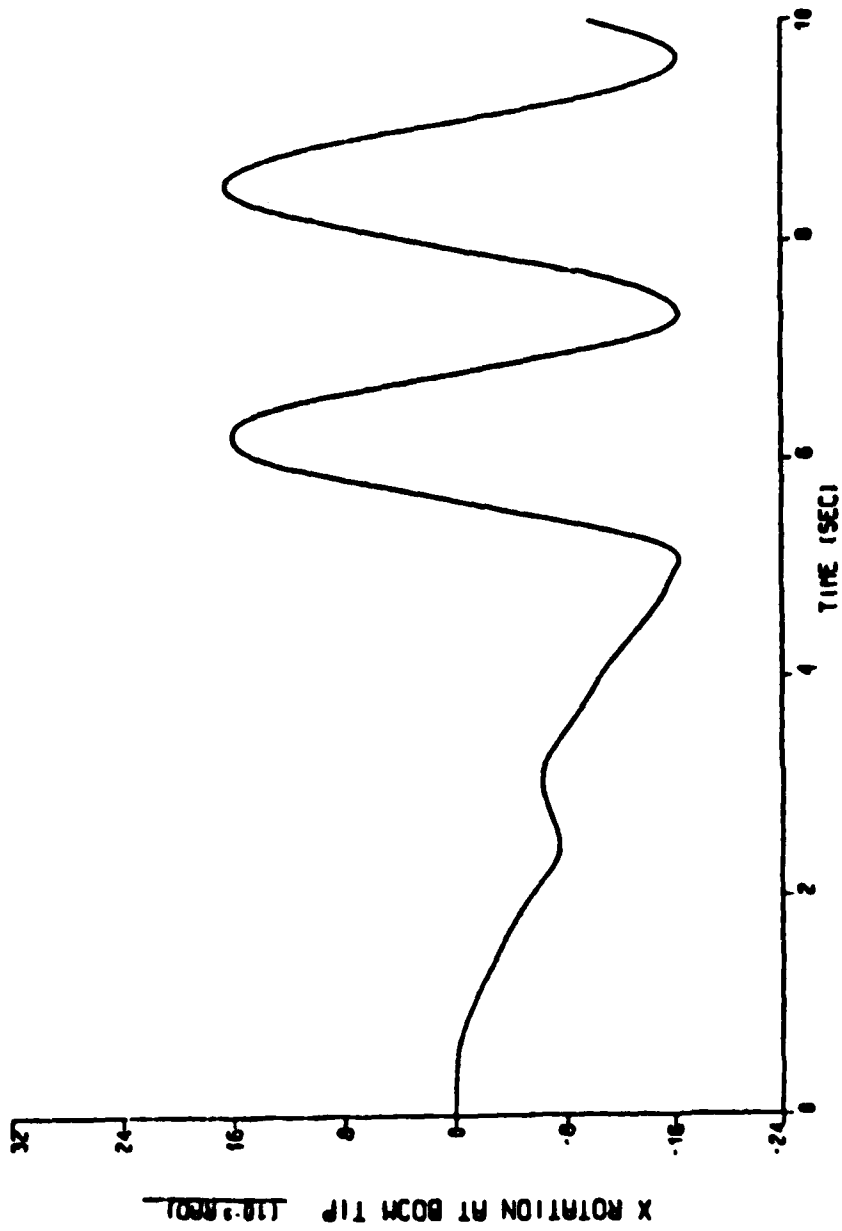


Figure C.7

Rotation of Boom Tip About Horizontal Axis
of Stiffer Reflector at -135°

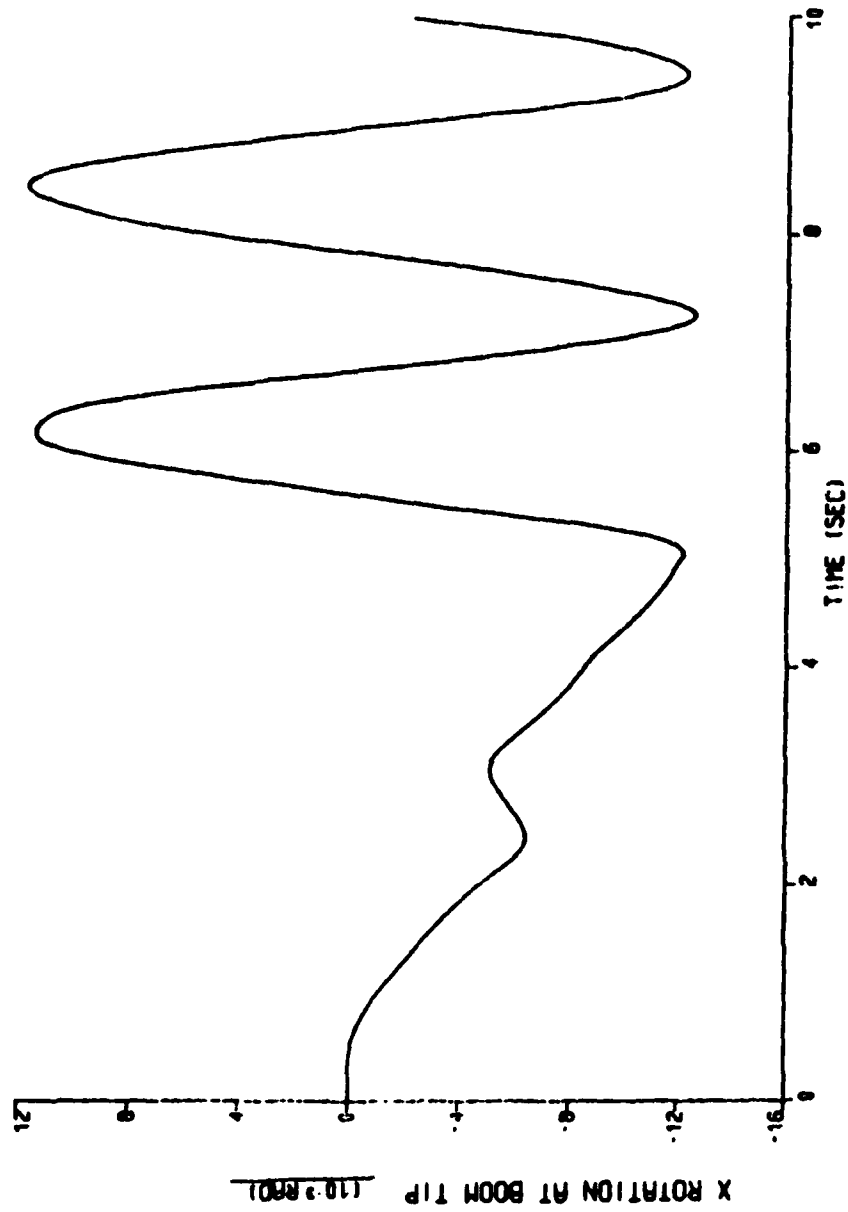


Figure C.8

**Rotation of Boom Tip About Horizontal Axis
of Stiffer Reflector at -145°**

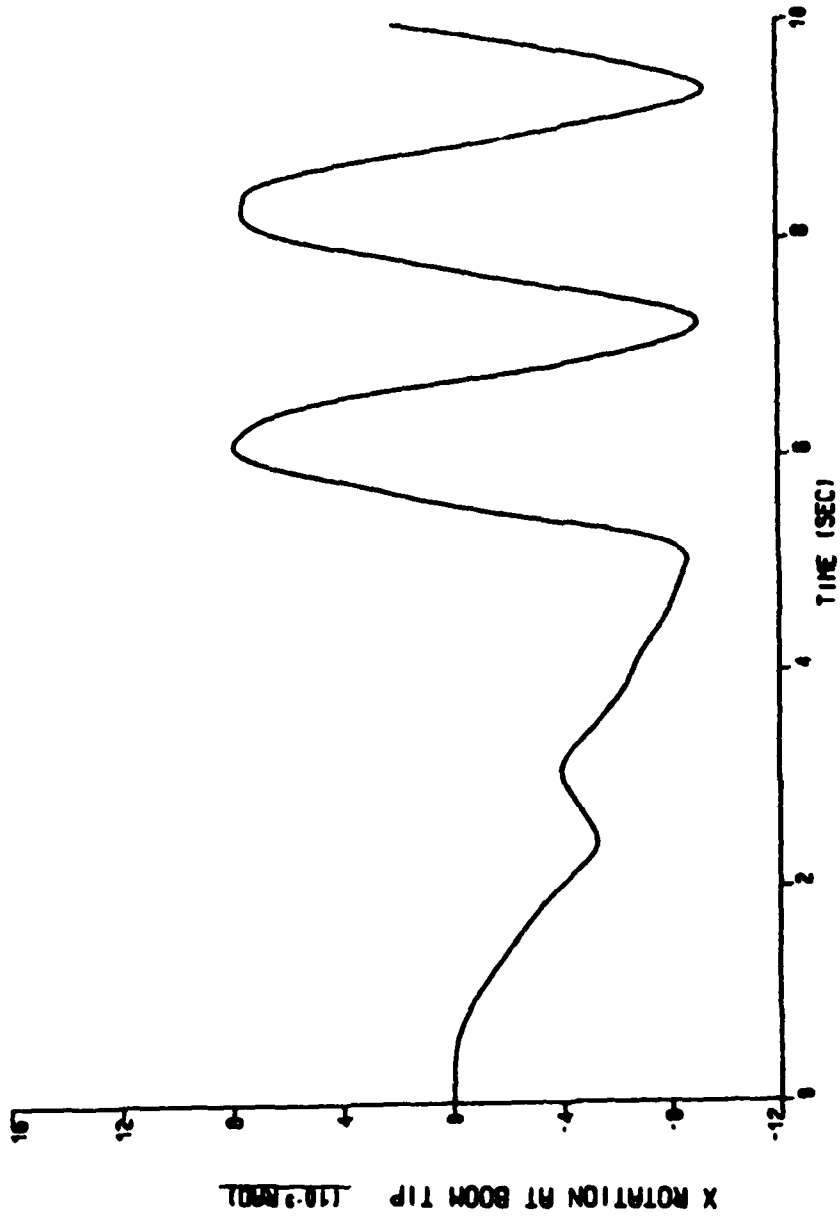


Figure C.9

**Rotation of Boom Tip About Horizontal Axis
of Stiffer Reflector at -155°**

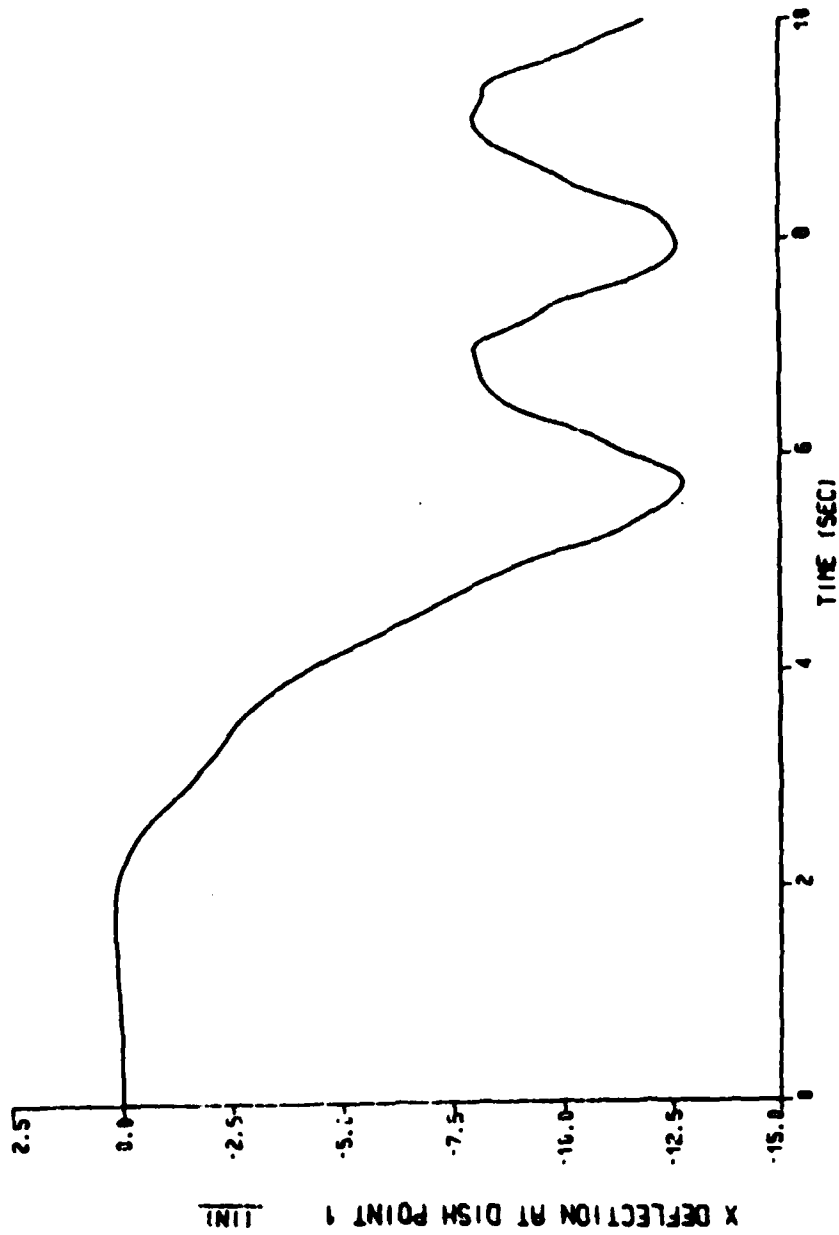


Figure C.10

Horizontal Deflection of Dish Point 1 of Stiffer Reflector at -135'

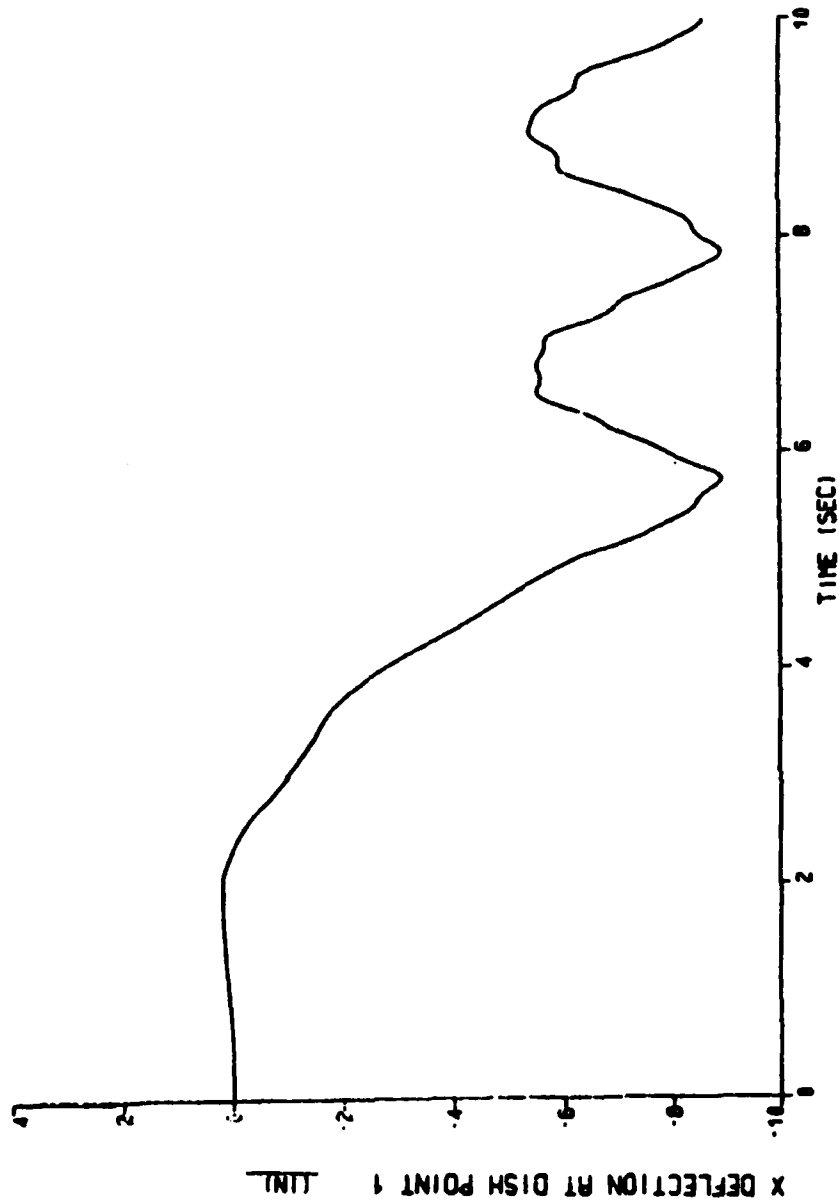


Figure C.11

Horizontal Deflection of Dish Point 1 of Stiffer Reflector at -145°

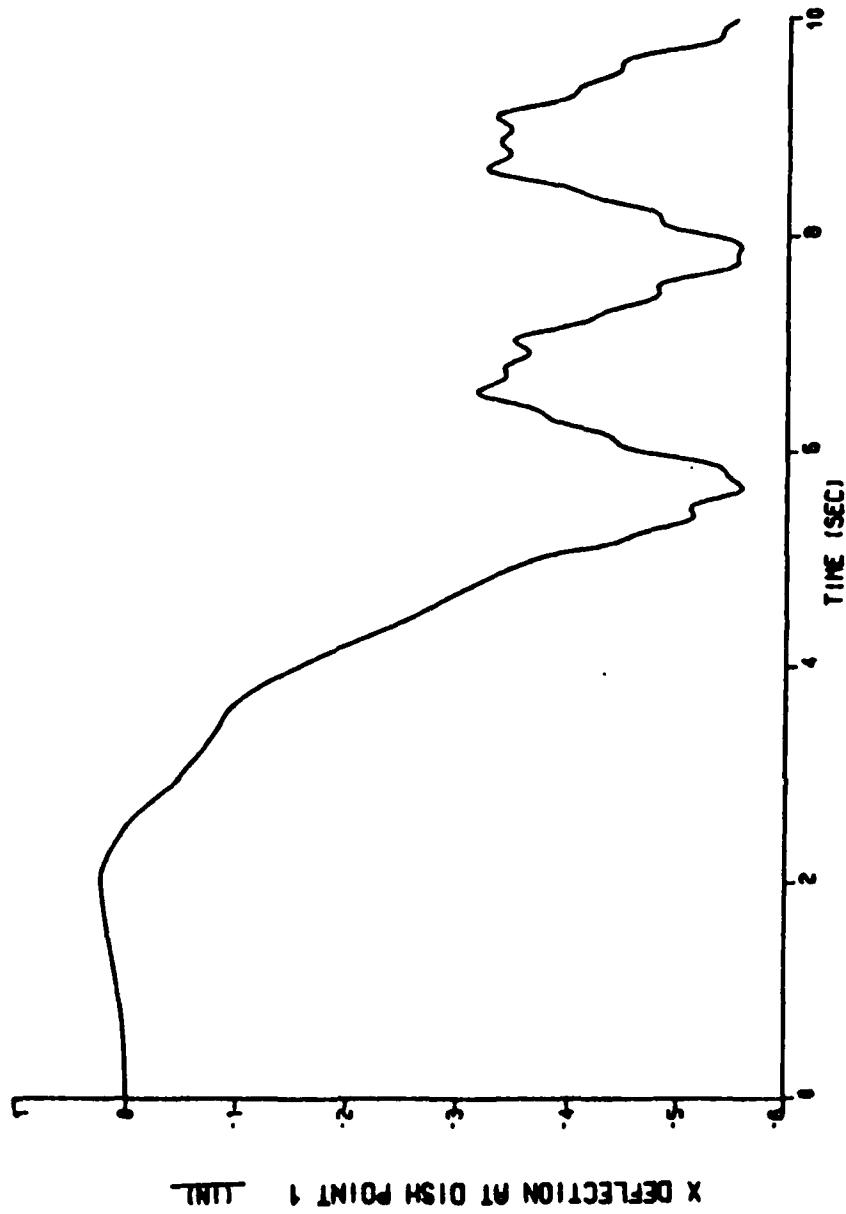


Figure C.12

Horizontal Deflection of Dish Point 1 of Stiffer Reflector at -135°

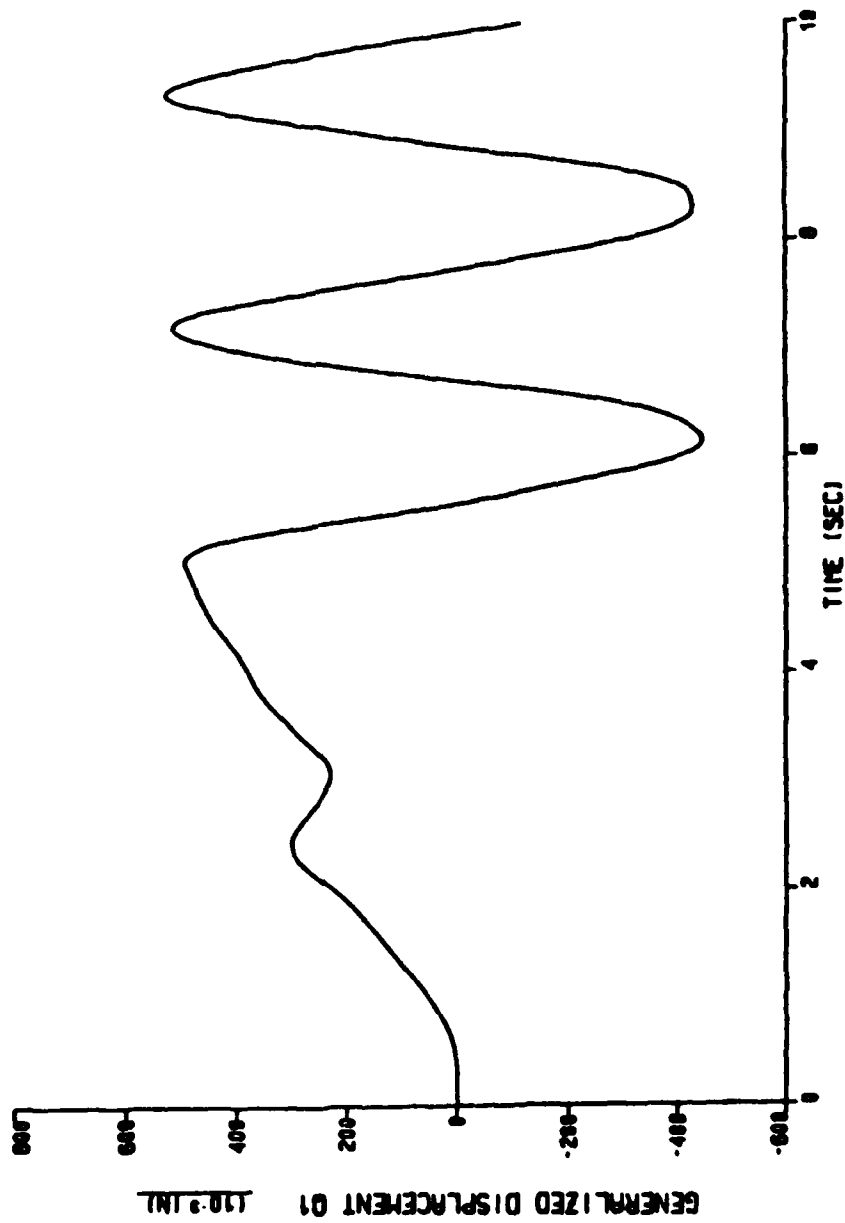


Figure D.1

First Boom Generalized Coordinate of Stiffer Reflector at -155°

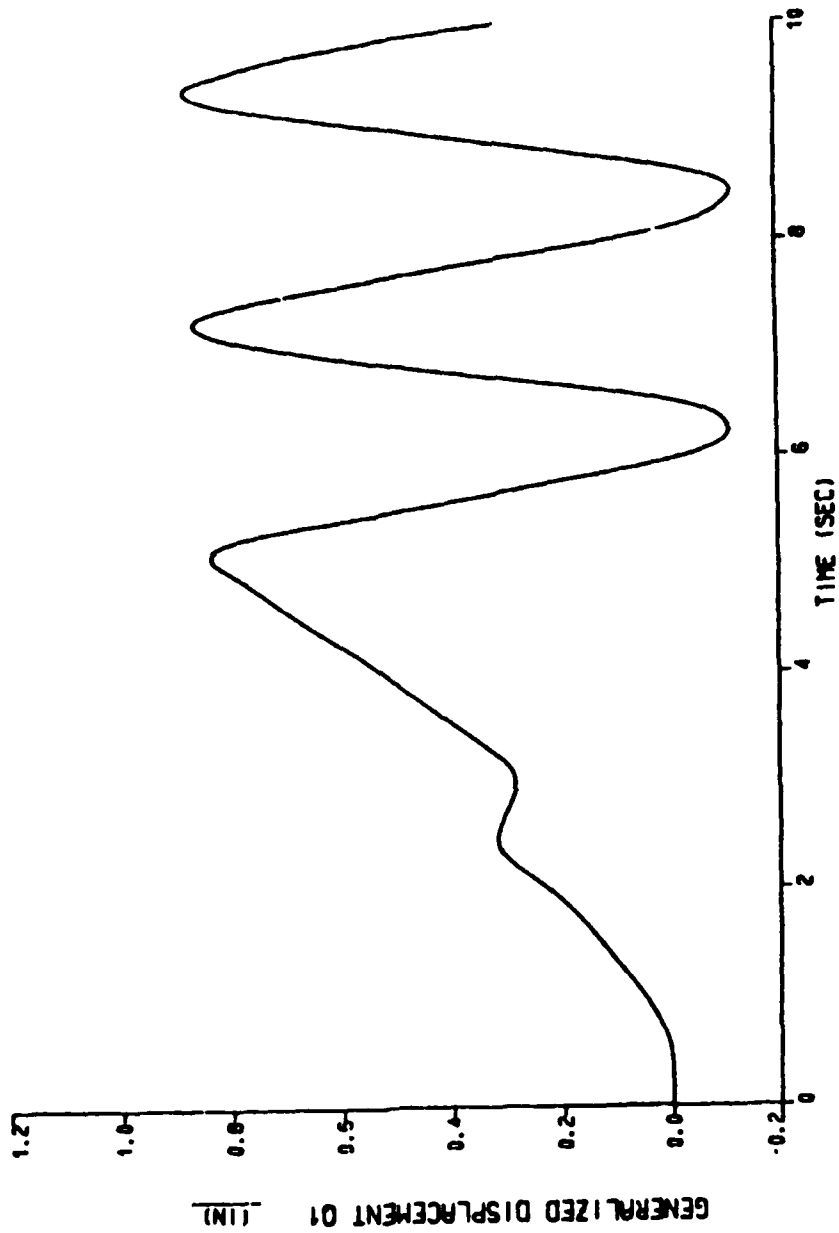


Figure D.2

**First Boom Generalized Coordinate of
Stiffer Reflector Tilted 5' Out of Plane**

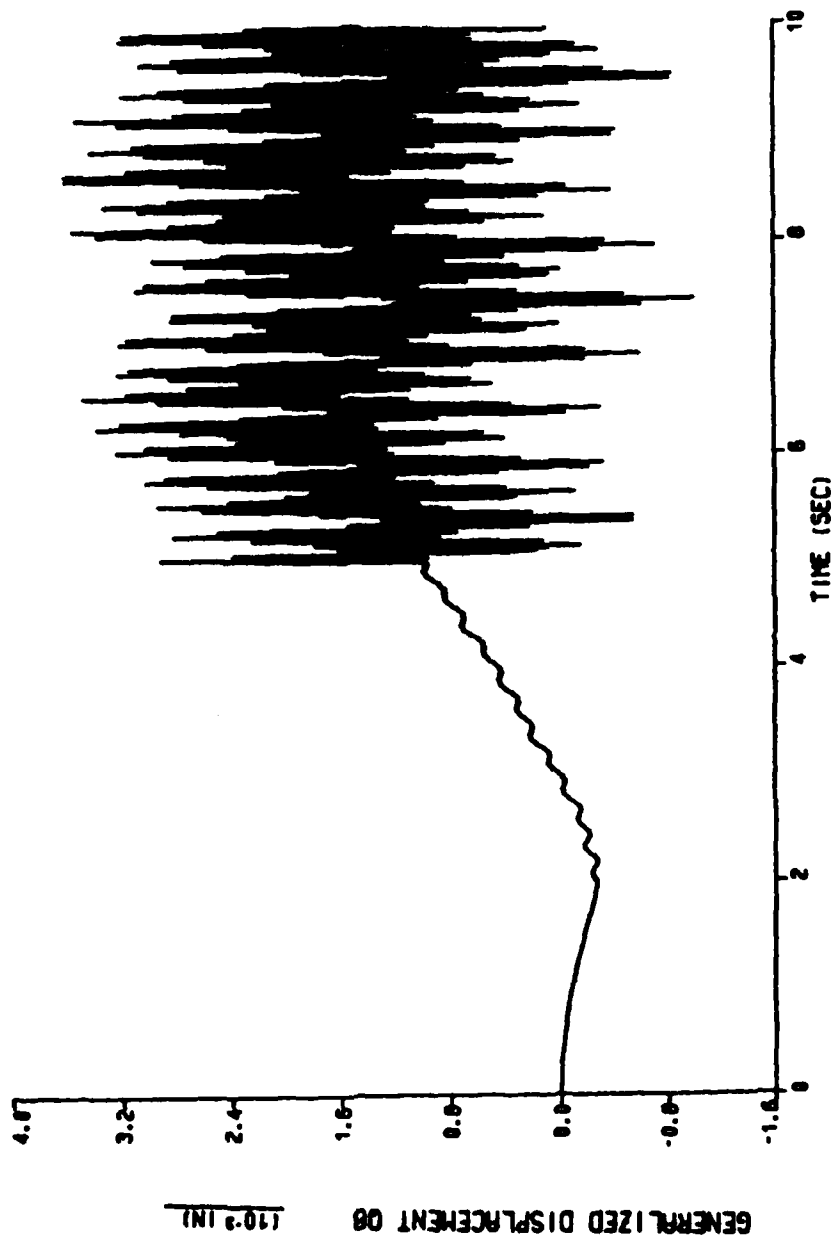


Figure D.3

**Fourth Reflector Generalized Coordinate
of Stiffer Reflector at -155°**

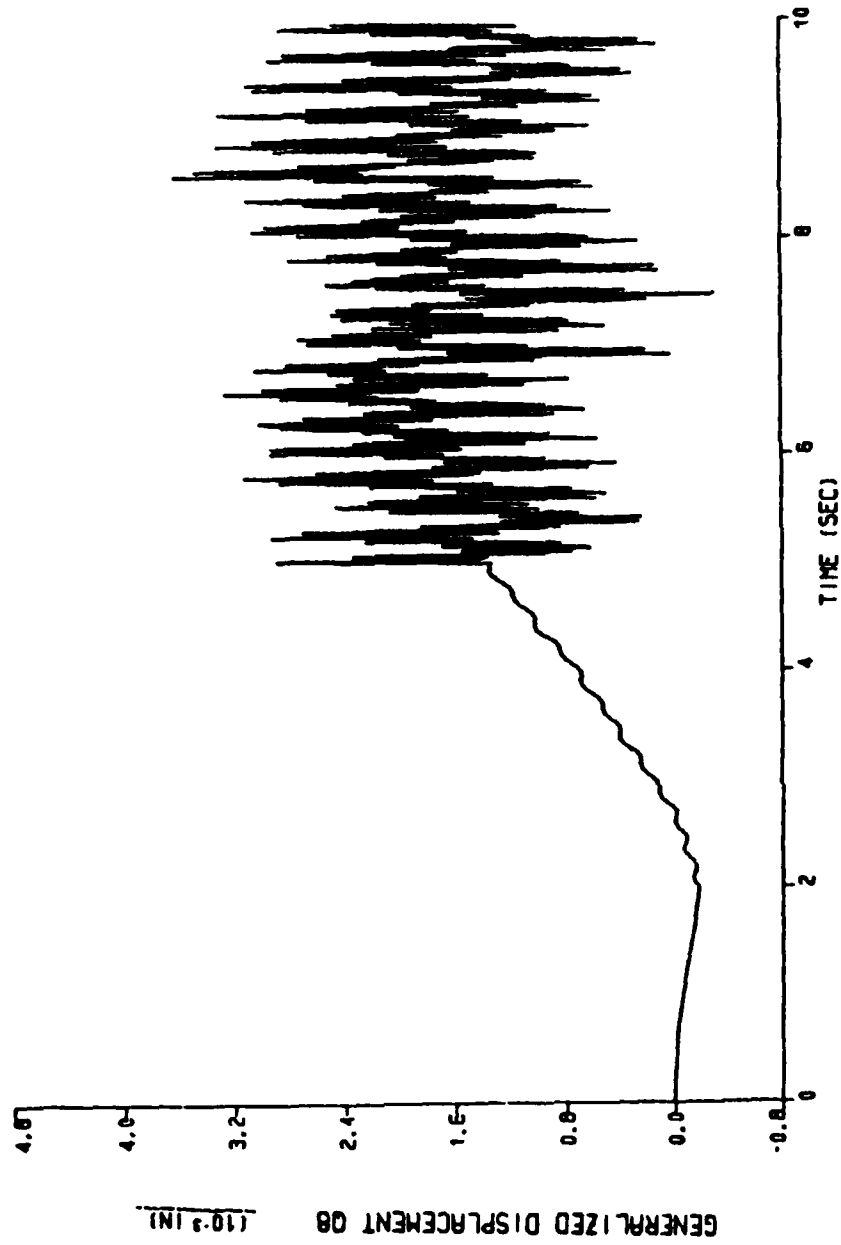


Figure D.4

**Fourth Reflector Generalized Coordinate
of Stiffer Reflector Tilted 5° Out of Plane**

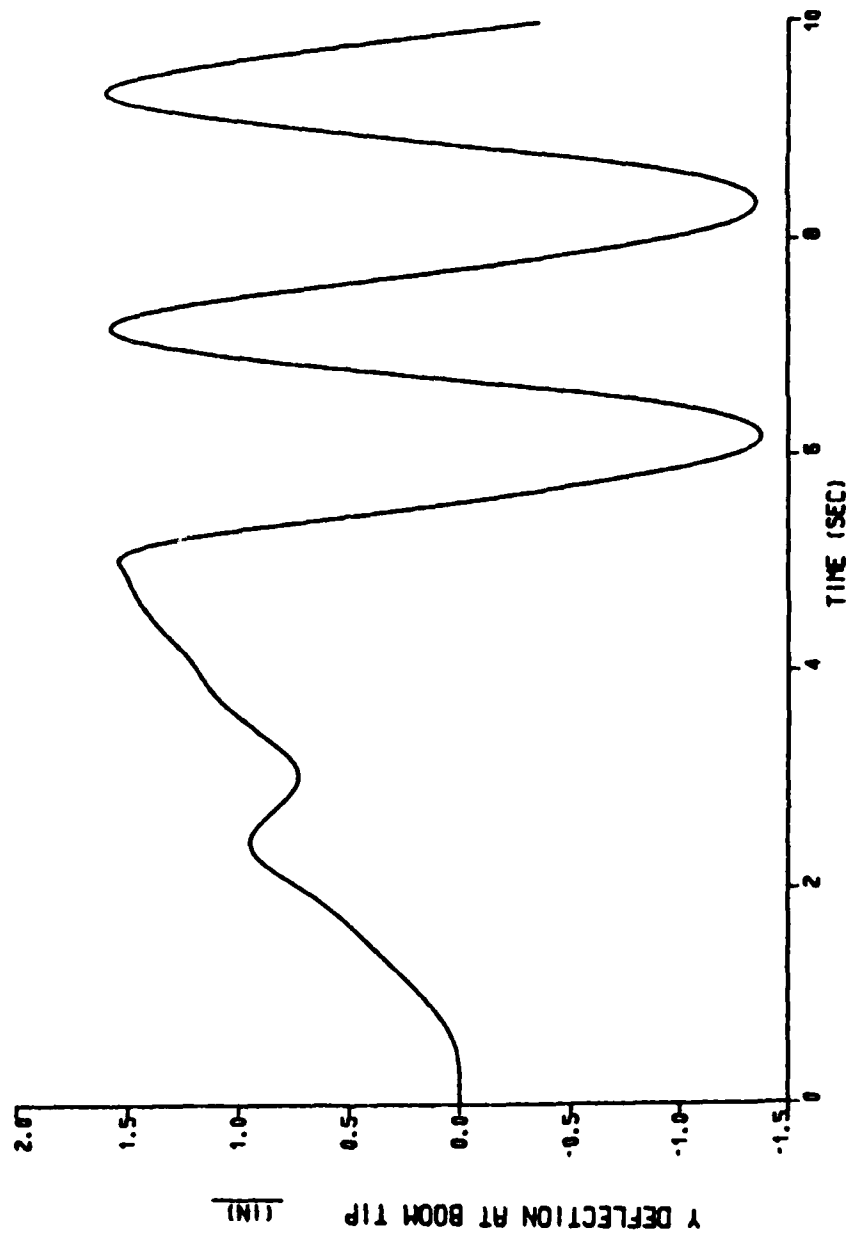


Figure D.5
 Out-of-Plane Deflection at Boom Tip of Stiffer Reflector at -155°

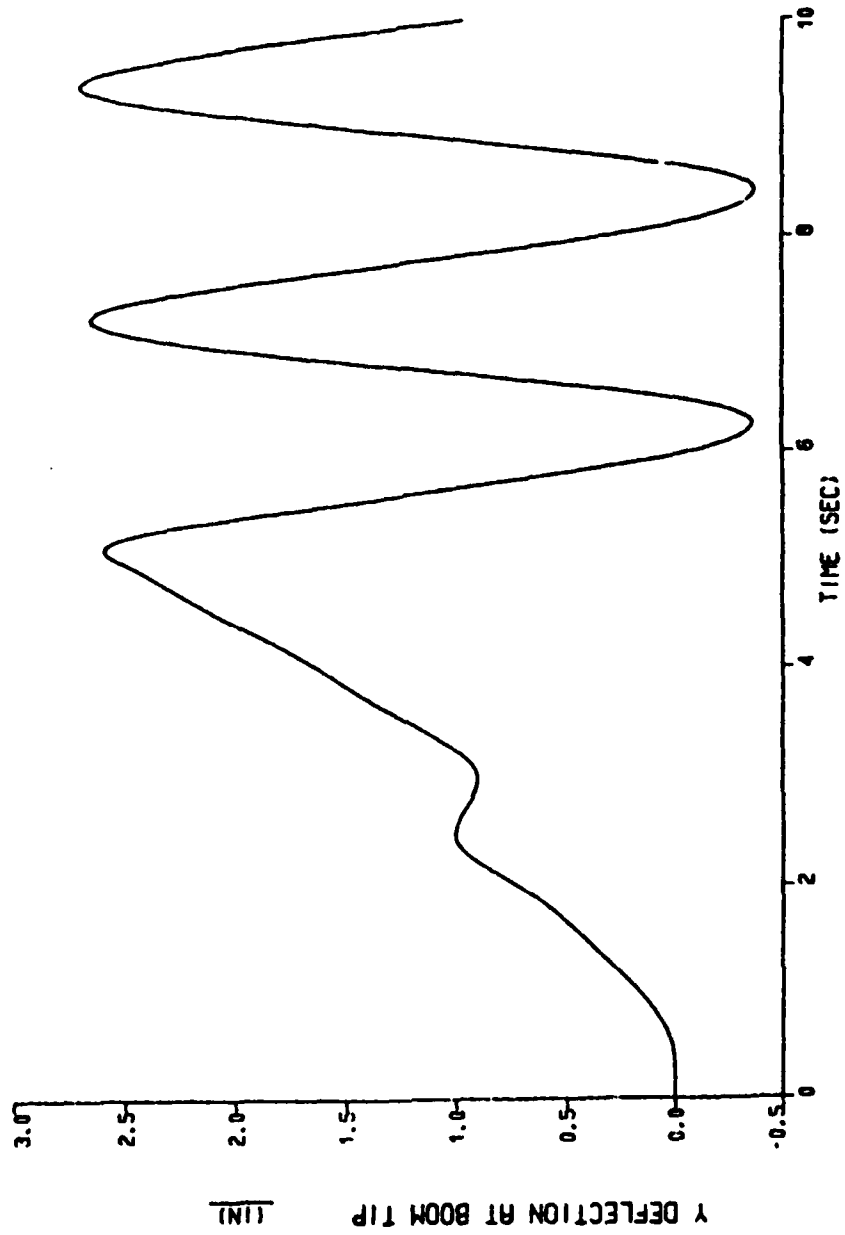


Figure D.6

**Out-of-Plane Deflection at Boom Tip of
Stiffer Reflector Tilted 5° Out of Plane**

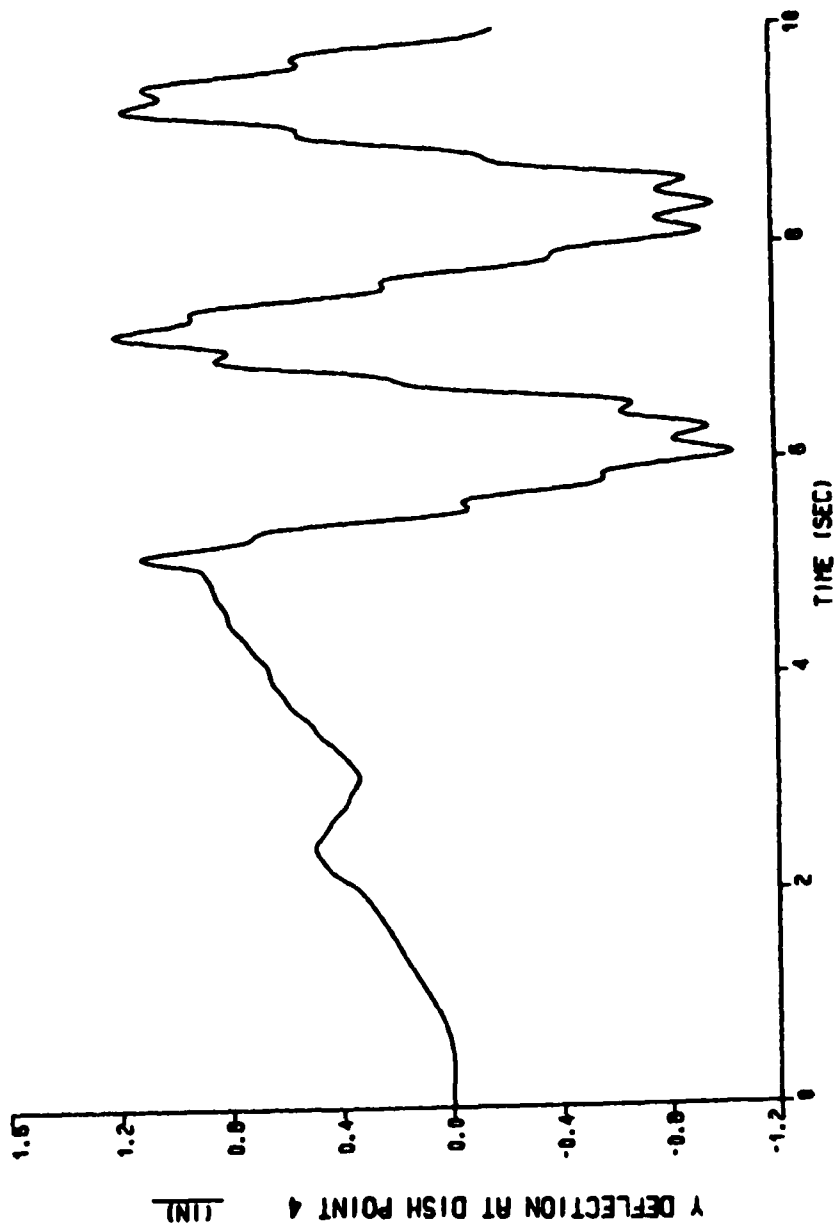


Figure D.7

**Out-of-Plane Deflection at Dish Point 4
of Stiffer Reflector at -155°**

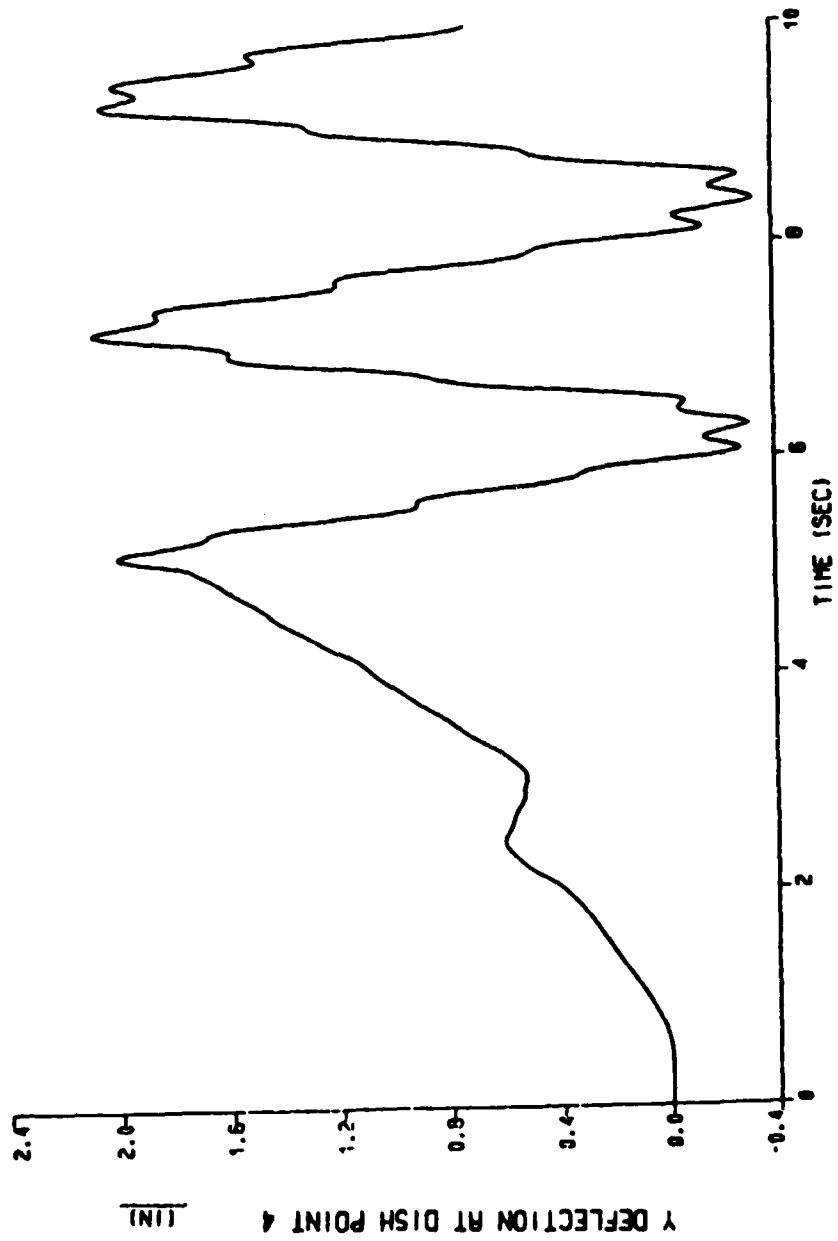


Figure D.8

**Out-of-Plane Deflection at Dish Point 4
of Stiffer Reflector Tilted 5' Out of Plane**

LIST OF REFERENCES

1. Defense Meteorological Satellite Program (DMSP), "Technical Operating Report System Engineering Task 0007-11 Preliminary Study for Navy Remote Sensing System (N-ROSS)," issued July 1985, DMSP Program Office, RCA Aerospace and Defense, Astro-Electronics Division, Princeton, New Jersey.
2. Defense Meteorological Satellite Program (DMSP), "Technical Operating Report System Engineering Task 0007-11 Preliminary Study for Navy Remote Sensing System (N-ROSS)," issued April 1984, DMSP Program Office, RCA Aerospace and Defense, Astro-Electronics Division, Princeton, New Jersey.
3. Kang, Choong Soon, Dynamic Analysis of the Flexible Boom in the N-ROSS Satellite, Thesis, Naval Postgraduate School, Monterey, California, March 1987.
4. Sing, R. P. and R. J. Vandervoort, Paper 84-1024, AIAA Dynamics Specialists Conference, Palm Springs, CA, 1984, "Dynamics of Flexible Bodies in Tree Topology—A Computer-Oriented Approach."
5. Kane, T. R., Dynamics, 3rd ed., Academic Press, Stanford University, 1978.
6. Kane, T. R., P. W. Likins, and D. A. Levinson, Spacecraft Dynamics, McGraw-Hill Inc., New York, 1983.
7. MSC/NASTRAN User's Manual Vol. 1 & 2, The MacNeal-Schwendler Corporation.
8. Dynamic Simulation Language/VS Program Description/Operation Manual, Program Number 5798-PXJ. IBM Corporation, 2d ed., September 1985.
9. Tsai, S. W. and H. T. Hahn, Introduction to Composite Materials, Technomic Publishing Co., Inc., Westport, Connecticut, 1980.

INITIAL DISTRIBUTION LIST

		No. Copies
1.	Defense Technical Information Center Cameron Station Alexandria, VA 22304-6145	2
2.	Library, Code 0142 Naval Postgraduate School Monterey, CA 93943-5002	2
3.	Professor Y.S. Shin, Code 69Sg Department of Mechanical Engineering Naval Postgraduate School Monterey, CA 93943	4
4.	Department Chairman, Code 69 Department of Mechanical Engineering Naval Postgraduate School Monterey, CA 93943	1
5.	Dr. Kilsoo Kim, Code 69Ki Department of Mechanical Engineering Naval Postgraduate School Monterey, CA 93943	1
6.	LCDR Scott Palmer, USN Pdw 106-7 Space & Naval Warfare System Command Washington, D.C. 20363-5100	1
7.	CAPT N.E. Holben, USN Pdw 106-7 Space & Naval Warfare System Command Washington, D.C. 20363-5100	1
8.	Dr. Robert Lindberg Head of Advanced Concepts Section Space System & Technology Division Naval Research Laboratory Washington, D.C. 30275	1
9.	LT Natalie F. Heffernan P.O. Box 416 Callao, VA 22435	5

END

10-87

DTIC